Evaluation of ReaxFF potentials for the interactions between 3-fold coordinated carbon systems and molecules

Zacharias G. Fthenakis

Instituto Nanoscienze – Consiglio Nazionale delle Ricerche, Italy

Theoretical and Physical Chemistry Institute, National Hellenic Research Foundation, Greece

Collaborators



- Vallentina Tozzini, Nano-CNR, Pisa, Italy
- Nektarios Lathiotakis, National Hellenic Research Foundation, Greece
- Ioannis Petsalakis, National Hellenic Research Foundation, Greece

Funding

- EU-H2020 FETPROACT LESGO (Agreement No. 952068)
- MONSTRE-2D PRIN2017 KFMJ8E (Italian Ministry of University and Research)
- nanoporous GrAphene membrane made without TransfEr for gas Separation GATES (MIS 5041612)
- Advanced Materials and Devices (MIS 5002409)
- National Infrastructure in Nanotechnology, Advanced Materials and Micro-/Nanoelectronics (MIS 5002772) of the Operational Program Competitiveness, Enterprenueurship and Innovation (NSRF 2014-2020), co-financed by Greek and European Union (European Regional Development Fund)

Theoretical methods for calculations
Which method to use? Why we need classical potentials?

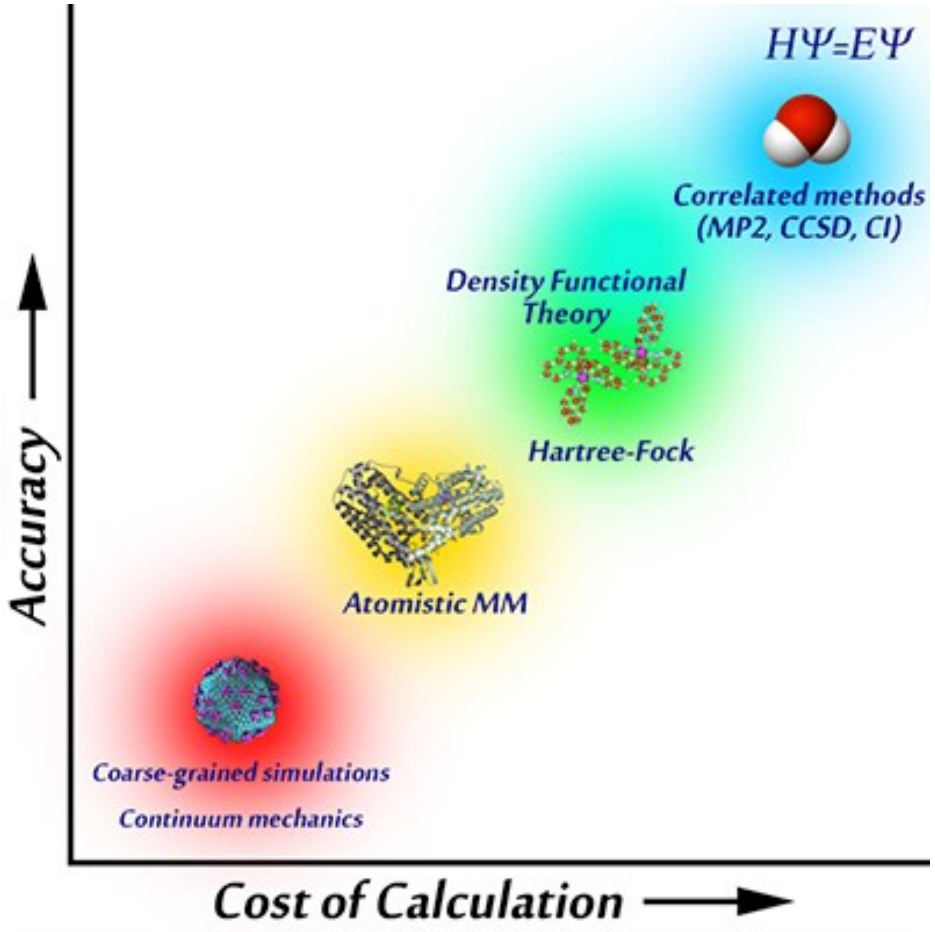

leeping.github.io/forcebalance/doc/html/

- Several different levels of accuracy depending on the approximations
- A more accurate method is more time consuming

Computational time (cost of calculation) increases as:

- the accuracy inceases
- the system size increases

Method	Cost	Example for N=10
CCSD(T)	$\propto N^7$	T ~ 4 months
CCSD and MP4	$\propto N^6$	T ~ 12 days
MP2	$\propto N^5$	T ~ 28 hours
HF > DFT > TB	$\propto N^2 - N^3$	T ~ 1.5 – 20 min
Classical Potentials	$\propto N - N^2$	T ~ 10-100 sec
Continuum mechanics	$\propto N$	T ~ 10 sec

Conclusion: The system size selects the method

Theoretical methods for calculations
Which method to use? Why we need classical potentials?

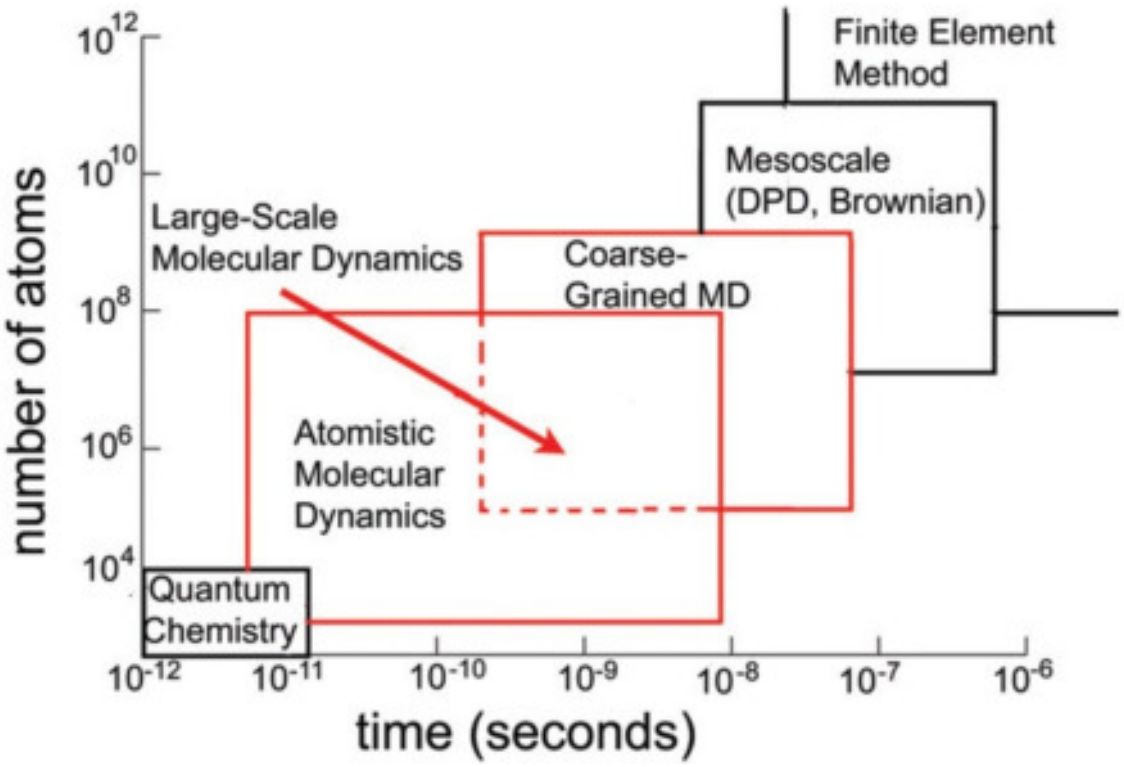

Greathouse et al, Minerals **4**, 519 (2014)

- Several different levels of accuracy depending on the approximations
- A more accurate method is more time consuming

Computational time (cost of calculation) increases as:

- the accuracy inceases
- the system size increases

Method	Cost	Example for N=10
CCSD(T)	$\propto N^7$	T ~ 4 months
CCSD and MP4	$\propto N^6$	T ~ 12 days
MP2	$\propto N^5$	T ~ 28 hours
HF > DFT > TB	$\propto N^2 - N^3$	T ~ 1.5 – 20 min
Classical Potentials	$\propto N - N^2$	T ~ 10-100 sec
Continuum mechanics	$\propto N$	T ~ 10 sec

Conclusion: The system size selects the method

Theoretical methods for calculations
Which method to use? Why we need classical potentials?

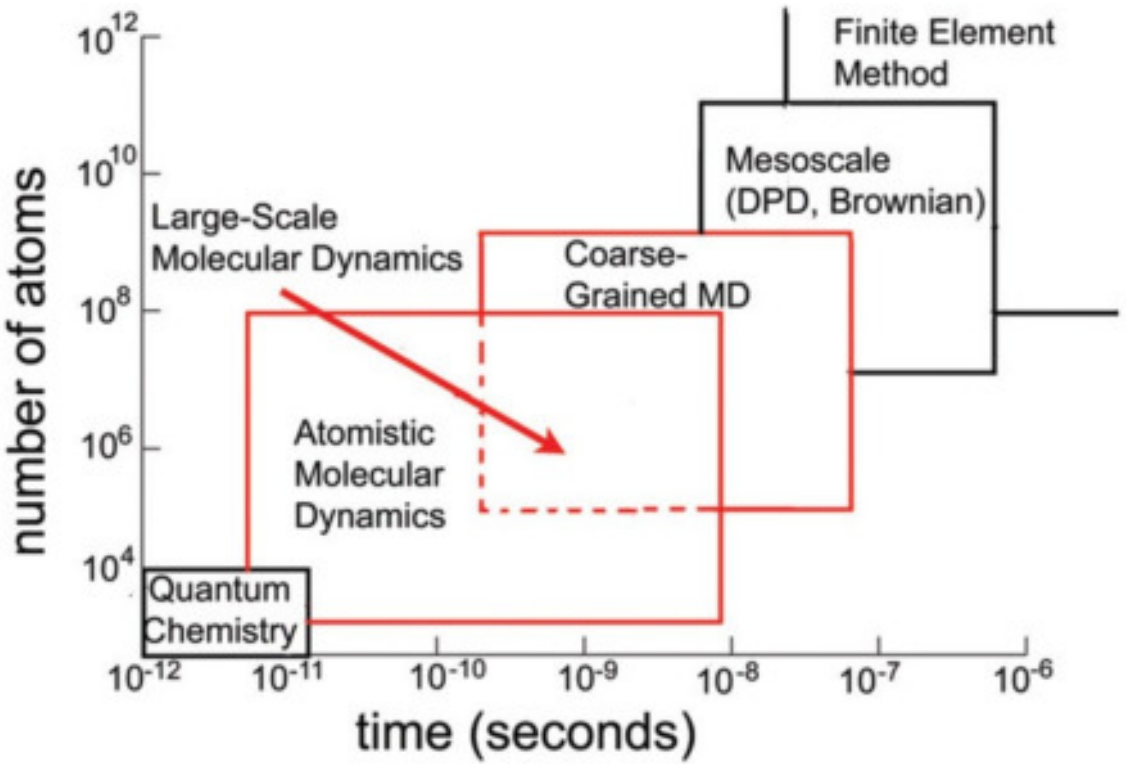

Greathouse et al, Minerals **4**, 519 (2014)

Main parameters to be taken in account

- Size of the system
- **Properties** to be calculated
  - Information to be extracted decreases as less accurate methods are used (e.g. quantum mechanical character is lost in calculations using classical potentials).
  - Properties that require large system simulations can not be calculated using accurate methods (e.g. melting temperature, dislocations, etc)
  - Calculations may be different, not only due to the accuracy of the methods, but also due to the size of the simulated system.

For example …

Theoretical methods for calculations
Which method to use? Why we need classical potentials?

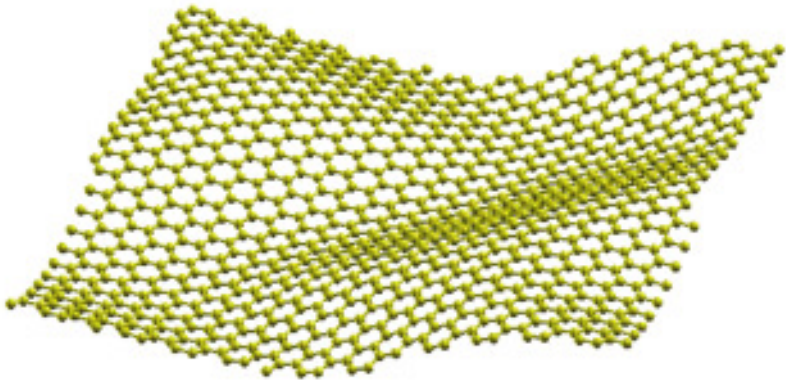

Main parameters to be taken in account

- Size of the system
- **Properties** to be calculated
  - Information to be extracted decreases as less accurate methods are used (e.g. quantum mechanical character is lost in calculations using classical potentials).
  - Properties that require large system simulations can not be calculated using accurate methods (e.g. melting temperature, dislocations, etc)
  - Calculations may be different, not only due to the accuracy of the methods, but also due to the size of the simulated system.

- **Approximations are unavoidable for the study of large systems.**
- **Improving the accuracy of approximations (e.g. classical potentials) for large systems is essential.**

Classical potentials for Carbon materials

- Simple «old» potentials
- Molecular Mechanics potentials
- Bond Order Potentials (BOPs)
- ReaxFF potentials
- Machine learning potentials

Classical potentials for Carbon materials

- **Simple «old» potentials**
- Molecular Mechanics potentials
- Bond Order Potentials (BOPs)
- ReaxFF potentials
- Machine learning potentials

Pair potentials

$$\Phi_1 = \phi_2 = \sum_{i<j} U_{ij} .$$

- **Exp-6 potential**

(C-C, C-H, C-Cl, C-Br, C-N, C-S, C-O, C-N interactions) (1967-197

$$U_{ij} = Be^{-Cr_{ij}} - \frac{A}{r_{ij}^6} .$$

- **Giglio et al**

(C-C, C-CH_3, C-Cl, C-S) (1970-1973)

$$U_{ij} = \frac{B}{r_{ij}^6} e^{-Cr_{ij}} - \frac{A}{r_{ij}^6} .$$

- **Gamba – Bonadeo**
  (C-C,C-N,C-H) (1981)

$$U_{ij} = Be^{-Cr_{ij}} - \frac{A}{r_{ij}^6} + D\frac{\mu_i \mu_j}{r_{ij}^3} .$$

(for benzene and azabenzene)

All these potentials suffer from the absence of n-body terms, n>2.

They are nor reliable for graphene.

Classical potentials for Carbon materials

- **Simple «old» potentials**
- Molecular Mechanics potentials
- Bond Order Potentials (BOPs)
- ReaxFF potentials
- Machine learning potentials

Many body potentials

$$\Phi = \phi_2 + \phi_3 = \sum_{i<j} U_{ij} + \sum_{i<j<k} W_{ijk},$$

3-body terms

- **Keating potential** **(for covalent semiconductors)**

$$U_{ij} = \frac{3\alpha}{16R_{ij}^2}(r_{ij}^2 - R_{ij}^2)^2,$$

$$W_{ijk} = \frac{3\beta}{8R_{ij}R_{ik}}(\mathbf{r}_{ij}\cdot\mathbf{r}_{ik} - \mathbf{R}_{ij}\cdot\mathbf{R}_{ik})^2 + \frac{3\sigma}{4R_{ij}R_{ik}}(r_{ij}^2 - R_{ij}^2)(r_{ik}^2 - R_{ik}^2).$$

- Atoms j and k are the first neighbors to atom i.
- R_{ij} is the equilibrium distance in the bulk.

P. N. Keating, *Phys. Rev.* **145**, 637 (1966).
V. K. Bashenov, D. I. Marvakov, and A. M. Mutal, *Phys. Stat. Sol. (b)* **86**, K7 (1978).
R. M. Martin, *Phys. Rev. B* **1** , 4005 (1970)

Classical potentials for Carbon materials

- **Simple «old» potentials**
- Molecular Mechanics potentials
- Bond Order Potentials (BOPs)
- ReaxFF potentials
- Machine learning potentials

Many body potentials

$$\Phi = \phi_2 + \phi_3 = \sum_{i<j} U_{ij} + \sum_{i<j<k} W_{ijk} ,$$

- **Murrell et al I potential** **(for cubic crystals)**

$$U_{ij} = -D(1 + a_2\rho_{ij})e^{-a_2\rho_{ij}} ,$$

$$W_{ijk} = D \cdot P(Q_1, Q_2, Q_3)e^{-a_3 Q_1} ,$$

$$P(Q_1, Q_2, Q_3) = C_0 + C_1 Q_1 + C_2 Q_1^2 + C_3(Q_2^2 + Q_3^2) + C_4 Q_1^3 + C_5 Q_1(Q_2^2 + Q_3^2) + C_6(Q_3^3 - 3Q_3 Q_2^2) ,$$

$$\begin{bmatrix} Q_1 \\ Q_2 \\ Q_3 \end{bmatrix} = \begin{bmatrix} \frac{1}{\sqrt{3}} & \frac{1}{\sqrt{3}} & \frac{1}{\sqrt{3}} \\ 0 & \frac{1}{\sqrt{2}} & -\frac{1}{\sqrt{2}} \\ \frac{\sqrt{2}}{\sqrt{3}} & -\frac{1}{\sqrt{6}} & -d\frac{1}{\sqrt{6}} \end{bmatrix} \begin{bmatrix} \rho_1 \\ \rho_2 \\ \rho_3 \end{bmatrix} ,$$

$$\rho_1 = \rho_{ij} , \quad \rho_2 = \rho_{ik} , \quad \rho_3 = \rho_{jk} , \quad \rho_{ij} = \frac{r_{ij} - r_e}{r_e} .$$

J. N. Murrell and R. E. Mottram, *Mol. Phys.* **69**, 571 (1990).
J. N. Murrell and J. A. Rodriguez-Ruiz, *Mol. Phys.* **71**, 823 (1990).

Classical potentials for Carbon materials

- **Simple «old» potentials**
- Molecular Mechanics potentials
- Bond Order Potentials (BOPs)
- ReaxFF potentials
- Machine learning potentials

Many body potentials

$$\Phi = \phi_2 + \phi_3 = \sum_{i<j} U_{ij} + \sum_{i<j<k} W_{ijk} ,$$

- **Murrell et al I potential** **(for cubic crystals)**

$$U_{ij} = -D(1 + a_2\rho_{ij})e^{-a_2\rho_{ij}} ,$$

$$W_{ijk} = D \cdot P(Q_1, Q_2, Q_3)e^{-a_3 Q_1} ,$$

$$P(Q_1, Q_2, Q_3) = C_0 + C_1 Q_1 + C_2 Q_1^2 + C_3(Q_2^2 + Q_3^2) + C_4 Q_1^3 + C_5 Q_1(Q_2^2 + Q_3^2) + C_6(Q_3^3 - 3Q_3 Q_2^2) ,$$

$$\begin{bmatrix} Q_1 \\ Q_2 \\ Q_3 \end{bmatrix} = \begin{bmatrix} \frac{1}{\sqrt{3}} & \frac{1}{\sqrt{3}} & \frac{1}{\sqrt{3}} \\ 0 & \frac{1}{\sqrt{2}} & -\frac{1}{\sqrt{2}} \\ \frac{\sqrt{2}}{\sqrt{3}} & -\frac{1}{\sqrt{6}} & -d\frac{1}{\sqrt{6}} \end{bmatrix} \begin{bmatrix} \rho_1 \\ \rho_2 \\ \rho_3 \end{bmatrix} ,$$

$$\rho_1 = \rho_{ij} , \quad \rho_2 = \rho_{ik} , \quad \rho_3 = \rho_{jk} , \quad \rho_{ij} = \frac{r_{ij} - r_e}{r_e} .$$

- **Murrell et al II potential**

$$P(Q_1, Q_2, Q_3) = C_0 + C_1 Q_1 + C_2 Q_1^2 + C_3(Q_2^2 + Q_3^2) + C_4 Q_1^3 + C_5 Q_1(Q_2^2 + Q_3^2) + C_6(Q_3^3 - 3Q_3 Q_2^2) + C_7 Q_1^4 + C_8 Q_1^2(Q_2^2 + Q_3^2) + C_9(Q_2^2 + Q_3^2)^2 + C_{10} Q_1(Q_3^3 - 3Q_3 Q_2^2) .$$

A. R. Al-Derzi, R. L. Johnston, J. N. Murrell, and J. A. Rodriguez-Ruiz, *Mol. Phys.* **73**, 265 (1991).
B. R. Eggen, R. L. Johnston, S. Li, and J. N. Murrell, *Mol. Phys.* **76**, 619 (1992).

Classical potentials for Carbon materials

- **Simple «old» potentials**
- Molecular Mechanics potentials
- Bond Order Potentials (BOPs)
- ReaxFF potentials
- Machine learning potentials

- Fit of the phonons in graphite.
- Applied to calculate the vibrations of C_{60}.

C. Lobo and J. L. Martins, *Z. Phys. D* **39**, 159 (1997)

Many body potentials

$$\Phi = \phi_1 + \phi_2 + \phi_3 ,$$

- **Lobo - Martins potential** **(for graphene and fullerenes)**

$$\phi_1 = \sum_{i=1}^{N} \gamma \mathbf{D}_i \cdot \mathbf{D}_i , \qquad \mathbf{D}_i = \mathbf{r}_{i1} + \mathbf{r}_{i2} + \mathbf{r}_{i3}$$

"dangling bond vector"

$$\phi_2 = \frac{1}{2} \sum_{i=1}^{N} \sum_{j=1}^{3} \frac{\alpha}{4r_0^2} (\mathbf{r}_{ij} \cdot \mathbf{r}_{ij} - r_0^2)^2$$

r_0 = 1.421 Å

Keating type potentials

over first neighbors ,

$$+ \frac{1}{2} \sum_{i=1}^{N} \sum_{k=1} \gamma' \mathbf{D}_i \cdot \mathbf{D}_{i_k} + \frac{1}{2} \sum_{i=1}^{N} \sum_{j=1}^{6} \frac{\alpha'}{4R_0^2} (\mathbf{R}_{ij} \cdot \mathbf{R}_{ij} - R_0^2)^2$$

$$R_0 = \sqrt{3} r_0 .$$

over second neighbors ,

$$\phi_3 = \sum_{i=1}^{N} \sum_{j=1}^{2} \sum_{k=j+1}^{3} \frac{\beta}{r_0^2} \left(\mathbf{r}_{ij} \cdot \mathbf{r}_{ik} + \frac{1}{2} r_0^2 \right)^2$$

i_k: Nearest neighbors of atom i

over first neighbors .

Classical potentials for Carbon materials

- Simple «old» potentials
- **Molecular Mechanics potentials**
- Bond Order Potentials (BOPs)
- ReaxFF potentials
- Machine learning potentials

Molecular Mechanics (MM) potential

General Form

Bond stretching

Bond angle bending

$$E = \sum_{bonds} K_b(b - b_0)^2 + \sum_{angles} K_\theta(\theta - \theta_0)^2$$

$$+ \sum_{dihedrals} K_{\phi,n}[1 + \cos(n\phi - \delta_n)]$$

$$+ \sum_{impropers} K_\phi(\phi - \phi_0)^2 + \sum_{i \neq j} \left(\frac{q_i q_j}{r_{ij}}\right) + E_{LJ}.$$

Dihedral angles contribution

Improper angles contribution

Charge contribution

Interatomic contribution

Classical potentials for Carbon materials

- Simple «old» potentials
- **Molecular Mechanics potentials**
- Bond Order Potentials (BOPs)
- ReaxFF potentials
- Machine learning potentials

Valence Force Field MM Potential
(for tetrahedrally coordinated systems)

$$\Phi = \phi_2 + \phi_3 + \phi_4 = \sum_{i<j} U_{ij} + \sum_{i<j<k} W_{ijk} + \sum_{i<j<k<l} Z_{ijkl} ,$$

$$U_{ij} = \frac{1}{4} f_r (\Delta r_{ij})^2 ,$$

$$W_{ijk} = \frac{1}{2} r_0^2 f_\theta (\Delta\theta_{jik})^2 + f_{rr} \Delta r_{ij} \Delta r_{ik} + r_0 f_{r\theta} (\Delta r_{ij} + \Delta r_{ik}) \Delta\theta_{jik} ,$$

$$Z_{ijkl} = r_0^2 f_{\theta\theta} (\Delta\theta_{jik} \Delta\theta_{kil} + \Delta\theta_{kil} \Delta\theta_{lij} + \Delta\theta_{lij} \Delta\theta_{jik}) .$$

D. W. Bullett, *J. Phys. C: Solid State Phys.* **8**, 3108 (1975).
M. J. P. Musgrave and J. A. Pople, *Proc. R. Soc. A* **268**, 474 (1962).

Classical potentials for Carbon materials

- Simple «old» potentials
- **Molecular Mechanics potentials**
- Bond Order Potentials (BOPs)
- ReaxFF potentials
- Machine learning potentials

$$\Phi = V_{\text{intra}} + V_{\text{inter}} + V_{\text{wall}} ,$$

$$V_{\text{intra}} = V_{\text{Morse}} + V_{\text{bend}} + V_{\text{wag}} + V_{\text{torsion}} + V_{\text{L-J}} ,$$

$$V_{\text{inter}} = V_{\text{RDX-Xe}} + V_{\text{Xe-Xe}} ,$$

$$V_{\text{wall}} = \sum_i \frac{A\rho_i^2}{R^2} e^{-b(R-\rho_i)} ,$$

$\sigma_{ij} = (\sigma_i + \sigma_j)/2$, $\varepsilon_{ij} = (\varepsilon_i\varepsilon_j)^{1/2}$.

$V_{\text{RDX-Xe}}$ and $V_{\text{Xe-Xe}}$ potentials are represented by $V_{\text{L-J}}$

Wallis et al MM Potential

(for hexahydro-l,3,5-trinitro-l,3,5-triazine (RDX))

RDX potential (C, N, O, H - Xe)

$$V_{\text{Morse}} = \sum_{i=1}^{21} D_{e,i}[1 - e^{-\alpha_i(r_i - r_i^0)}]^2 \quad \text{(bond stretching)} ,$$

$$V_{\text{bend}} = \sum_{i=1}^{36} \frac{1}{2} k_b(\theta_i - \theta_i^0)^2 \quad \text{(bending angles)} ,$$

$$V_{\text{wag}} = \sum_{i=1}^{3} \frac{1}{2} k_\gamma(\gamma_i - \gamma_i^0)^2 \quad \text{(wagging angles)} ,$$

$$V_{\text{torsion}} = \sum_{i=1}^{9} \sum_{j=0}^{2} a_j \cos(j\tau_i) \quad \text{(torsional angles)} ,$$

$$V_{\text{L-J}} = \sum_i \sum_j 4\epsilon \left[\left(\frac{\sigma_{ij}}{r_{ij}} \right)^{12} - \left(\frac{\sigma_{ij}}{r_{ij}} \right)^{6} \right] \quad \text{(nonbonded)} .$$

E. P. Wallis and D. L. Thompson, *J. Chem. Phys.* **99**, 2661 (1993).

Classical potentials for Carbon materials

- Simple «old» potentials
- **Molecular Mechanics potentials**
- Bond Order Potentials (BOPs)
- ReaxFF potentials
- Machine learning potentials

Fthenakis et al MM Potential
(for graphene and sp^2 Carbon systems)

$$U = U_{str} + U_{bend} + U_{tors}$$

$$V_s(r) = D[e^{-a(r-r_0)} - 1]^2,$$

$$V_b(\theta) = \frac{k}{2}\left(\theta - \frac{2\pi}{3}\right)^2 - \frac{k'}{3}\left(\theta - \frac{2\pi}{3}\right)^3,$$

$$V_t(\omega) = \frac{1}{2}V_1[1 + \cos(\omega)] + \frac{1}{2}V_2[1 - \cos(2\omega)],$$

Z. G. Fthenakis et al, *Phys. Chem. Chem. Phys.* **19**, 30925 (2017)

Classical potentials for Carbon materials

- Simple «old» potentials
- **Molecular Mechanics potentials**
- Bond Order Potentials (BOPs)
- ReaxFF potentials
- Machine learning potentials

Other well known general MM potentials

- Assisted Model Building with Energy Refinement (**AMBER**)
- Chemistry at HARvard Macromolecular Mechanics (**CHARM**)
- Optimized Potentials for Liquid Simulations (**OPLS-AA**)
- GROningen Molecular Simulation **(GROMOS)**
- Transferable Potentials for Phase Equilibria (**TraPPE**)

Classical potentials for Carbon materials

- Simple «old» potentials
- Molecular Mechanics potentials
- **Bond Order Potentials (BOPs)**
- ReaxFF potentials
- Machine learning potentials

Abel – Tersoff Bond order potentials (BOPs)

Abell showed that for covalent systems the binding energy E_b can be written as a sum over nearest neighbors in the form

$$E_b = \sum_i \sum_{j\,(>i)} [V^R(r_{ij}) - b_{ij} V^A(r_{ij})].$$

Repulsion term

Bond order between atoms i and j

Attraction term

- V^A and V^R are pair potentials
- b_{ij} includes n-body terms (n>2)
- In a first approximation, $b_{ij} \propto N^{-1/2}$, N = local coordination

Abell G C, *Phys. Rev.* B **31** 6184 (1985)

Classical potentials for Carbon materials

- Simple «old» potentials
- Molecular Mechanics potentials
- **Bond Order Potentials (BOPs)**
- ReaxFF potentials
- Machine learning potentials

Tersoff potential (1st generation BOPs)

$$\Phi_{II} = \phi_{2,3} = \sum_{i<j;k} U_{ij;k} .$$

$$U_{ij;k} = f_c(r_{ij})(Ae^{-\lambda_1 r_{ij}} - B_{ij}e^{-\lambda_2 r_{ij}}) ,$$

$$B_{ij} = B_0 e^{-z_{ij}/b} ,$$

cutoff function

$$f_c(r) = \begin{cases} 1 & \text{for } r < R - D , \\ \frac{1}{2} - \frac{1}{2}\sin\left[\frac{\pi}{2}(r - R)/D\right] & \text{for } R - D < r < R + D , \\ 0 & \text{for } r > R + D . \end{cases}$$

$$z_{ij} = \sum_{k \neq i,j} \left[\frac{w(r_{ik})}{w(r_{ij})}\right]^n \times \left[c + e^{-d\cos\theta_{ijk}}\right]^{-1} ,$$

$$w(r) = f_c(r)e^{-\lambda_2 r} ,$$

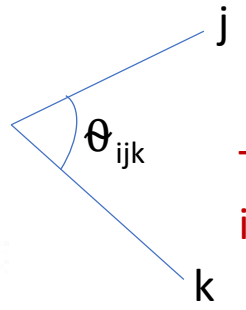

Three body interaction

The simplest potential which includes three body terms initially parametrized for Si (Tersoff J, *Phys. Rev. Lett.* **56,** 632 (1986); Tersoff J, *Phys. Rev.* B **37,** 6991 (1988)), then for C (Tersoff J, *Phys. Rev. Lett.* **61,** 2879 (1988)) and for Si-C and Si-Ge systems (Tersoff J,*Phys. Rev.* B **39** 5566 (1989)).

Classical potentials for Carbon materials

- Simple «old» potentials
- Molecular Mechanics potentials
- **Bond Order Potentials (BOPs)**
- ReaxFF potentials
- Machine learning potentials

Used to study the formation of C_{60}

Similar approaches: **Chelikowsky – Phillips potential**

$$E[\{\mathbf{R}\}] = \sum_{\substack{i,j \\ (i<j)}} [A \exp(-\beta_1 R_{ij}^2)/R_{ij}^2 - g_{ij} \exp(-\beta_2 R_{ij}^2)/R_{ij}]$$

$$g_{ij} = g_0 + g_1 S_{ij} S_{ji}$$

$$S_{ij} = 1 + \langle \cos(3\theta_{ijk}) \rangle$$

$$\langle f(\theta_{ijk}) \rangle = [f]/[1] ,$$

$$[f(\theta_{ijk})] = \sum_{\substack{k \\ k \neq i,j}} f(\theta_{ijk}) \exp(-\lambda_1 \theta_{ijk}^4) \exp(-\lambda_2 R_{ijk}^4)$$

$$R_{ijk} = (R_{ij} + R_{ik})/2.$$

J. R. Chelikowsky, *Phys. Rev. B* **45**, 12062 (1992)

Classical potentials for Carbon materials

- Simple «old» potentials
- Molecular Mechanics potentials
- **Bond Order Potentials (BOPs)**
- ReaxFF potentials
- Machine learning potentials

Similar approaches: **Khor – Das Sarma potential**

(for tetrahedrally bonded C)

$$\Phi = \phi_{2,3} = \sum_{i<j;k} U_{ij;k} \,,$$

$$U_{ij;k} = A f_{ij}(r_{ij})[e^{-\theta r_{ij}} - g_{ij}(1 + h_{ij})] \,,$$

$$f_{ij}(r_{ij}) = e^{-\beta(r_{ij} - R_i)^\tau} \,,$$

$$g_{ij} = \frac{B_0}{Z_i^\alpha} e^{-\lambda r_{ij}} \,,$$

$$Z_i = \sum_j f_{ij}(r_{ij}) \,,$$

$$h_{ij} = \sum_{k \neq i,j} [\cos \eta(\theta_{ijk} - \theta_i) - 1] \,.$$

θ_i = equilibrium angle
θ_{ijk} = angle between bonds ij and ik

K. E. Khor and S. Das Sarma, *Phys. Rev. B* **38**, 3318 (1988)

Classical potentials for Carbon materials

- Simple «old» potentials
- Molecular Mechanics potentials
- **Bond Order Potentials (BOPs)**
- ReaxFF potentials
- Machine learning potentials

Similar approaches: **Takai et al potential**

(for tetrahedrally bonded C)

$$\Phi = \phi_2 + \phi_3 = \sum_{i<j} U_{ij} + \sum_{i<j<k} W_{ijk} ,$$

$$U_{ij} = e^{(q_1 - q_2 r_{ij})} - q_3 \left[\frac{1}{2} - \frac{1}{\pi} \arctan[q_4 (r_{ij} - q_5)] \right]^{12} ,$$

$$W_{ijk} = Z[p + g(\theta_i, \theta_j, \theta_k)] e^{-b^2 (r_{ij}^2 + r_{ik}^2 + r_{jk}^2)} ,$$

$$g(\theta_i, \theta_j, \theta_k) = (\cos\theta_i + h)(\cos\theta_j + h)(\cos\theta_k + h) .$$

T. Takai, C. Lee, T. Hahcioglu, and W. A. Tiller, *J. Phys. Chem.* **94**, 4480 (1990)

Classical potentials for Carbon materials

- Simple «old» potentials
- Molecular Mechanics potentials
- **Bond Order Potentials (BOPs)**
- ReaxFF potentials
- Machine learning potentials

Brenner potential (improvement of Tersoff)

for carbon and hydrocarbons

- $b_{ij} \longrightarrow \bar{b}_{ij}=(b_{ij}+b_{ji})/2$ + corrections

(to avoid unphysical behavior of Tersoff potential)

- If an sp^2 and an sp^3 atom are bonded, the Tersoff potential treats their bond as an intermediate between a single and a double bond, although the bond is better described as a single bond.
- Non physical description for conjugated and non conjugated bonds.

D.W.Brenner, *Phys. Rev. B* **42**, 9458 (1990)

Brenner potential for carbon and hydrocarbons

General form

$$E_b = \sum_i \sum_{j(>i)} [V^R(r_{ij}) - b_{ij} V^A(r_{ij})].$$

$$V_A(r_{ij}) = f_{ij}(r_{ij}) D_{ij}^{(e)} S_{ij}/(S_{ij}-1) e^{-\sqrt{2S_{ij}}\beta_{ij}(r-R_{ij}^{(e)})}$$

Attraction pair potential

$$V_R(r_{ij}) = f_{ij}(r_{ij}) D_{ij}^{(e)}/(S_{ij}-1) e^{-\sqrt{2S_{ij}}\beta_{ij}(r-R_{ij}^{(e)})}$$

Repulsion pair potential

Number of H atoms bonded to atom i

$$N_i^{(H)} = \sum_{j(=\text{hydrogen})} f_{ij}(r_{ij}),$$

$$N_i^{(C)} = \sum_{j(=\text{carbon})} f_{ij}(r_{ij}),$$

Number of C atoms bonded to atom i

$$f_{ij}(r) = \begin{cases} 1, & r < R_{ij}^{(1)} \\ \left[1+\cos\left(\dfrac{\pi(r-R_{ij}^{(1)})}{(R_{ij}^{(2)}-R_{ij}^{(1)})}\right)\right]/2, & R_{ij}^{(1)} < r < R_{ij}^{(2)} \\ 0, & r > R_{ij}^{(2)}. \end{cases}$$

Cutoff function
(1st n.n. restriction)

$$N_{ij}^{\text{conj}} = 1 + \sum_{\text{carbons } k(\neq i,j)} f_{ik}(r_{ik}) F(x_{ik}) + \sum_{\text{carbons } l(\neq i,j)} f_{jl}(r_{jl}) F(x_{jl})$$

$$\bar{B}_{ij} = (B_{ij} + B_{ji})/2 + F_{ij}(N_i^{(t)}, N_j^{(t)}, N_{ij}^{\text{conj}})$$

Average bond order form + corrections

$$B_{ij} = \left[1 + \sum_{k(\neq i,j)} G_i(\theta_{ijk}) f_{ik}(r_{ik}) e^{\alpha_{ijk}[(r_{ij}-R_{ij}^{(e)})-(r_{ik}-R_{ik}^{(e)})]} + H_{ij}(N_i^{(H)}, N_i^{(C)})\right]^{-\delta_i}$$

Bond order

Angle between bonds ij and ik

$$G_C(\theta) = a_0\{1 + c_0^2/d_0^2 - c_0^2/[d_0^2 + (1+\cos\theta)^2]\}$$

for Carbon

$$F(x_{ik}) = \begin{cases} 1, & x_{ik} \le 2 \\ \{1+\cos[\pi(x_{ik}-2)]\}/2, & 2 < x_{ik} < 3 \\ 0, & x_{ik} \ge 3 \end{cases}$$

$$x_{ik} = N_k^{\text{tot}} - f_{ik}(r_{ik})$$

D.W.Brenner, *Phys. Rev. B* **42**, 9458 (1990)

Brenner potential for carbon and hydrocarbons

General form

$$E_b = \sum_i \sum_{j(>i)} [V^R(r_{ij}) - b_{ij} V^A(r_{ij})].$$

- For making the potential continuous, **H_{ij}** and **F_{ij}** are selected as two and three dimensional **cubic splines** to interpolate between values at discrete number of neighbors.
- Two different parametrizations have been determined:
  - **Brenner I**
  - **Brenner II**
- Also a third parametrization without the correction b_{ij}, F_{ij} and H_{ij} occurs (Brenner, in *Atomic Scale Calculations in Materials Science*, **vol. 141,** MRS Symposia Proc. (1989) p.59

Number of H atoms bonded to atom i

$$N_i^{(H)} = \sum_{j(=\text{hydrogen})} f_{ij}(r_{ij}),$$

$$N_i^{(C)} = \sum_{j(=\text{carbon})} f_{ij}(r_{ij}),$$

Number of C atoms bonded to atom i

$$\bar{B}_{ij} = (B_{ij} + B_{ji})/2 + F_{ij}(N_i^{(t)}, N_j^{(t)}, N_{ij}^{\text{conj}})$$ Average bond order form + corrections

$$N_{ij}^{\text{conj}} = 1 + \sum_{\text{carbons } k(\neq i,j)} f_{ik}(r_{ik}) F(x_{ik}) + \sum_{\text{carbons } l(\neq i,j)} f_{jl}(r_{jl}) F(x_{jl})$$

$$B_{ij} = \left[1 + \sum_{k(\neq i,j)} G_i(\theta_{ijk}) f_{ik}(r_{ik}) e^{\alpha_{ijk}[(r_{ij} - R_{ij}^{(e)}) - (r_{ik} - R_{ik}^{(e)})]} + H_{ij}(N_i^{(H)}, N_i^{(C)})\right]^{-\delta_i}$$ Bond order

Angle between bonds ij and ik

$$G_C(\theta) = a_0\{1 + c_0^2/d_0^2 - c_0^2/[d_0^2 + (1+\cos\theta)^2]\}$$ for Carbon

$$F(x_{ik}) = \begin{cases} 1, & x_{ik} \le 2 \\ \{1 + \cos[\pi(x_{ik} - 2)]\}/2, & 2 < x_{ik} < 3 \\ 0, & x_{ik} \ge 3 \end{cases}$$

$$x_{ik} = N_k^{\text{tot}} - f_{ik}(r_{ik})$$

D.W.Brenner, *Phys. Rev. B* **42**, 9458 (1990)

Classical potentials for Carbon materials

- Simple «old» potentials
- Molecular Mechanics potentials
- **Bond Order Potentials (BOPs)**
- ReaxFF potentials
- Machine learning potentials

Reactive empirical bond order (REBO) potential

(improvement of Brenner – Second generation of BOPs)

for carbon and hydrocarbons

- It allows for covalent bond breaking and forming
- Fitted to describe intramolecular bonding

$$E_b = \sum_i \sum_{j(>i)} [V^R(r_{ij}) - b_{ij} V^A(r_{ij})].$$

$$V^R(r) = f^c(r)(1 + Q/r)Ae^{-\alpha r} \qquad V^A(r) = f^c(r) \sum_{n=1,3} B_n e^{-\beta_n r}$$

Cutoff function

$$f_{ij}^c(r) = \begin{cases} 1 & r < D_{ij}^{\min} \\ [1 + \cos((r - D_{ij}^{\min})/(D_{ij}^{\max} - D_{ij}^{\min}))]/2 & D_{ij}^{\min} < r < D_{ij}^{\max} \\ 0 & r > D_{ij}^{\max} \end{cases}$$

Bond order: $\overline{b}_{ij} = \frac{1}{2}[b_{ij}^{\sigma-\pi} + b_{ji}^{\sigma-\pi}] + b_{ij}^{\pi}$

Contributions from **sigma-pi** and **pi** bonds

D.W.Brenner, *Phys. Rev. B* **42**, 9458 (1990)

Reactive empirical bond order (REBO) potential (Second generation of BOPs)

$$\overline{b}_{ij} = \tfrac{1}{2}[b_{ij}^{\sigma-\pi} + b_{ji}^{\sigma-\pi}] + b_{ij}^{\pi}.$$

Number of H and C atoms bonded to atom i

$$b_{ij}^{\sigma-\pi} = \left[1 + \sum_{k\,(\neq i,j)} f_{ik}^{c}(r_{ik}) G(\cos(\theta_{ijk})) e^{\lambda_{ijk}} + P_{ij}(N_i^{C}, N_i^{H})\right]^{-1/2}.$$

P_{ij} is a bicubic spline

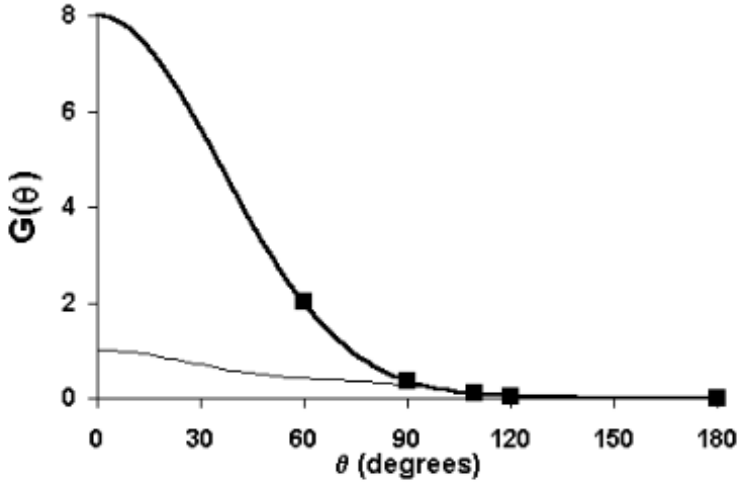

Figure 3. The angular contribution to the bond order equation (8). Squares: fitting data derived from the discrete bond order values. Heavy curve: spline fit to the data. Light curve: modified form for low-coordination structures.

$$b_{ij}^{\pi} = \Pi_{ij}^{\mathrm{RC}} + b_{ij}^{\mathrm{DH}}.$$

$$\pi_{ij}^{\mathrm{RC}} = F_{ij}(N_i^t, N_j^t, N_{ij}^{\mathrm{conj}})$$

$$b_{ij}^{\mathrm{DH}} = T_{ij}(N_i^t, N_j^t, N_{ij}^{\mathrm{conj}}) \left[\sum_{k\,(\neq i,j)} \sum_{l\,(\neq i,j)} (1 - \cos^2(\Theta_{ijkl})) f_{ik}^{c}(r_{ik}) f_{jl}^{c}(r_{jl})\right]$$

$\Theta_{ijkl} = \boldsymbol{e}_{jik} \boldsymbol{e}_{ijl}.$

Dihedral angle

$\boldsymbol{e}_{jik}$ and $\boldsymbol{e}_{ijl}$ are unit vectors in the directions $\boldsymbol{R}_{ij} \times \boldsymbol{R}_{jl}$, and $\boldsymbol{R}_{ji} \times \boldsymbol{R}_{ik}$ respectively

Classical potentials for Carbon materials

- Simple «old» potentials
- Molecular Mechanics potentials
- **Bond Order Potentials (BOPs)**
- ReaxFF potentials
- Machine learning potentials

Other (REBO) potentials

For C, Si, H

- K. Beardmore and R. Smith, *Philos. Mag. A* **74**, 1439 (1996)
- A. J. Dyson and P. V. Smith, *Surf. Sci.* **355**, 140 (1996)

For C, O, H

- B.Ni, K. H. Lee and S.B.Sinnott, *J. Phys. Cond. Matter* **16**, 7261 (2004)
- A. F. Fonseca et al, *Phys. Rev. B* **84**, 075460 (2011)

For C, F, H

- I. Jang and S. b. Sinnott, *J. Phys. Chem. B* **108**, 18993 (2004)

Classical potentials for Carbon materials

- Simple «old» potentials
- Molecular Mechanics potentials
- **Bond Order Potentials (BOPs)**
- ReaxFF potentials
- Machine learning potentials

Adaptive Intermolecular Reactive Empirical Bond Order (AIREBO) potentials

REBO: - Good to describe intramolecular interactions
- NOT good to describe **intermolecular** interactions

AIREBO: **Covers that gap**
- Intermolecular interactions include dispersion and short range repulsion effects
- Dispersion and intermolecular repulsion:

$$V_{ij}^{\mathrm{LJ}}(r_{ij}) = 4\epsilon_{ij}\left[\left(\frac{\sigma_{ij}}{r_{ij}}\right)^{12} - \left(\frac{\sigma_{ij}}{r_{ij}}\right)^{6}\right].$$

Classical potentials for Carbon materials

- Simple «old» potentials
- Molecular Mechanics potentials
- Bond Order Potentials (BOPs)
- **ReaxFF potentials**
- Machine learning potentials

A. C. T. van Duin, S. Dasgupta, F. Lorant and W. A. Goddard, J. Phys. Chem. A **105**, 9396 (2001)

- **ReaxFF potentials:**

General form: that of Molecular Mechanics Potentials + Bond Order

$$E^{tot} = E^{bond} + E^{over} + E^{angle} + E^{tor} + E^{vdw} + E^{Coulomb} + E^{specific}.$$

- E^{bond} assumes that the bond-order is determined directly from the interatomic distance and valence
- E^{over} (over-coordination term): penalties when the coordination number is outside the range of the ideal valence
- $E^{Coulomb}$: Coulomb interactions. ReaxFF utilizes the electronegativity equalization method to distribute charges in atoms
- $E^{specific}$: System-specific terms not usually included
- Parameters are fitted from quantum MD simulations

Primary advantage: Ability to model reactive chemistry with low computational cost

Classical potentials for Carbon materials

- Simple «old» potentials
- Molecular Mechanics potentials
- Bond Order Potentials (BOPs)
- **ReaxFF potentials**
- Machine learning potentials

Available ReaxFF potentials for C:

• RDX	for RDX explosives (C/H/O/N)
• CHO-2008	for combustion of hydrocarbons (C/H/O)
• Budzien et al	LAMMPS database (C/H/O/N)
• Mattsson et al	LAMMPS database (C/H/O)
• CHON-2010	for soot particles and their interactions with molecules (C/H/O/N/S/Si/Pt/Zr/Ni/Cu/Co/He/Ne/Ar/Kr/Xe)
• Lg	(low gradient) – RDX improvement (C/H/O/N)
• ci-CH	(charge implicit) – for hydrocarbons (C/H)
• C-2013	for carbon condensed phases
• CHO-2016	improvement of CHO-2008, including information from C-2013 (C/H/O)
• CHON-2019	improvement of CHO-2016 including nitrogen interactions (C/H/O/N)
• GR-RDX-2021	developed by us combining RDX and C-2013 potentials (Cg/C/H/O/N, Cg = graphene carbon)

Combining the two ReaxFF (RDX and C-2013) to develop a new potential

- **RDX**:
  - C-C, C-H, C-N, C-O, H-H, H-N, H-O, N-N, N-O and O-O interactions.
  - Not good for graphene
- **C-2013**:
  - C-C interactions in condensed carbon phases.

Assumption No 1: C atoms of graphene will be considered as atoms of a **new species (Cg),** which will be described by C-C interactions of C-2013 potential.

Interactions:

- C-C, C-H, C-N, C-O, H-H, H-N, H-O, N-N, N-O, O-O described by RDX ReaxFF
- Cg-Cg described by C-2013 ReaxFF
- Cg-C, Cg-H, Cg-O, Cg-N described by ?

Assumption No 2: Cg-C, Cg-H, Cg-O and Cg-N interactions will be the same as the interactions between C-C, C-H, C-O and C-N interactions, respectively, (i.e. they will be described by RDX ReaxFF).

… but what about the *general parameters* of the combined potential ?

Combining the two ReaxFF (RDX and C-2013) to develop a new potential

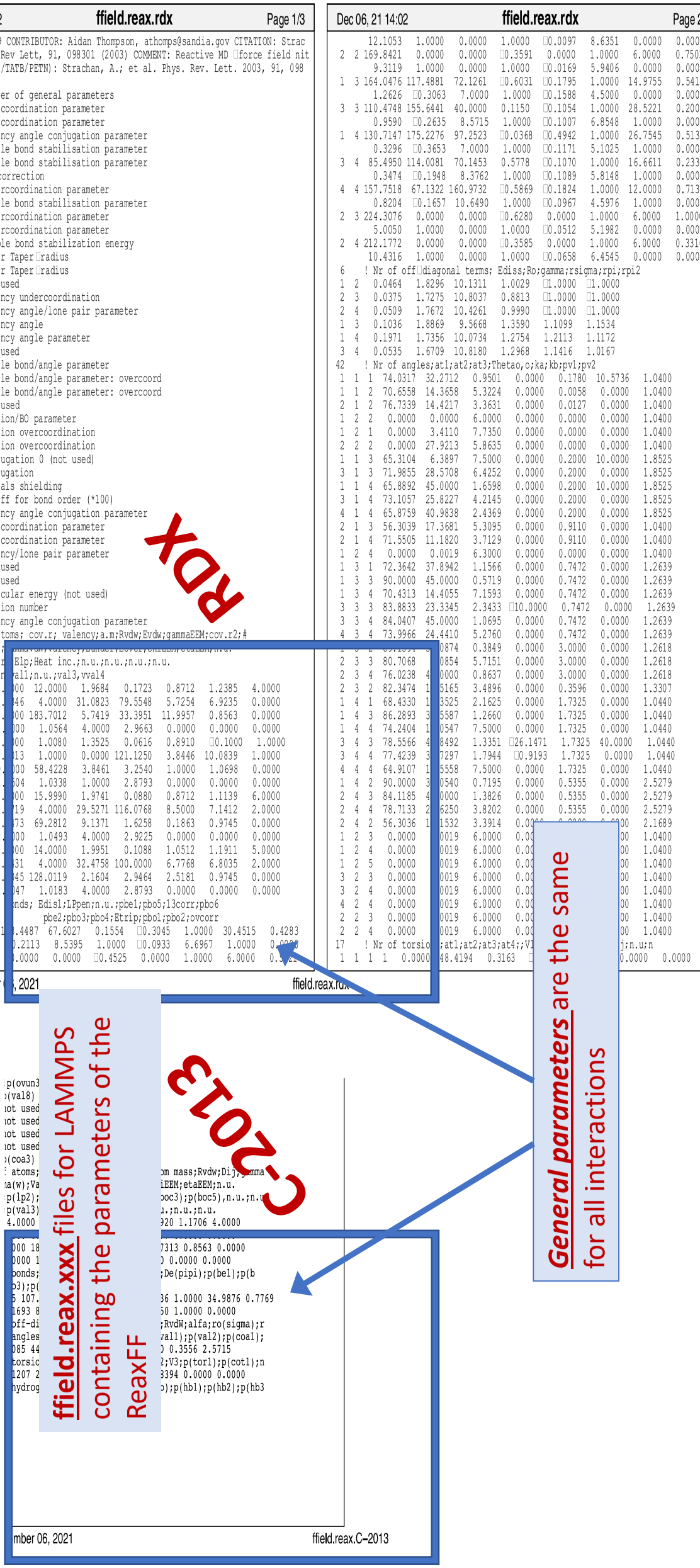

Combining the two ReaxFF (RDX and C-2013) to develop a new potential

C-2013

RDX

```
 0 !Cutoff for bond order (*100)
 6 !Valency angle conjugation parameter
 1 !Overcoordination parameter
 1 !Overcoordination parameter
 3 !Valency/lone pair parameter
 0 !Not used
 0 !Not used
 0 !Molecular energy (not used)
 0 !Version number
 0 !Valency angle conjugation parameter
Nr of atoms; cov.r; valency;a.m;Rvdw;Evdw;
   alfa;gammavdW;valency;Eunder;Eover;chiE
    cov r3;Elp;Heat inc.;n.u.;n.u.;n.u.;n.u
     ov/un;val1;n.u.;val3,val4
742    4.0000   12.0000    1.9684    0.1723
606    2.1346    4.0000   31.0823   79.5548
104    0.0000  183.7012    5.7419   33.3951
983    2.5000    1.0564    4.0000    2.9663    0.0000    0.0000
867    1.0000    1.0080    1.3525    0.0616    0.8910   -0.1000    1.0000
858    5.0013    1.0000    0.0000  121.1250    3.8446   10.0839    1.0000
000    0.0000   58.4228    3.8461    3.2540    1.0000    1.0698    0.0000
683    2.1504    1.0338    1.0000    2.8793    0.0000    0.0000    0.0000
142    2.0000   15.9990    1.9741    0.0880    0.8712    1.1139    6.0000
186    7.7719    4.0000   29.5271  116.0768    8.5000    7.1412    2.0000
909   14.9473   69.2812    9.1371    1.6258    0.1863    0.9745    0.0000
965    2.5000    1.0493    4.0000    2.9225    0.0000    0.0000    0.0000
450    3.0000   14.0000    1.9951    0.1088    1.0512    1.1911    5.0000
303    7.8431    4.0000   32.4758  100.0000    6.7768    6.8035    2.0000
636    0.1045  128.0119    2.1604    2.9464    2.5181    0.9745    0.0000
959    0.0047    1.0183    4.0000    2.8793    0.0000    0.0000    0.0000
   ir of bonds; Edis1;LPpen;n.u.;pbe1;pbo5;13corr;pbo6
                pbe2;pbo3;pbo4;Etrip;pbo1;pbo2;ovcorr
1.  3.0  113.4487   67.6027    0.1554   -0.3045    1.0000   30.4515    0.4283
0.0801   -0.2113    8.5395    1.0000   -0.0933    6.6967    1.0000    0.0000
3.6889    0.0000    0.0000   -0.4525    0.0000    1.0000    6.0000    0.5921
```

The general parameters of the two potentials are NOT the same…

… however,…
… assumption No 3

```
 3  1  4  73.1057  25.822
 4  1  4  65.8759  40.983
 2  1  3  56.3039  17.368
 1  2  4   0.0000   0.001
 1  3  1  72.3642  37.894
 1  3  3  90.0000  45.000
 1  3  4  70.4313  14.405
 3  3  3  83.8833  23.334
 3  3  4  84.0407  45.000
 4  3  4  73.9966  24.441
 1  3  2  89.1394  37.087
 2  3  3  80.7068   5.085
 2  3  4  76.0238  45.000
 2  3  2  82.3474  13.516
 1  4  1  68.4330  19.352
 1  4  3  86.2893  37.558
 1  4  4  74.2404  12.054
 3  4  3  78.5566  43.849
 3  4  4  77.4239  33.729
 4  4  4  64.9107  17.555
 1  4  2  90.0000  32.054
 2  4  3  84.1185  45.000
 2  4  4  78.7133  24.625
 2  4  2  56.3036  14.153
 1  2  3   0.0000   0.001
 1  2  4   0.0000   0.001
 1  2  5   0.0000   0.001
 3  2  3   0.0000   0.001
 3  2  4   0.0000   0.001
 4  2  4   0.0000   0.001
 2  2  3   0.0000   0.001
 2  2  4   0.0000   0.001
17    ! Nr of torsions;at
 1  1  1   0.0000  48.
```

Combining the two ReaxFF (RDX and C-2013) to develop a new potential

- **RDX**:
  - C-C, C-H, C-N, C-O, H-H, H-N, H-O, N-N, N-O and O-O interactions.
  - Not good for graphene
- **C-2013**:
  - C-C interactions in condensed carbon phases.

Assumption No 1: C atoms of graphene will be considered as atoms of a new species (Cg), which will be described by C-C interactions of C-2013 potential.

Interactions:

- C-C, C-H, C-N, C-O, H-H, H-N, H-O, N-N, N-O, O-O described by RDX ReaxFF
- Cg-Cg described by C-2013 ReaxFF
- Cg-C, Cg-H, Cg-O, Cg-N described by ?

Assumption No 2: Cg-C, Cg-H, Cg-O and Cg-N interactions will be the same as the interactions between C-C, C-H, C-O and C-N interactions, respectively, (i.e. they will be described by RDX ReaxFF).

Assumption No 3: The new potential will have the parameters of the RDX potential, hoping that it will provide reasonable predictions.

Advantages and disadvantages of the new potential

- The potential has to be tested…
- Different type of C atoms specialized in different bonding environments may provide more accurate predictions. This might improve transferability.
- In principle, Cg and C atoms should not interchange their roles during the simulations.

We call the new potential GR-RDX-2021 potential.

Studied structures and properties

- **Graph**
  - Stru
  - Mec
    stra
  - Resp
  - Pho
  - Ener
    Wal
  - Ener
    mol

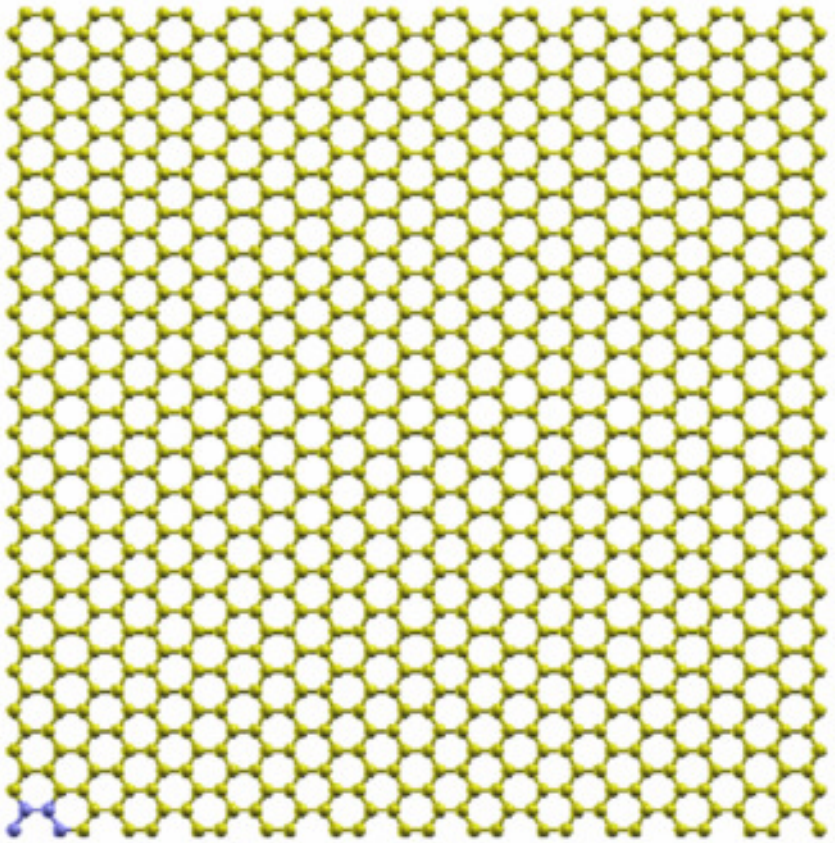

graphene

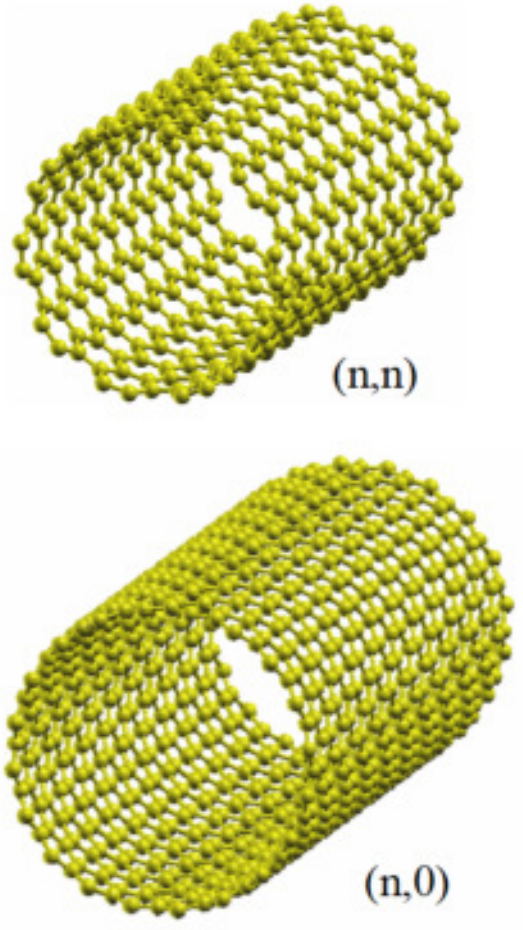

carbon nantotubes

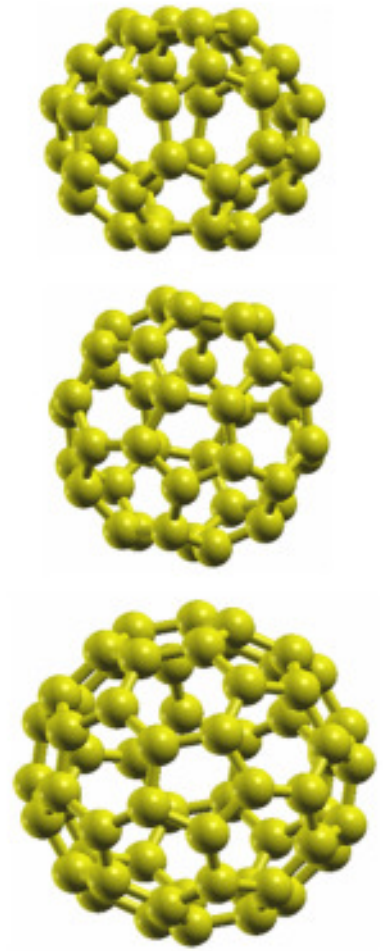

fullerenes

s
axial
:
with
n
erene

Testing the performance of ReaxFF for graphene - Optimization

Cohesive Energy U_{coh}
and
Bond Length a_0

12x21 supercell of
1008 atoms

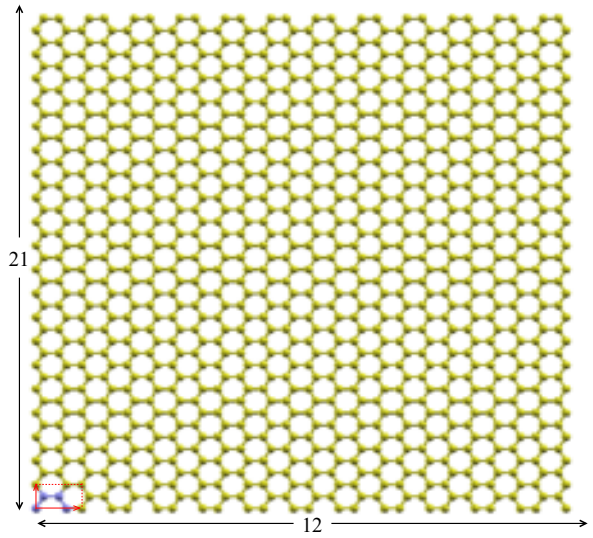

Potential	U_{coh} (eV/atom)	a_0 (Å)
Mattsson et al	-8.912227	1.48495
RDX	-8.681633	1.45003
lg	-8.773100	1.44998
Budzien et al	-8.527977	1.44761
CHO-2008	-8.479561	1.44385
CHON-2010	-8.479561	1.44385
ci-CH	**-8.423060**	**1.43777**
ci-CH (2nd min)	**-8.411486**	**1.45497**
GR-RDX-2021	-7.431757	1.42183
C-2013	-7.434825	1.42159
CHO-2016	-7.404626	1.41991
CHON-2019	-7.404626	1.41991
Expimental or ab-initio	-7.464	1.424 – 1.429

Planar and periodic

Interestingly **two** minima were found for ci-CH potential

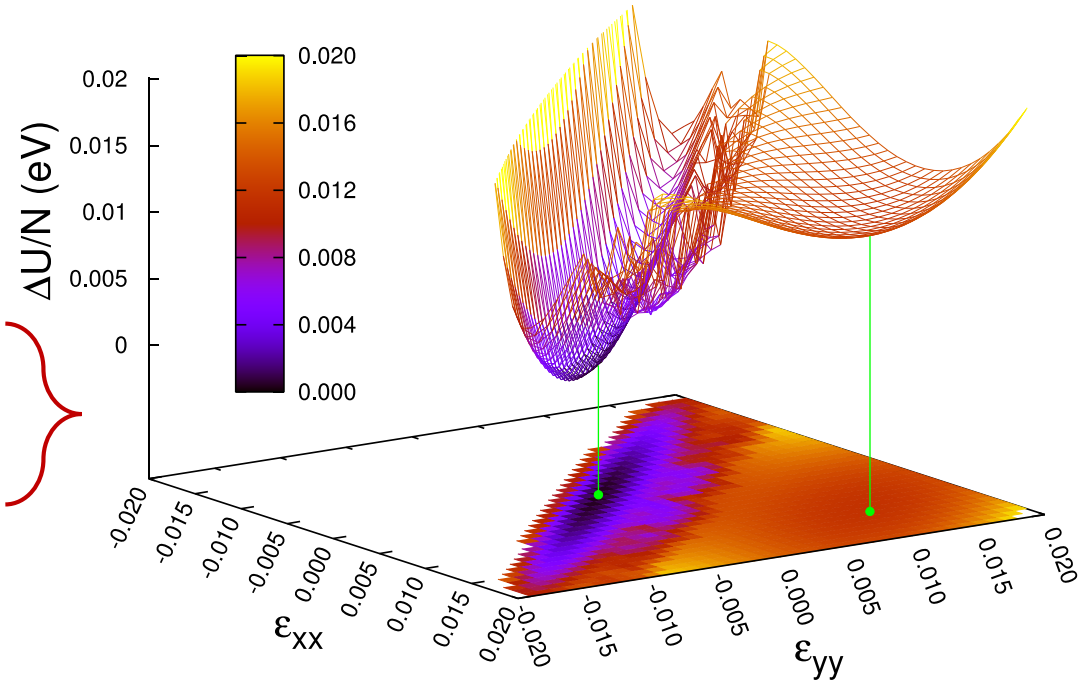

δU_{coh} = 0.012 eV

Testing the performance of ReaxFF for graphene - Optimization

Cohesive Energy U_{coh}
and
Bond Length a_0

12x21 supercell of
1008 atoms

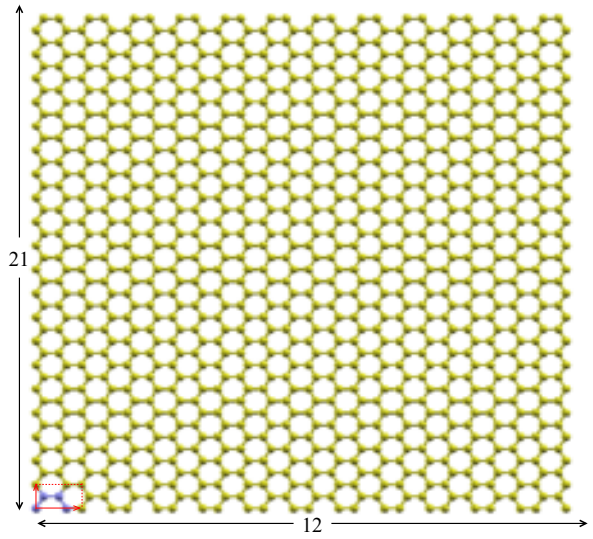

Potential	U_{coh} (eV/atom)	a_0 (Å)
Mattsson et al	-8.912227	1.48495
RDX	-8.681633	1.45003
lg	-8.773100	1.44998
Budzien et al	-8.527977	1.44761
CHO-2008	-8.479561	1.44385
CHON-2010	-8.479561	1.44385
ci-CH	-8.423060	1.43777
ci-CH (2nd min)	-8.411486	1.45497
GR-RDX-2021	-7.431757	1.42183
C-2013	-7.434825	1.42159
CHO-2016	-7.404626	1.41991
CHON-2019	-7.404626	1.41991
Expimental or ab-initio	-7.464	1.424 – 1.429

Group A
-8.41 - -8.91 eV

Group B
-7.40 - -7.43 eV

Testing the performance of ReaxFF for graphene - Optimization

Cohesive Energy U_{coh}
and
Bond Length a_0

12x21 supercell of
1008 atoms

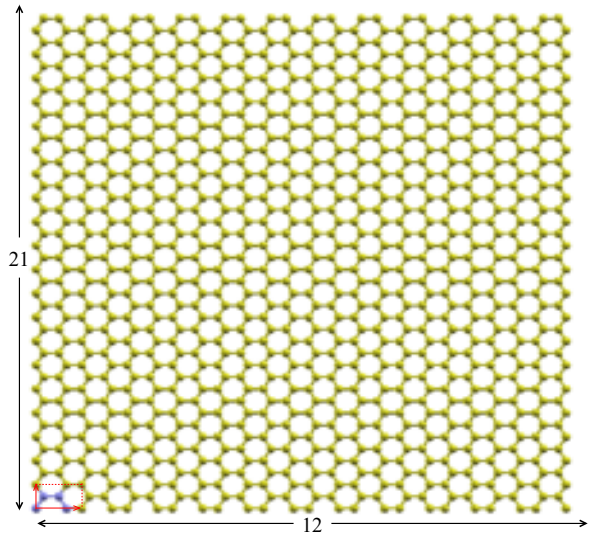

Potential	U_{coh} (eV/atom)	a_0 (Å)
Mattsson et al	-8.912227	1.48495
RDX	-8.681633	1.45003
lg	-8.773100	1.44998
Budzien et al	-8.527977	1.44761
CHO-2008	-8.479561	1.44385
CHON-2010	-8.479561	1.44385
ci-CH	-8.423060	1.43777
ci-CH (2nd min)	-8.411486	1.45497
GR-RDX-2021	-7.431757	1.42183
C-2013	-7.434825	1.42159
CHO-2016	-7.404626	1.41991
CHON-2019	-7.404626	1.41991
Expimental or ab-initio	-7.464	1.424 – 1.429

Group A
1.44 – 1.48 Å

Group B
1.42 Å

Testing the performance of ReaxFF for graphene
Calculation of Young's modulus E and Poisson's ratio ν

Strain along x (arm chair) direction

$\sigma_{yy}=0,\ \varepsilon_{xx} > 0$

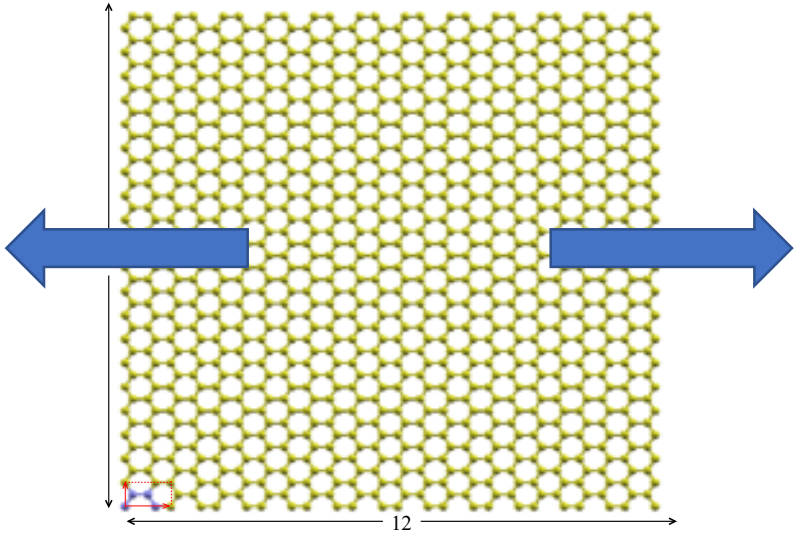

Strain along y (zig-zag) direction

$\sigma_{xx}=0,\ \varepsilon_{yy} > 0$

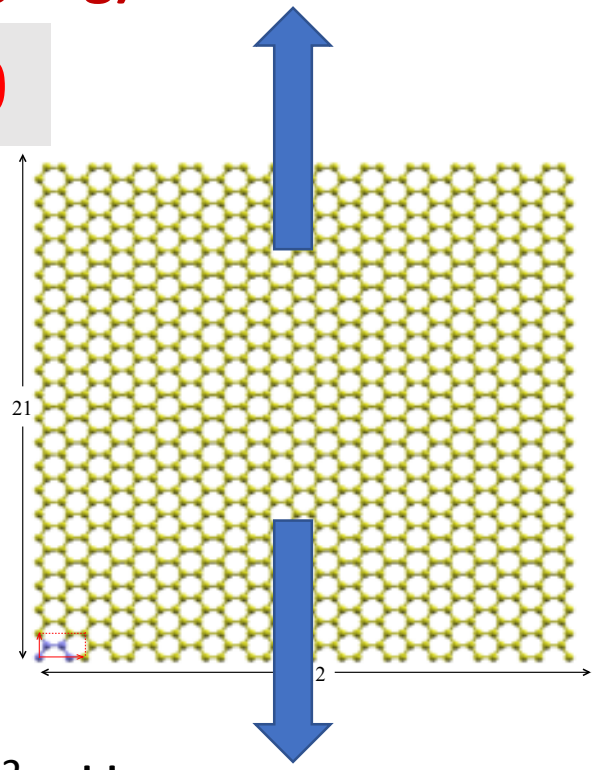

Energy	$U(\varepsilon_{xx}) = k_x\varepsilon_{xx}^2 + U_0$	$U(\varepsilon_{yy}) = k_y\varepsilon_{yy}^2 + U_0$
Young's modulus	$E_x = \sigma_{xx}/\varepsilon_{xx} = 2k_x/V$	$E_x = \sigma_{xx}/\varepsilon_{xx} = 2k_x/V$
Poisson's ratio	$\nu_x = -\varepsilon_{yy}/\varepsilon_{xx}$	$\nu_y = -\varepsilon_{xx}/\varepsilon_{yy}$
Unit cell Volume	$V=L_xL_yd_0$, d_0 = 3.34 Å	$V=L_xL_yd_0$, d_0 = 3.34 Å

Testing the performance of ReaxFF for graphene
Calculation of Young's modulus E and Poisson's ratio ν

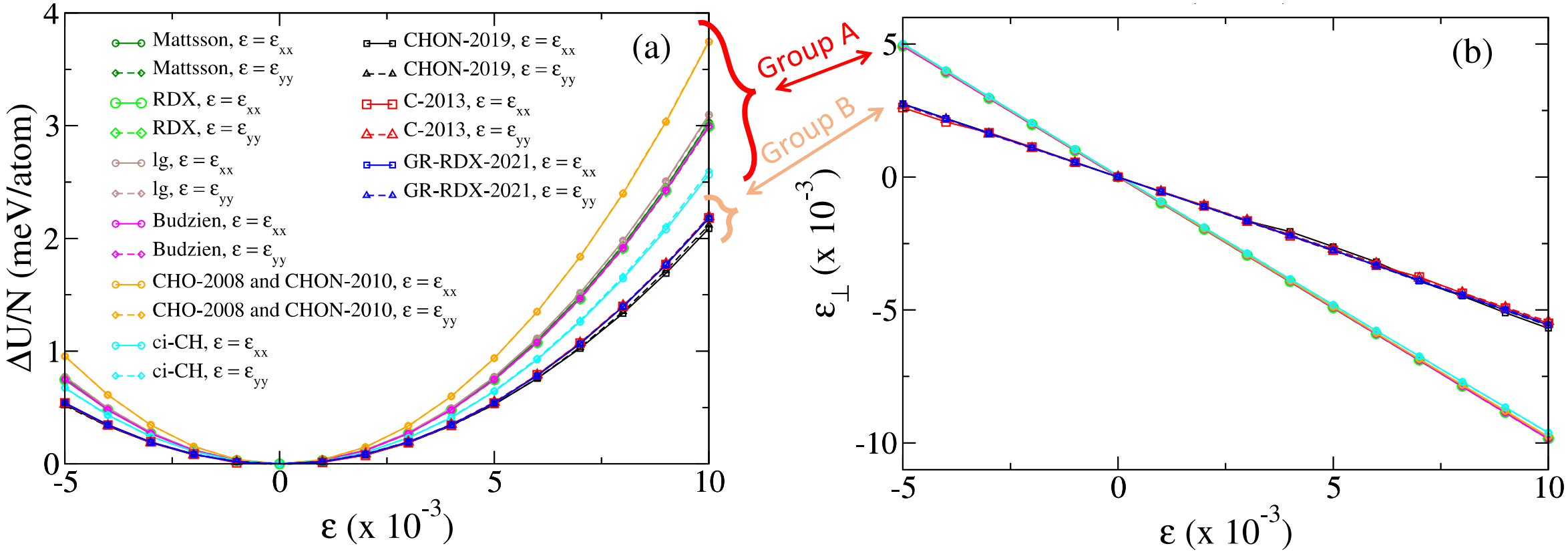

- Isotropic behavior (all potentials)
- Young's modulus: 3 values from Group A > 1 value from Group B
- Poisson's ratio: Same value for Group A > Same value from Group B

Testing the performance of ReaxFF for graphene

Young's modulus E
and
Poisson's ratio ν

12x21 supercell of
1008 atoms

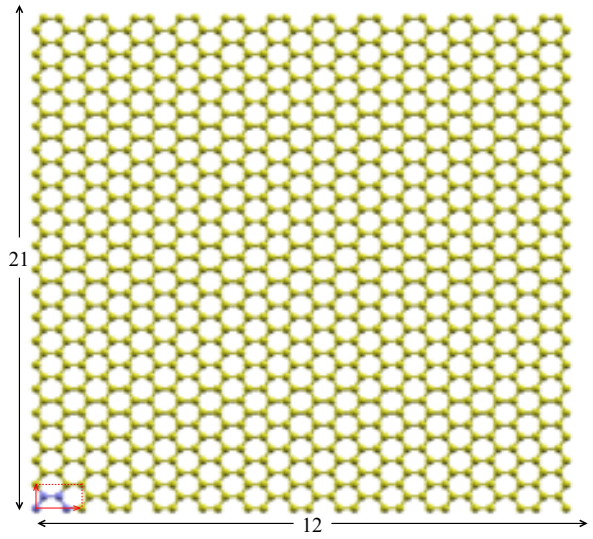

Potential	U_{coh} (eV/atom)	a_0 (Å)	E_x/E_y (GPa)	ν_x/ν_y
Mattsson et al	-8.912227	1.48495	1014/1016	0.987/0.987
RDX	-8.681633	1.45003	1051/1048	0.984/0.
lg	-8.773100	1.44998	1087/1084	0.983/0.
Budzien et al	-8.527977	1.44761	1060/1056	0.984/0.
CHO-2008	-8.479561	1.44385	1331/1334	0.983/0.
CHON-2010	-8.479561	1.44385	1331/1334	0.983/0
ci-CH	-8.423060	1.43777	926/936	0.975/0.976
ci-CH (2nd min)	-8.411486	1.45497	821/819	0.753/0.746
GR-RDX-2021	-7.431757	1.42183	795/797	0.550/0.550
C-2013	-7.434825	1.42159	801/795	0.537/0.
CHO-2016	-7.404626	1.41991	765/772	0.543/0.
CHON-2019	-7.404626	1.41991	765/772	0.543/0.554
Expimental or ab-initio	-7.464	1.424 – 1.429	1020 - 1092	0.125 – 0.18

Group A
E ≈ 1000-1100 GPa
or ≈ 1300 GPa
or ≈ 930 GPa

Group B
E ≈ 760-800 GPa

Testing the performance of ReaxFF for graphene

Young's modulus E
and
Poisson's ratio ν

12x21 supercell of
1008 atoms

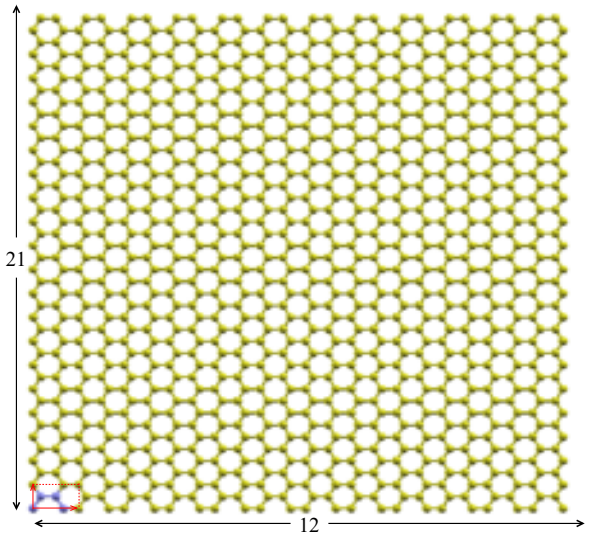

Potential	U_{coh} (eV/atom)	a_0 (Å)	E_x/E_y (GPa)	ν_x/ν_y
Mattsson et al	-8.912227	1.48495	1014/1016	0.987/0.987
RDX	-8.681633	1.45003	1051/1048	0.984/0.984
lg	-8.773100	1.44998	1087/1084	0.983/0.984
Budzien et al	-8.527977	1.44761	1060/1056	0.984/0.986
CHO-2008	-8.479561	1.44385	1331/1334	0.983/0.983
CHON-2010	-8.479561	1.44385	1331/1334	0.983/0.983
ci-CH	-8.423060	1.43777	926/936	0.975/0.976
ci-CH (2nd min)	-8.411486	1.45497	821/819	0.753/0.746
GR-RDX-2021	-7.431757	1.42183	795/797	0.550/0.550
C-2013	-7.434825	1.42159	801/795	0.537/0.540
CHO-2016	-7.404626	1.41991	765/772	0.543/0.554
CHON-2019	-7.404626	1.41991	765/772	0.543/0.554
Expimental or ab-initio	-7.464	1.424 – 1.429	1020 - 1092	0.125 – 0.18

Group A
ν = 0.98-0.99
≈ 1 !!!
Unreliable

Group B
ν = 0.54-0.55

Testing the performance of ReaxFF for graphene

Elastic constants

c_{11}, c_{12}, c_{66}
and spring constants
k_s and k_b
using the E and ν values

12x21 supercell of
1008 atoms

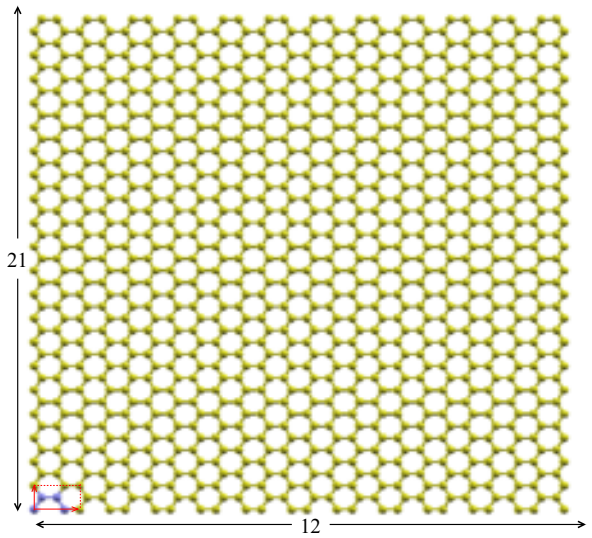

$$c_{11} = c_{22} = \frac{E}{1-\nu^2}$$

$$c_{12} = \lambda^* = \frac{E\nu}{1-\nu^2}$$

$$c_{66} = \mathrm{G} = \mu = \frac{E}{2(1+\nu)}$$

λ^* = First Lamé's coefficient

μ = Second Lamé's coefficient

G = shear modulus

$$\Delta U = \frac{1}{2}\sum_i (k_s\,\delta l_i^2 + \frac{1}{2}\sum_j k_b\,a_0^2\,\delta\phi_{ij}^2)$$

$$E = \frac{8\sqrt{3}}{d_0}\frac{k_s k_b}{k_s+18k_b}$$

$$\nu = \frac{k_s-6k_b}{k_s+18k_b}$$

$$k_s = \sqrt{3}d_0\frac{E}{1-\nu}$$

$$k_b = \frac{d_0}{2\sqrt{3}}\frac{E}{3\nu+1}$$

Testing the performance of ReaxFF for graphene

Elastic constants

c_{11}, c_{12}, c_{66}
and spring constants
k_s and k_b
using the E and ν values

12x21 supercell of
1008 atoms

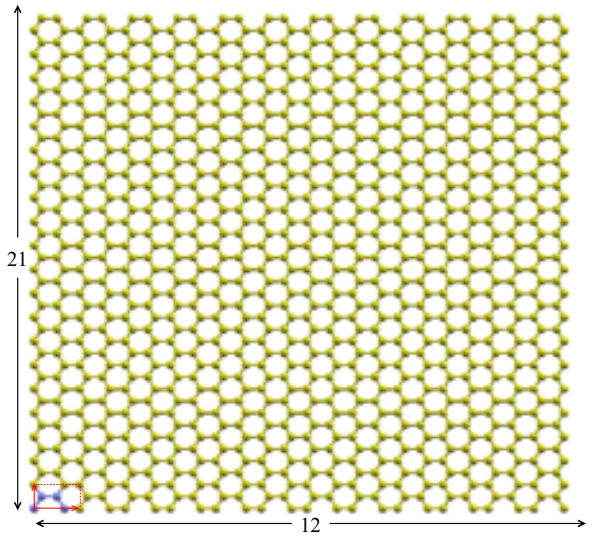

$$c_{11} = c_{22} = \frac{E}{1-\nu^2} \rightarrow \infty$$

$$c_{12} = \lambda^* = \frac{E\nu}{1-\nu^2} \rightarrow \infty$$

For ν =1

$$c_{66} = G = \mu = \frac{E}{2(1+\nu)} \rightarrow E/4$$

$$\Delta U = \frac{1}{2}\sum_i (k_s\, \delta l_i^2 + \frac{1}{2}\sum_j k_b\, a_0^2\, \delta\phi_{ij}^2)$$

$$E = \frac{8\sqrt{3}}{d_0}\frac{k_s k_b}{k_s+18k_b}$$

$$\nu = \frac{k_s-6k_b}{k_s+18k_b}$$

$$k_s = \sqrt{3}d_0\frac{E}{1-\nu} \rightarrow \infty$$

$$k_b = \frac{d_0}{2\sqrt{3}}\frac{E}{3\nu+1} \rightarrow E/4$$

Testing the performance of ReaxFF for graphene

Elastic constants

c_{11}, c_{12}, c_{66}
and spring constants
k_s and k_b
using the E and ν values

12x21 supercell of
1008 atoms

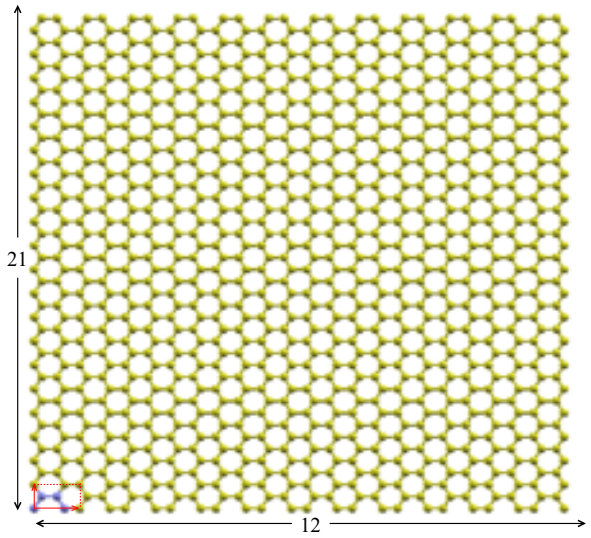

Potential	c_{11} (GPa)	c_{12} (GPa)	c_{66} (GPa)	k_s (eV/Å^2)	k_b (eV/Å^2)
Mattsson et al	38752	38241	255	2884	1.54
RDX	33102	32573	264	2375	1.60
lg	33698	33151	273	2417	1.66
Budzien et al	35407	34874	267	2541	1.61
CHO-2008	40234	39562	336	2885	2.03
CHON-2010	40234	39562	336	2885	2.03
ci-CH	19006	18534	236	1357	1.43
ci-CH (2nd min)	1869	1400	234	118	1.52
GR-RDX-2021	1141	628	257	64.0	1.81
C-2013	1124	605	259	62.5	1.84
CHO-2016	1099	603	248	61.5	1.75
CHON-2019	1099	603	248	61.5	1.75
Expimental or ab-initio	1100	140-180	400-500	45	4.1-4.8

Testing the performance of ReaxFF for graphene

Elastic constants

c_{11}, c_{12}, c_{66}
and spring constants
k_s and k_b
using the E and ν values

Potential	c_{11} (GPa)	c_{12} (GPa)	c_{66} (GPa)	k_s (eV/Å^2)	k_b (eV/Å^2)
Mattsson et al	38752	38241	255	2884	1.54
RDX	33102	32573	264	2375	1.60
lg	33698	33151	273	2417	1.66
Budzien et al	35407	34874	267	2541	1.61
CHO-2008	40234	39562	336	2885	2.03
CHON-2010	40234	39562	336	2885	2.03
ci-CH	19006	18534	236	1357	1.43
ci-CH (2nd min)	1869	1400	234	118	1.52
GR-RDX-2021	1141	628	257	64.0	1.81
C-2013	1124	605	259	62.5	1.84
CHO-2016	1099	603	248	61.5	1.75
CHON-2019	1099	603	248	61.5	1.75
Expimental or ab-initio	**1100**	**140-180**	**400-500**	**45**	**4.1-4.8**

33-40x exper.
unreliable

19x exper.
unreliable

reasonable

12x21 supercell of
1008 atoms

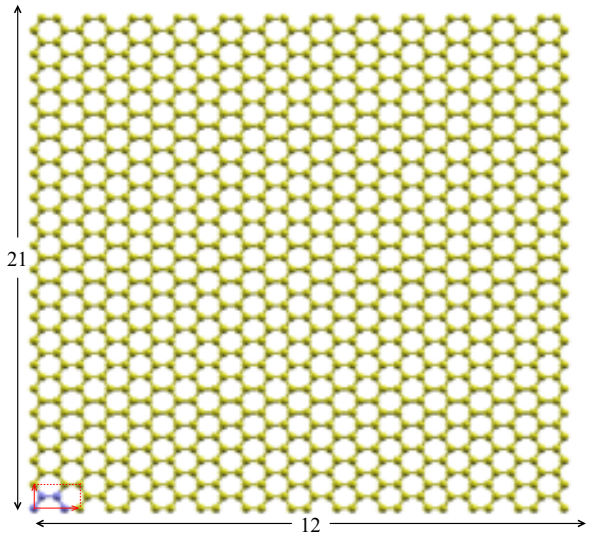

Testing the performance of ReaxFF for graphene

Elastic constants

c_{11}, c_{12}, c_{66}
and spring constants
k_s and k_b
using the E and ν values

12x21 supercell of
1008 atoms

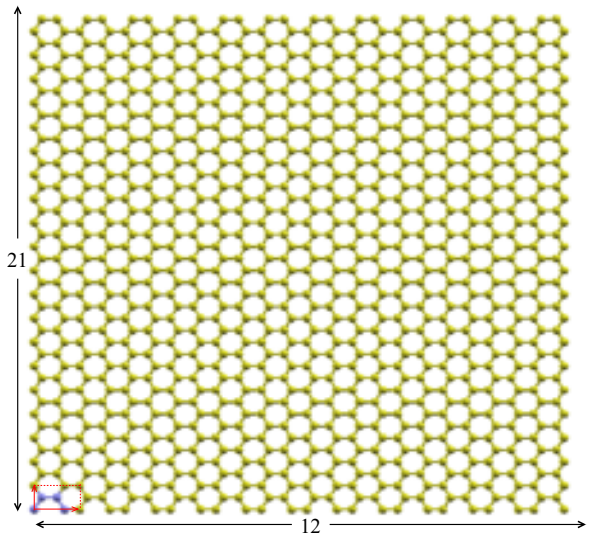

Potential	c_{11} (GPa)	c_{12} (GPa)	c_{66} (GPa)	k_s (eV/Å^2)	k_b (eV/Å^2)
Mattsson et al	38752	38241	255	2884	1.54
RDX	33102	32573	264	2375	1.60
lg	33693	33151	273	2417	1.66
Budzien et al	35407	34874	267	2541	1.61
CHO-2008	40234	39562	336	2885	2.03
CHON-2010	40234	39562	336	2885	2.03
ci-CH	19006	18534	236	1357	1.43
ci-CH (2nd min)	1869	1400	234	118	1.52
GR-RDX-2021	1141	628	257	64.0	1.81
C-2013	1124	605	259	62.5	1.84
CHO-2016	1099	603	248	61.5	1.75
CHON-2019	1099	603	248	61.5	1.75
Expimental or ab-initio	1100	140-180	400-500	45	4.1-4.8

220x exper.
unreliable

100x exper.
unreliable

4x exper.
overestimation

Testing the performance of ReaxFF for graphene

Elastic constants

c_{11}, c_{12}, c_{66}
and spring constants
k_s and k_b
using the E and ν values

12x21 supercell of
1008 atoms

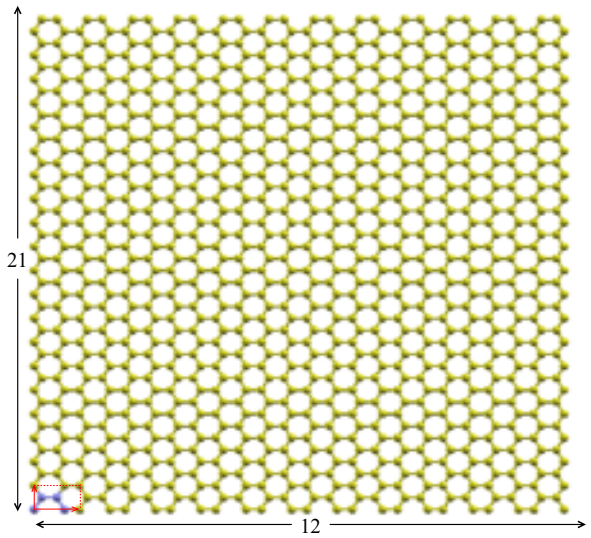

Potential	c_{11} (GPa)	c_{12} (GPa)	c_{66} (GPa)	k_s (eV/Å^2)	k_b (eV/Å^2)
Mattsson et al	38752	38241	255	2884	1.54
RDX	33102	32573	264	2375	1.60
lg	33698	33151	273	2417	1.66
Budzien et al	35407	34874	267	2541	1.61
CHO-2008	40234	39562	336	2885	2.03
CHON-2010	40234	39562	336	2885	2.03
ci-CH	19006	18534	236	1357	1.43
ci-CH (2nd min)	1869	1400	234	118	1.52
GR-RDX-2021	1141	628	257	64.0	1.81
C-2013	1124	605	259	62.5	1.84
CHO-2016	1099	603	248	61.5	1.75
CHON-2019	1099	603	248	61.5	1.75
Expimental or ab-initio	1100	140-180	400-500	45	4.1-4.8

1/2x exper.

A and B group Similar

Underestimation

1/2x exper.

Testing the performance of ReaxFF for graphene

Elastic constants

c_{11}, c_{12}, c_{66}
and spring constants
k_s and k_b
using the E and ν values

12x21 supercell of
1008 atoms

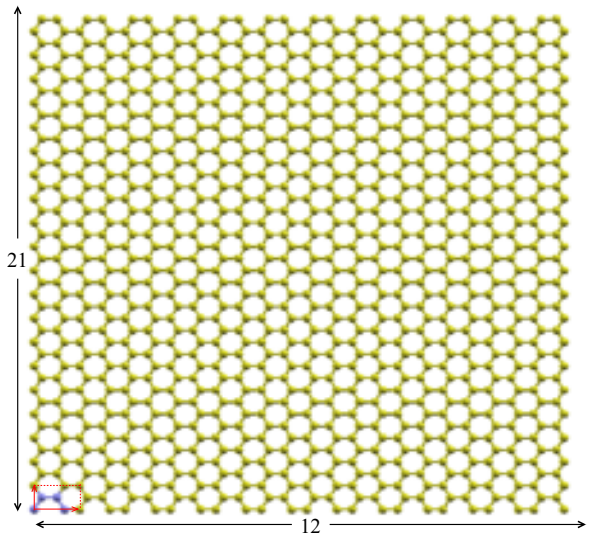

Potential	c_{11} (GPa)	c_{12} (GPa)	c_{66} (GPa)	k_s (eV/Å^2)	k_b (eV/Å^2)
Mattsson et al	38752	38241	255	2884	1.54
RDX	33102	32573	264	2375	1.60
lg	33698	33151	273	2417	1.66
Budzien et al	35407	34874	267	2541	1.61
CHO-2008	40234	39562	336	2885	2.03
CHON-2010	40234	39562	336	2885	2.03
ci-CH	19006	18534	236	1357	1.43
ci-CH (2nd min)	1869	1400	234	118	1.52
GR-RDX-2021	1141	628	257	64.0	1.81
C-2013	1124	605	259	62.5	1.84
CHO-2016	1099	603	248	61.5	1.75
CHON-2019	1099	603	248	61.5	1.75
Expimental or ab-initio	1100	140-180	400-500	45	4.1-4.8

50x exper.
unreliable

27x exper.
unreliable

4/3x exper.
similar

Testing the performance of ReaxFF for graphene

Elastic constants

c_{11}, c_{12}, c_{66}
and spring constants
k_s and k_b
using the E and ν values

12x21 supercell of
1008 atoms

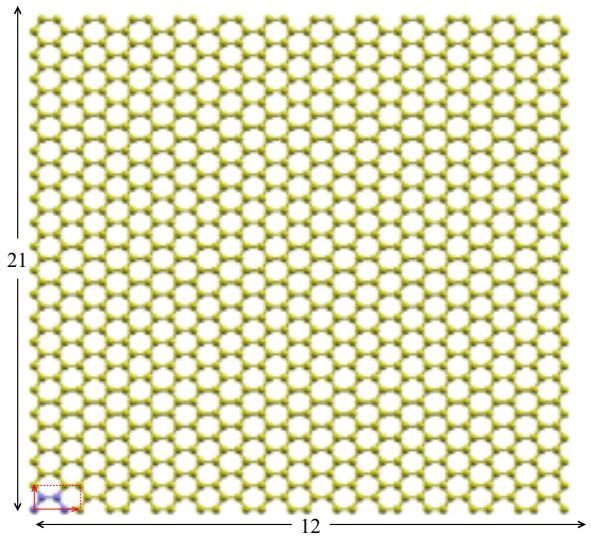

Potential	c_{11} (GPa)	c_{12} (GPa)	c_{66} (GPa)	k_s (eV/Å²)	k_b (eV/Å²)
Mattsson et al	38752	38241	255	2884	1.54
RDX	33102	32573	264	2375	1.60
lg	33698	33151	273	2417	1.66
Budzien et al	35407	34874	267	2541	1.61
CHO-2008	40234	39562	336	2885	2.03
CHON-2010	40234	39562	336	2885	2.03
ci-CH	19006	18534	236	1357	1.43
ci-CH (2nd min)	1869	1400	234	118	1.52
GR-RDX-2021	1141	628	257	64.0	1.81
C-2013	1124	605	259	62.5	1.84
CHO-2016	1099	603	248	61.5	1.75
CHON-2019	1099	603	248	61.5	1.75
Expimental or ab-initio	1100	140-180	400-500	45	4.1-4.8

1/3-1/2x exper.

A and B group Similar

Undrestimation

1/2x exper.

Testing the performance of ReaxFF for graphene

In conclusion:

	Group A	Group B	Experiment or ab-initio
Cohesive Energy (eV/atom)	-8.41 - -8.91	~ -7.4	-7.464
Bond length (Å)	1.44 - 1.48	1.42	1.42 – 1.43
Young's modulus (GPa)	1000 - 1300	760 - 800	1050
Poisson's ratio	0.98 !!!!!	0.54	0.125 – 0.180
c_{11} (GPa)	~ 35000 !!!!!	1100	1050
c_{12} (GPa)	~ 35000 !!!!!	600	150
c_{66} (GPa)	~ 250	~ 250	450
k_s (eV/Å^2)	~ 2500 !!!!!	62	45
k_b (eV/Å^2)	~ 1.8	~ 1.8	4 - 5

12x21 supercell of 1008 atoms

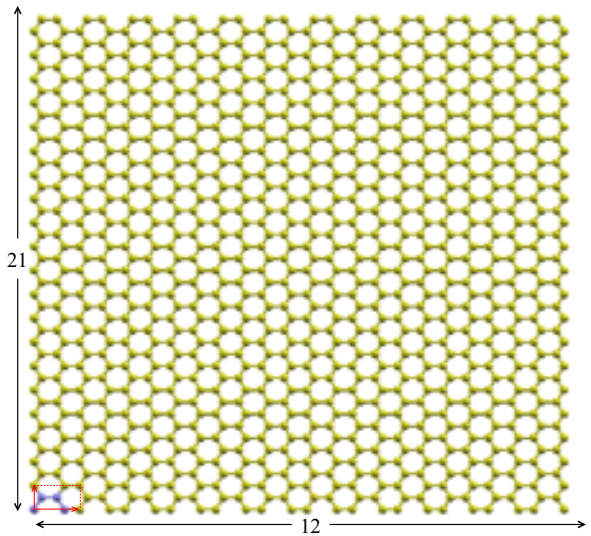

We focus our interest in group B potentials only.

Defective graphene: Stone – Wales (SW) defect and inverse SW defect

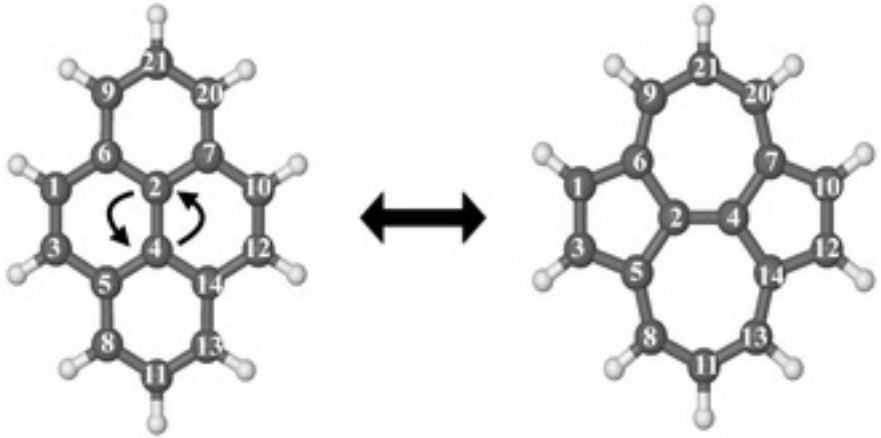

Pyrene (Pristine) **SW-Pyrene (Defect)**

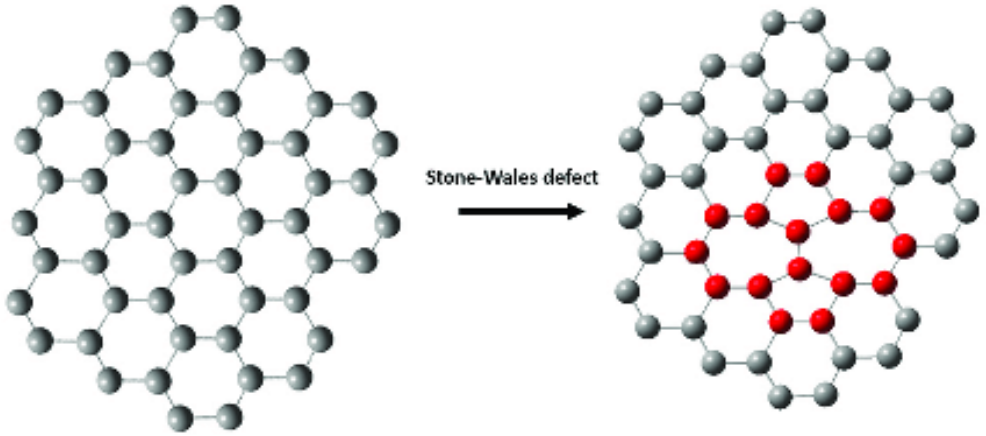

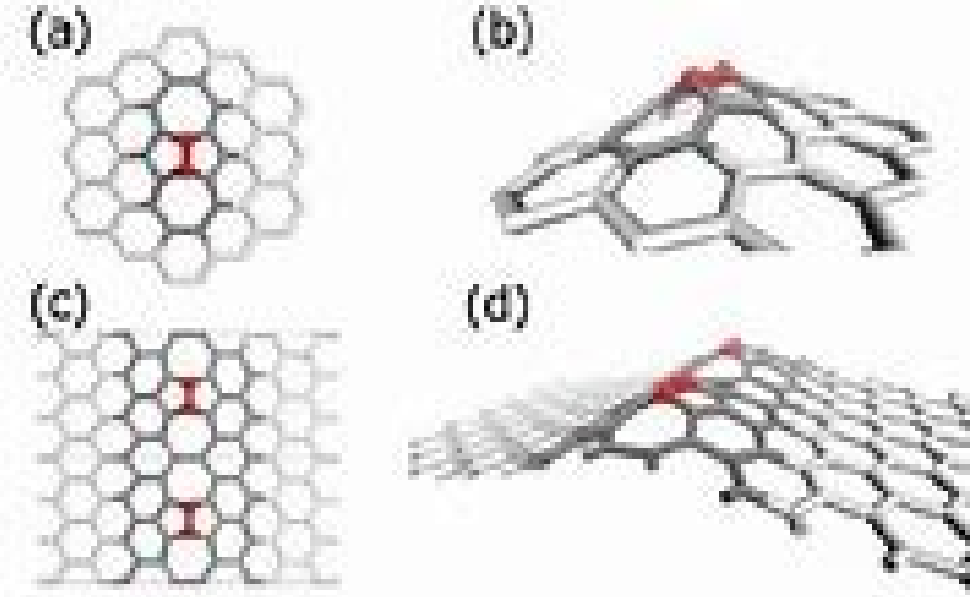

Topological defect: Stone Wales defect *(d=0)*

(AJ Stone and DJ Wales, Chem. Phys. Letters 128 (1986) 501.

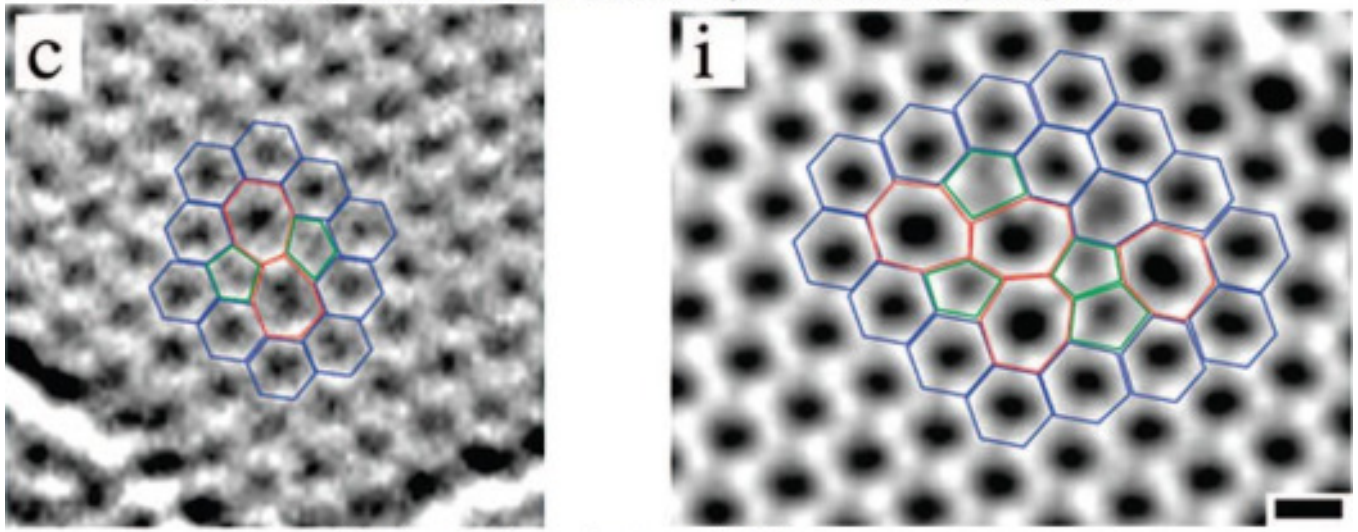

Zettl et al, Nano Letters (2008).

SW and inverse SW formation energy U_f for graphene

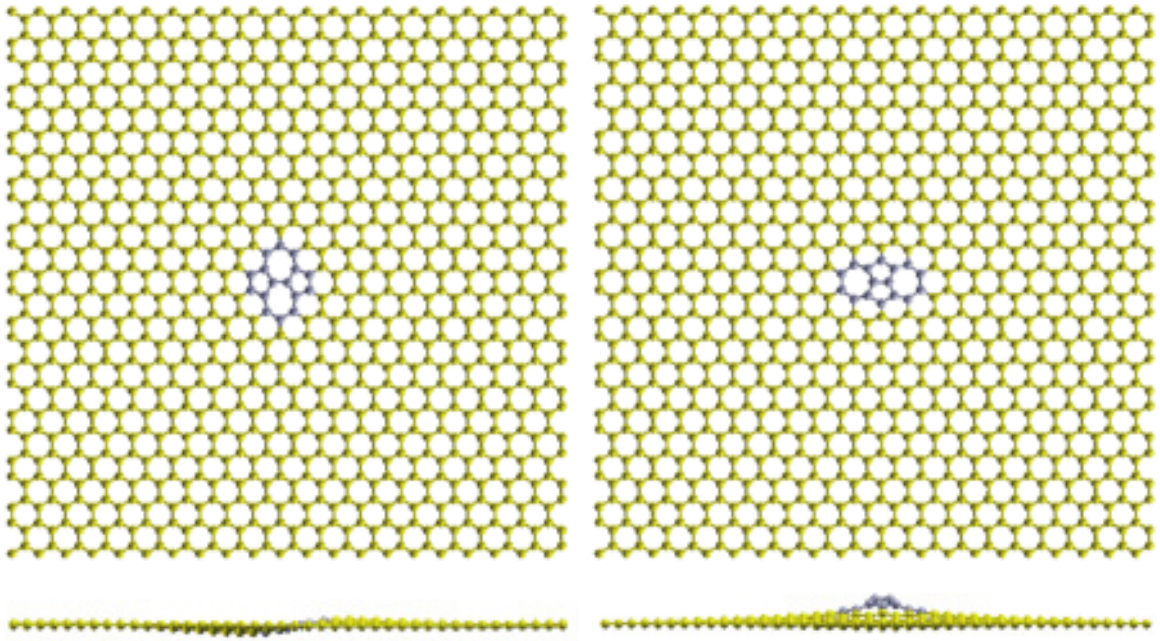

Similar geometries were predicted by DFT calculations

ReaxFF	SW U_f (eV)	inv. SW U_f (eV)
CHON-2019 - planar	3.6184	6.3057
CHON-2019 - not planar	3.5959	4.7356
C-2013 - planar	4.0717	
C-2013 - not planar	3.7809	
GR-RDX-2021 - planar	3.9874	
GR-RDX-2021 - not planar	3.7874	
DFT- GGA/PBE (DMOL)*	5.08	6.20
DFT-GGA/PW91 (CASTEP)**	4.8	

U_f for SW and inverse SW defects underestimated by ≈ 3/4

*Lusk and Carr, *Phys. Rev. Lett.* **100**, 175503 (2008)
**Reich and Robertson, Phys. Rev. B 72, 184109 (2005)

Vacancy formation energy U_f for graphene

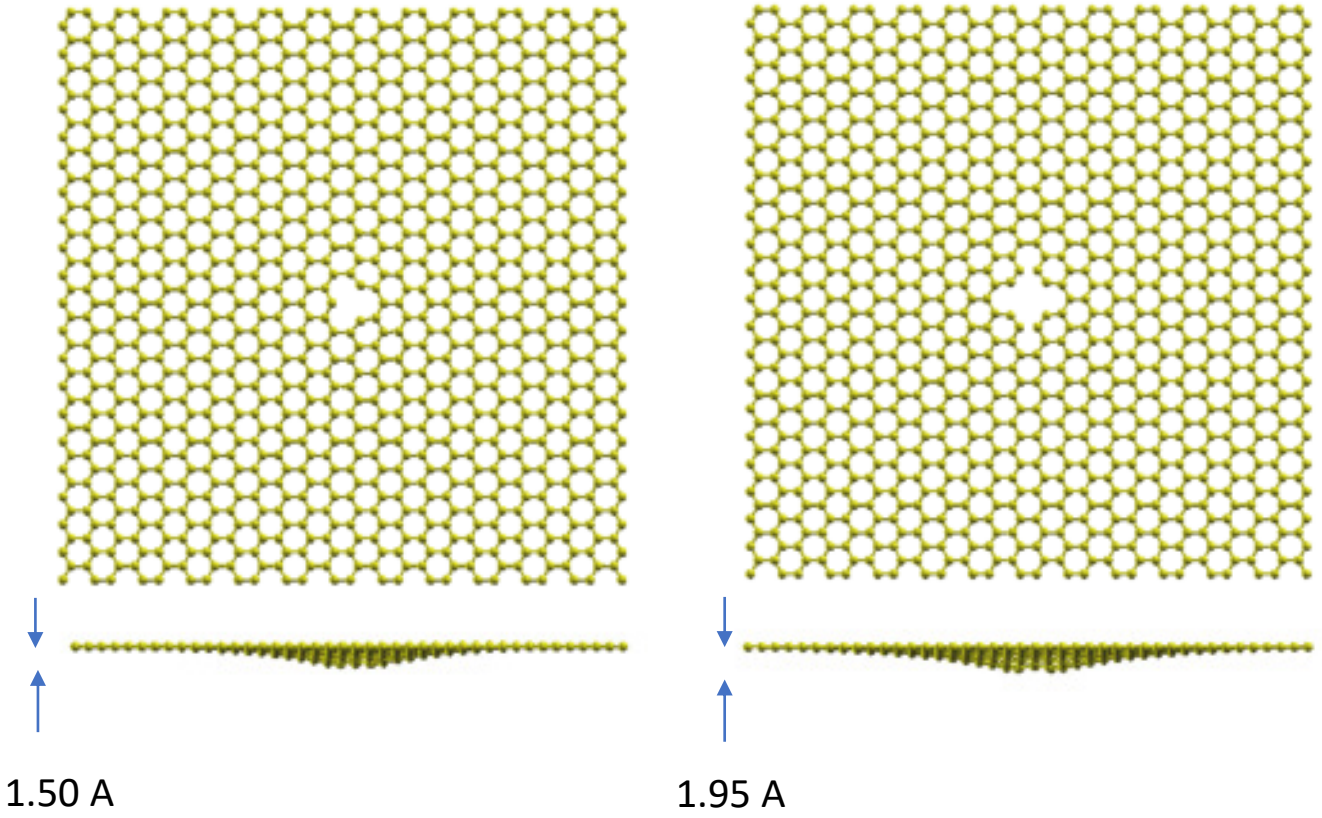

ReaxFF	1-vac. U_f (eV)	2-vac. U_f (eV)
CHON-2019 - planar	9.9013	12.9242
CHON-2019 - not planar	9.4651	12.1489
C-2013		
GR-RDX-2021		
DFT- GGA/PBE (DMOL)*	7.63	8.08
DFT-GGA/PW91 (CASTEP)**	7.6	

Overestimated values

*Lusk and Carr, *Phys. Rev. Lett.* **100**, 175503 (2008)
**Reich and Robertson, Phys. Rev. B 72, 184109 (2005)

Energy barriers for the permeation of CO_2 through pyridinic graphene pores

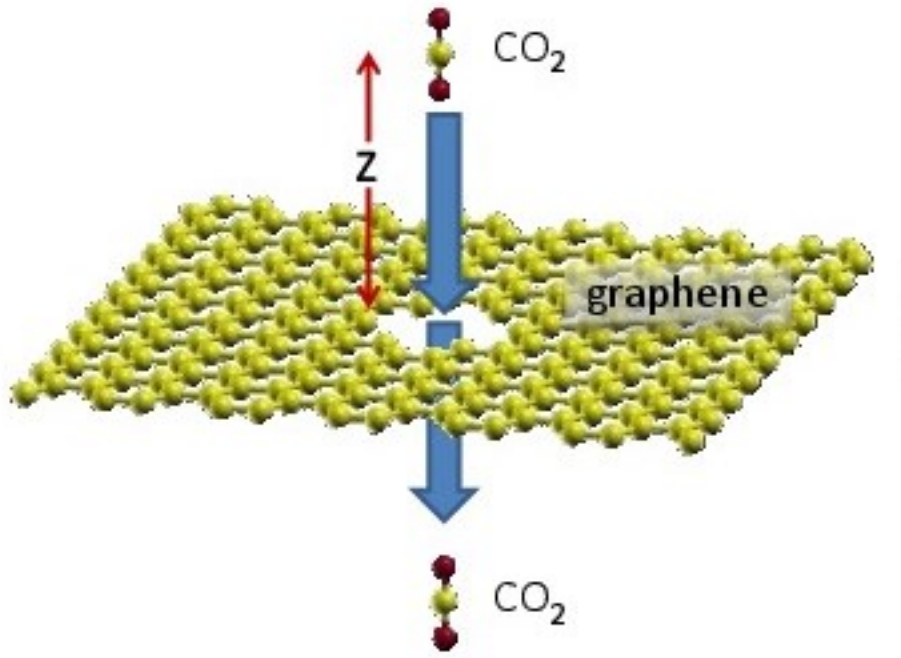

3vac–5N

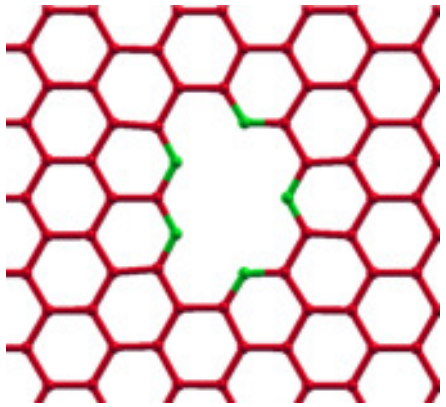

4vac-6N (a)

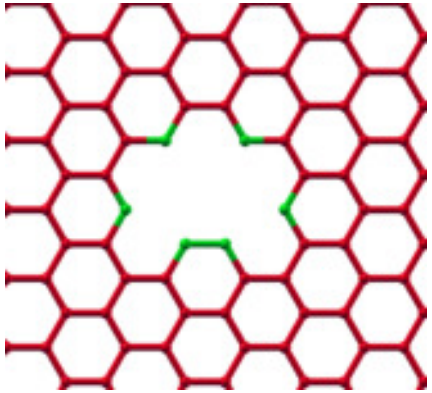

4vac-6N (b)

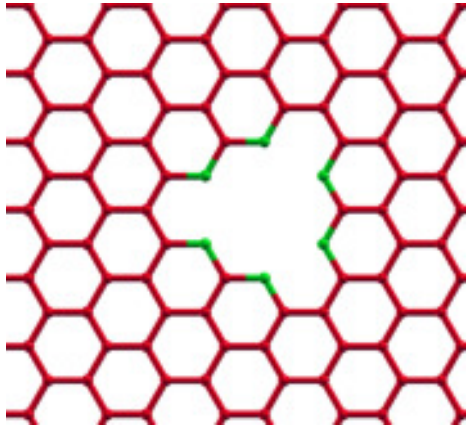

6vac-6N

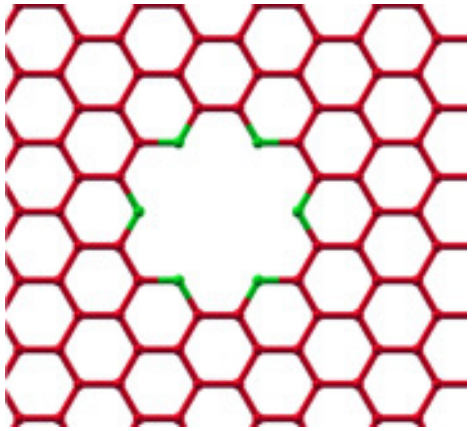

Energy barriers for the permeation of CO_2 through pyridinic graphene pores

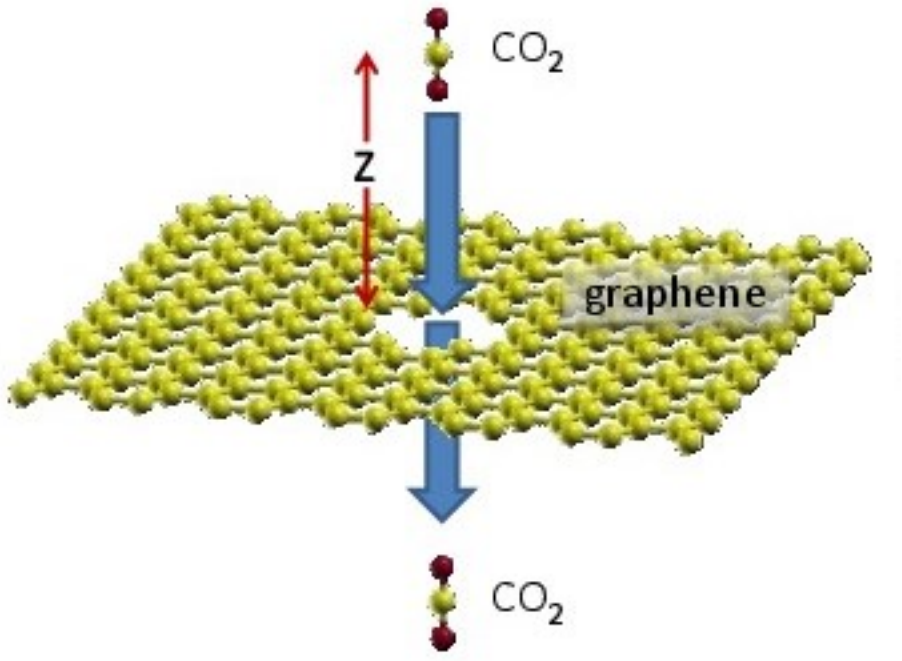

pore	CHON-2019	GR-RDX-2021	DFT
1vac-3 N			
2vac-4N	6.31	5.29	
3vac-5N	1.23	2.21	3.91
4vac-6N (a)	1.21	0.885	
4vac-6N (b)	0.37	0.485	0.54
6vac-6N	0.23	0	0

Energy barriers for the permeation of CO_2 through a pyridinic graphene pore

For the 6vac-6N pore

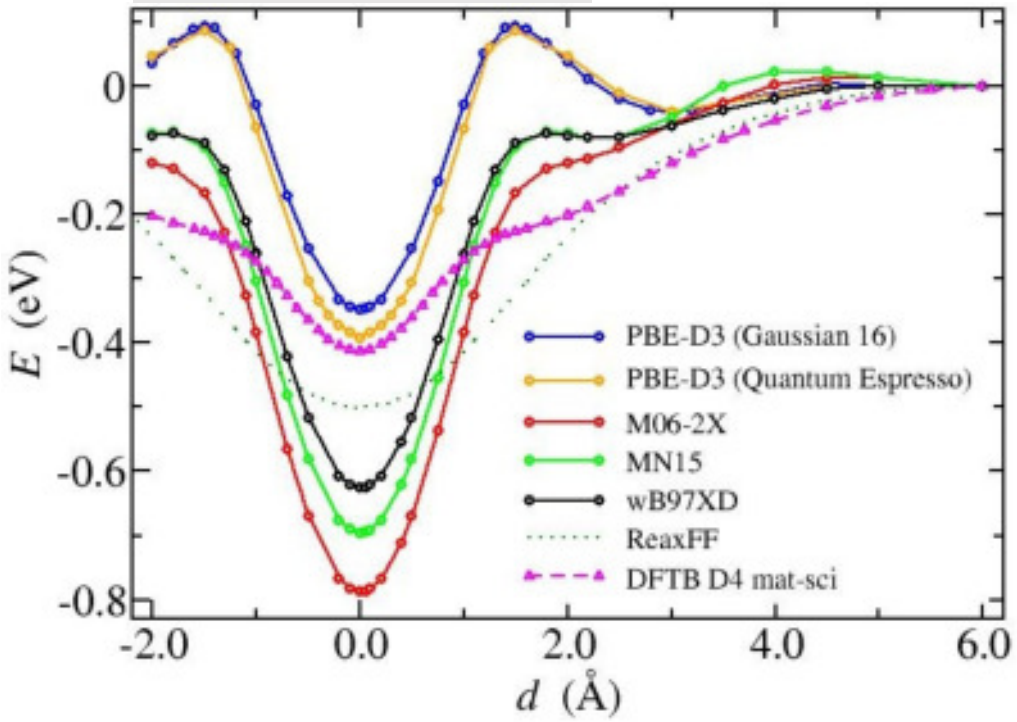

pore	CHON-2019	GR-RDX-2021	DFT
1vac-3 N			
2vac-4N	6.31	5.29	
3vac-5N	1.23	2.21	3.91
4vac-6N (a)	1.21	0.885	
4vac-6N (b)	0.37	0.489	0.54
6vac-6N	0.23	0	0

- Modern functionals: only attraction point (no barrier)
- PBE (small barrier, shallow min)
- Semiempirical/Reax-FF: shallow min, attraction point (no barrier) or small barrier

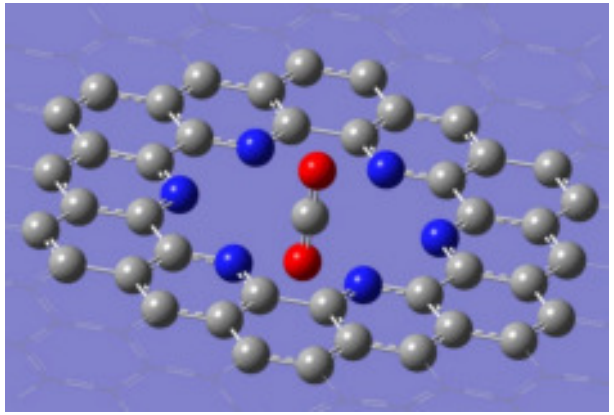

Graphene phonon dispersion relation

- Calculated using a hand made code implementing the **frozen phonon methods**.
- 7x7 hexagonal supercell.
- Atomic displacements in the two centered atoms.
- **δ**x = **δ**y = **δ**z = 0.0001 A

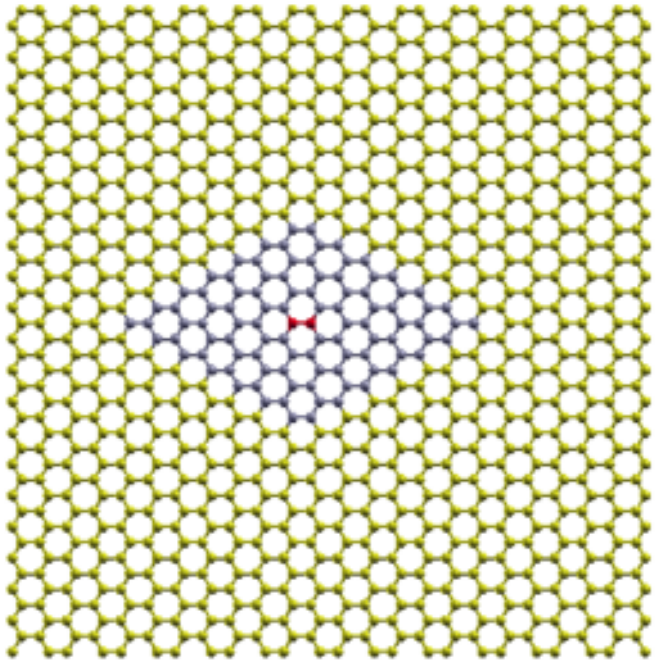

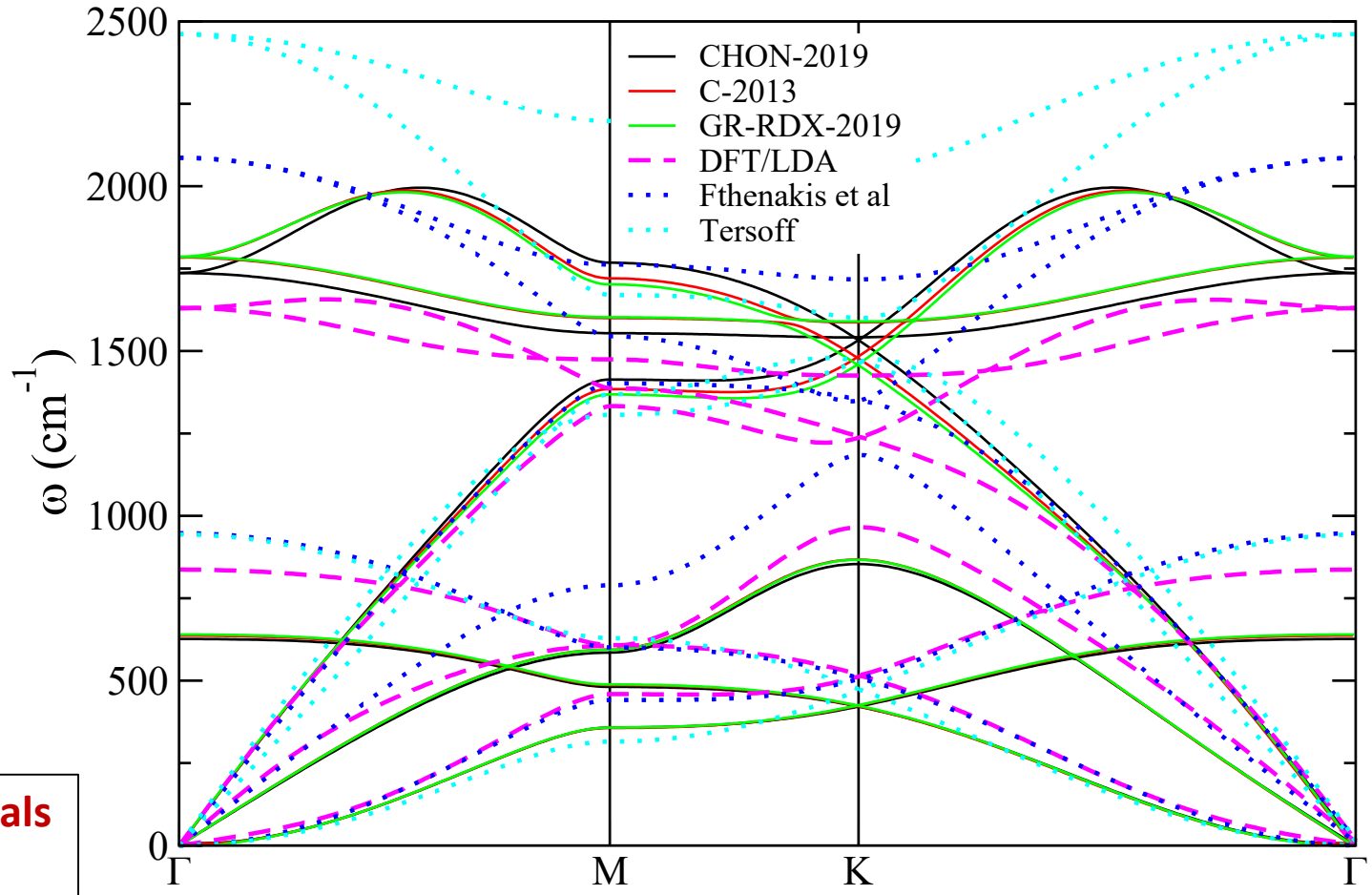

- **Very similar results for the three potentials**
- **Reasonable results compared to DFT**

Energy of Carbon nanotubes vs diameter D

(n,0) and (n,n) nanotubes
For (n,0) , n ≤ 100
For (n,n), n ≤ 20

$$\frac{U}{N} = U_0 + \frac{C_1}{D^2} + \frac{C_2}{D^4}$$

C_1 ranges between 5 and 10 eV/A^2

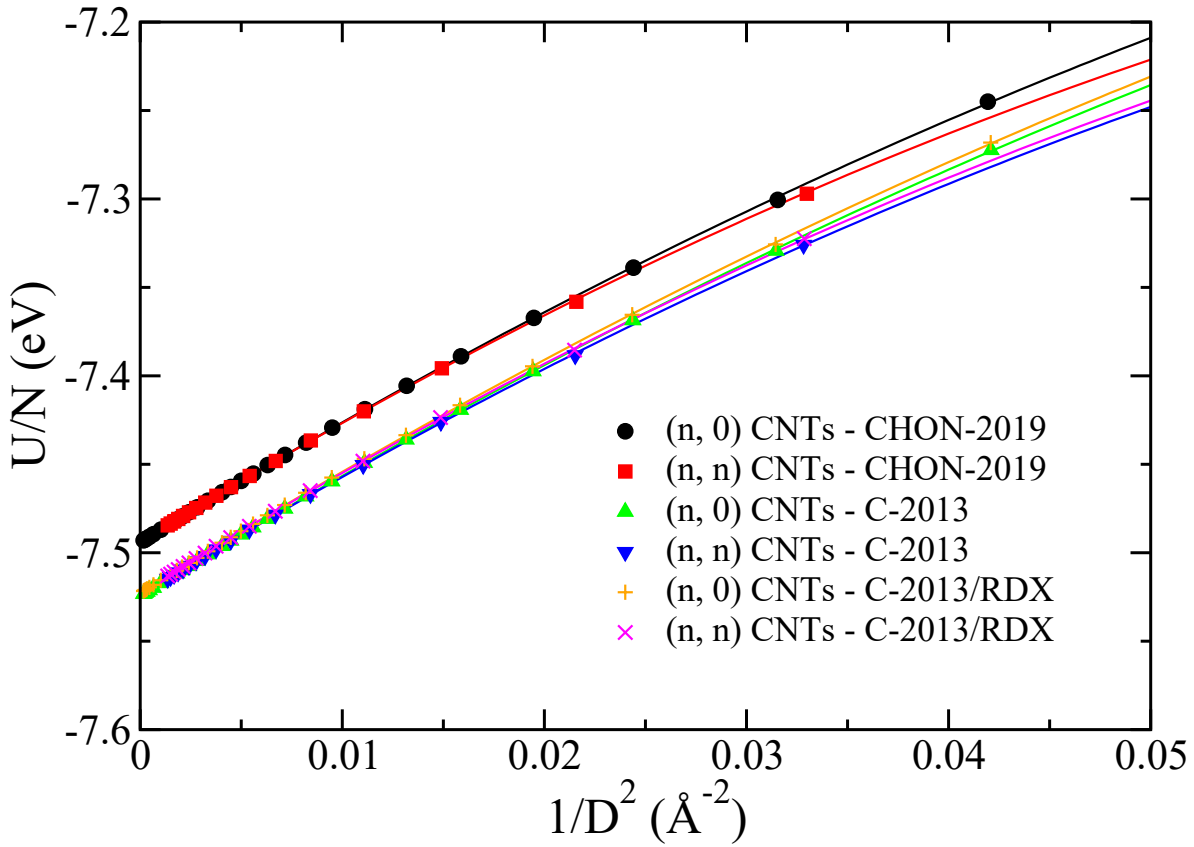

CNTs	Potential	Fitted equation (eV)
(n,0)	CHON-2019	U/N = -7.4043 + 7.0162/D^2 - 26.339/D^4
(n,0)	C-2013	U/N = -7.4346 + 7.0060/D^2 – 24.683/D^4
(n,0)	GR-RDX-2021	U/N = -7.4315 + 7.0798/D^2 – 24.900/D^4
(n,n)	CHON-2019	U/N = -7.4043 + 7.0385/D^2 – 31.710/D^4
(n,n)	C-2013	U/N = -7.4345 + 6.9853/D^2 – 29.267/D^4
(n,n)	GR-RDX-2021	U/N = -7.4315 + 7.0732/D^2 – 30.212/D^4

- 1/D^2 dependence:
  Tibbetts, J. Cryst. Growth **66**, 632 (1984)
- 1/D^4 additional term:
  Kanamitsou and Saito, J. Phys. Soc. Japan **71**, 483 (2002)
  Fthenakis et al, Phys. Chem. Chem. Phys. **19**, 30925 (2017))

Energy of Carbon nanotubes vs diameter D

(n,0) and (n,n) nanotubes
For (n,0) , n ≤ 100
For (n,n), n ≤ 20

$$\frac{U}{N} = U_0 + \frac{C_1}{D^2} + \frac{C_2}{D^4}$$

C_1 ranges between 5 and 10 eV/A^2

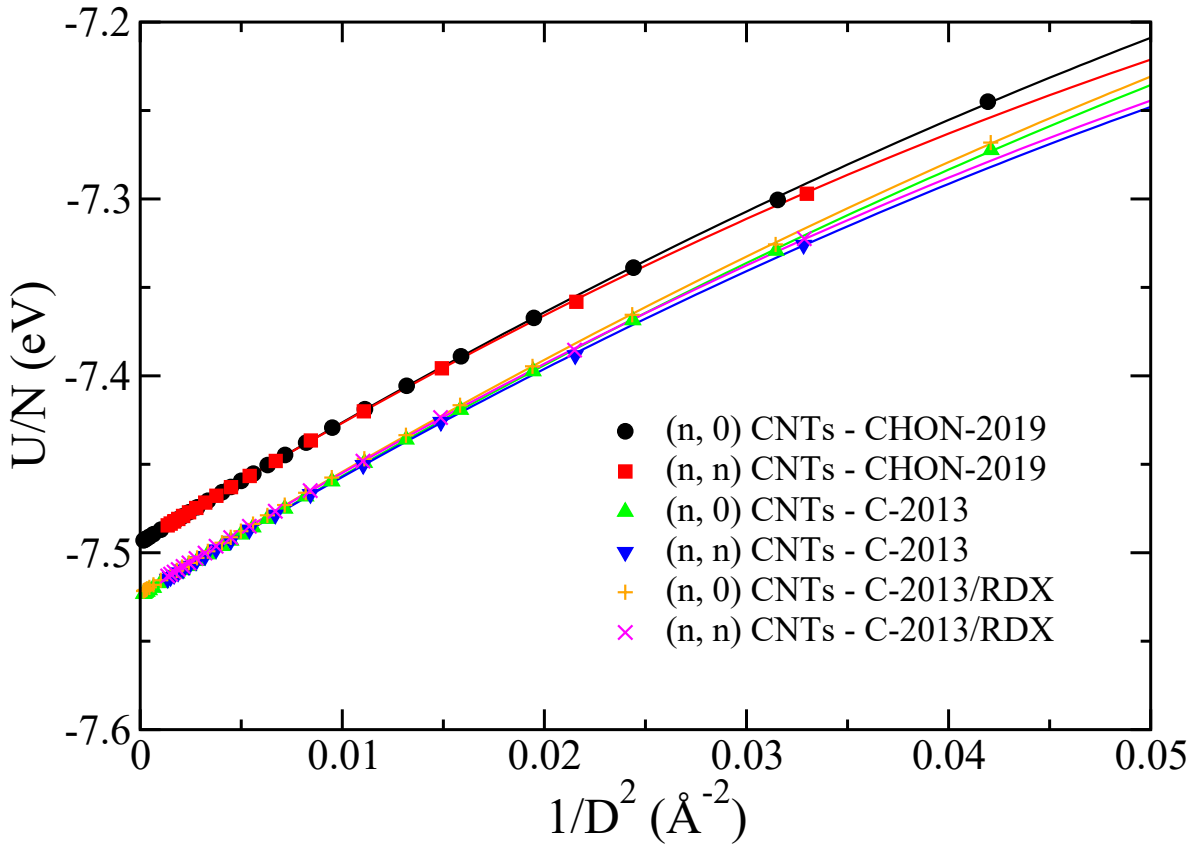

CNTs	Potential	Fitted equation (eV)
(n,0)	CHON-2019	U/N = -7.4043 + 7.0162/D^2 - 26.339/D^4
(n,0)	C-2013	U/N = -7.4346 + 7.0060/D^2 – 24.683/D^4
(n,0)	GR-RDX-2021	U/N = -7.4315 + 7.0798/D^2 – 24.900/D^4
(n,n)	CHON-2019	U/N = -7.4043 + 7.0385/D^2 – 31.710/D^4
(n,n)	C-2013	U/N = -7.4345 + 6.9853/D^2 – 29.267/D^4
(n,n)	GR-RDX-2021	U/N = -7.4315 + 7.0732/D^2 – 30.212/D^4

Energy of graphene ± 0.004%

ReaxFF	U/N (eV/atom)
CHON-2019	-7.404626
C-2013	-7.434825
GR-RDX-2021	-7.431757

Energy of Carbon nanotubes vs diameter D

(n,0) and (n,n) nanotubes
For (n,0) , n ≤ 100
For (n,n), n ≤ 20

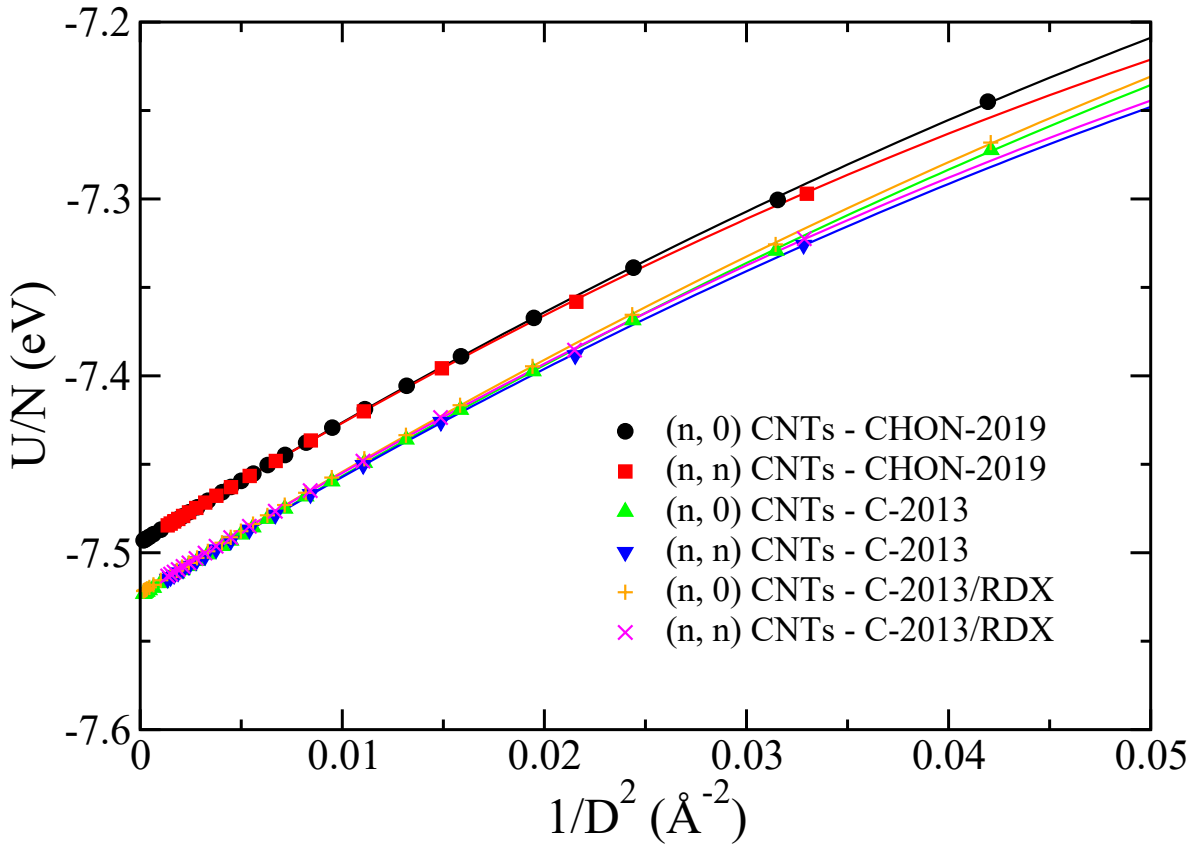

$$\frac{U}{N} = U_0 + \frac{C_1}{D^2} + \frac{C_2}{D^4}$$

C_1 ranges between 5 and 10 eV/A^2

CNTs	Potential	Fitted equation (eV)
(n,0)	CHON-2019	U/N = -7.4043 + 7.0162/D^2 - 26.339/D^4
(n,0)	C-2013	U/N = -7.4346 + 7.0060/D^2 – 24.683/D^4
(n,0)	GR-RDX-2021	U/N = -7.4315 + 7.0798/D^2 – 24.900/D^4
(n,n)	CHON-2019	U/N = -7.4043 + 7.0385/D^2 – 31.710/D^4
(n,n)	C-2013	U/N = -7.4345 + 6.9853/D^2 – 29.267/D^4
(n,n)	GR-RDX-2021	U/N = -7.4315 + 7.0732/D^2 – 30.212/D^4

≈ 7.0 eV/A^2, i.e. within the range [5, 10]
practically independent of the potential

Energy of Carbon nanotubes vs diameter D

(n,0) and (n,n) nanotubes
For (n,0) , n ≤ 100
For (n,n), n ≤ 20

$$\frac{U}{N} = U_0 + \frac{C_1}{D^2} + \frac{C_2}{D^4}$$

C_1 ranges between 5 and 10 eV·A^2

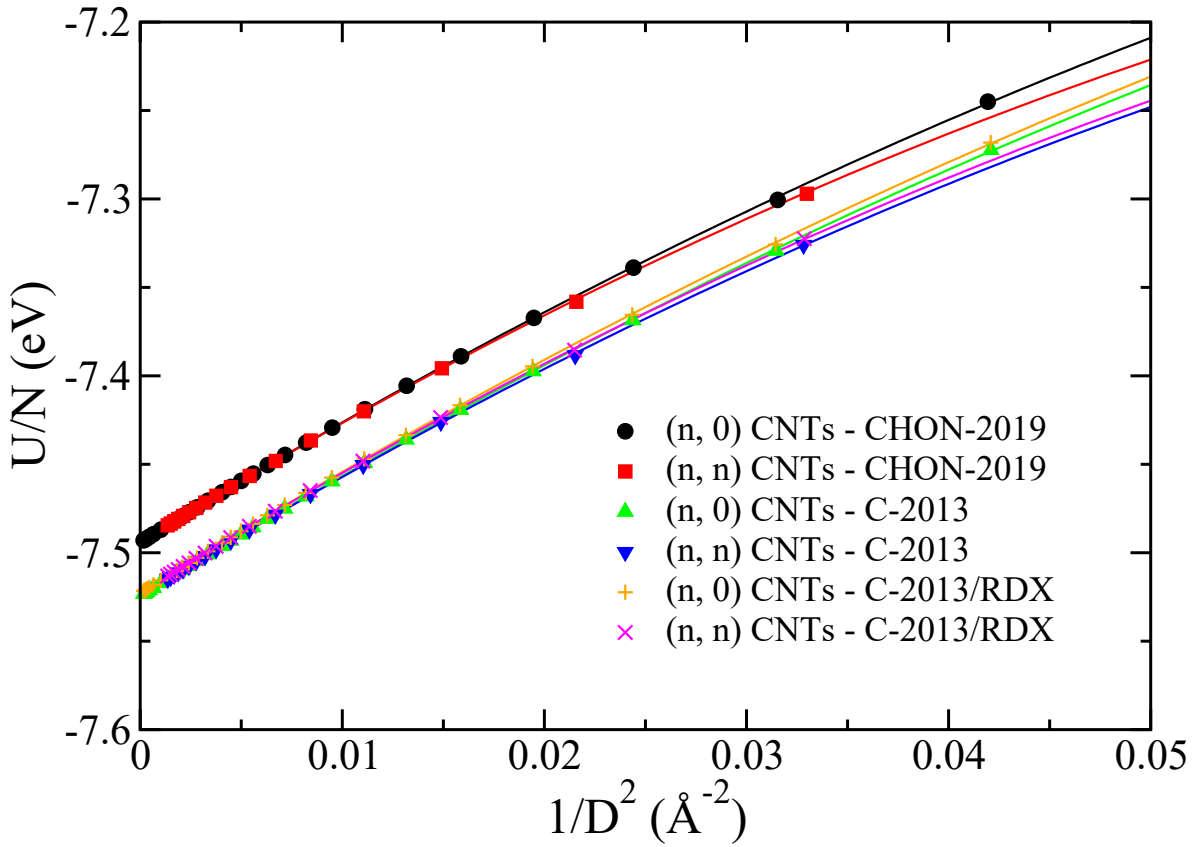

CNTs	Potential	Fitted equation (eV)
(n,0)	CHON-2019	U/N = -7.4043 + 7.0162/D^2 - 26.339/D^4
(n,0)	C-2013	U/N = -7.4346 + 7.0060/D^2 – 24.683/D^4
(n,0)	GR-RDX-2021	U/N = -7.4315 + 7.0798/D^2 – 24.900/D^4
(n,n)	CHON-2019	U/N = -7.4043 + 7.0385/D^2 – 31.710/D^4
(n,n)	C-2013	U/N = -7.4345 + 6.9853/D^2 – 29.267/D^4
(n,n)	GR-RDX-2021	U/N = -7.4315 + 7.0732/D^2 – 30.212/D^4

≈ -25 eV·A^4

≈ -30 eV·A^4

Almost independent of the potential

Mechanical properties of carbon nanotubes under uniaxial strain along the nanotube axis

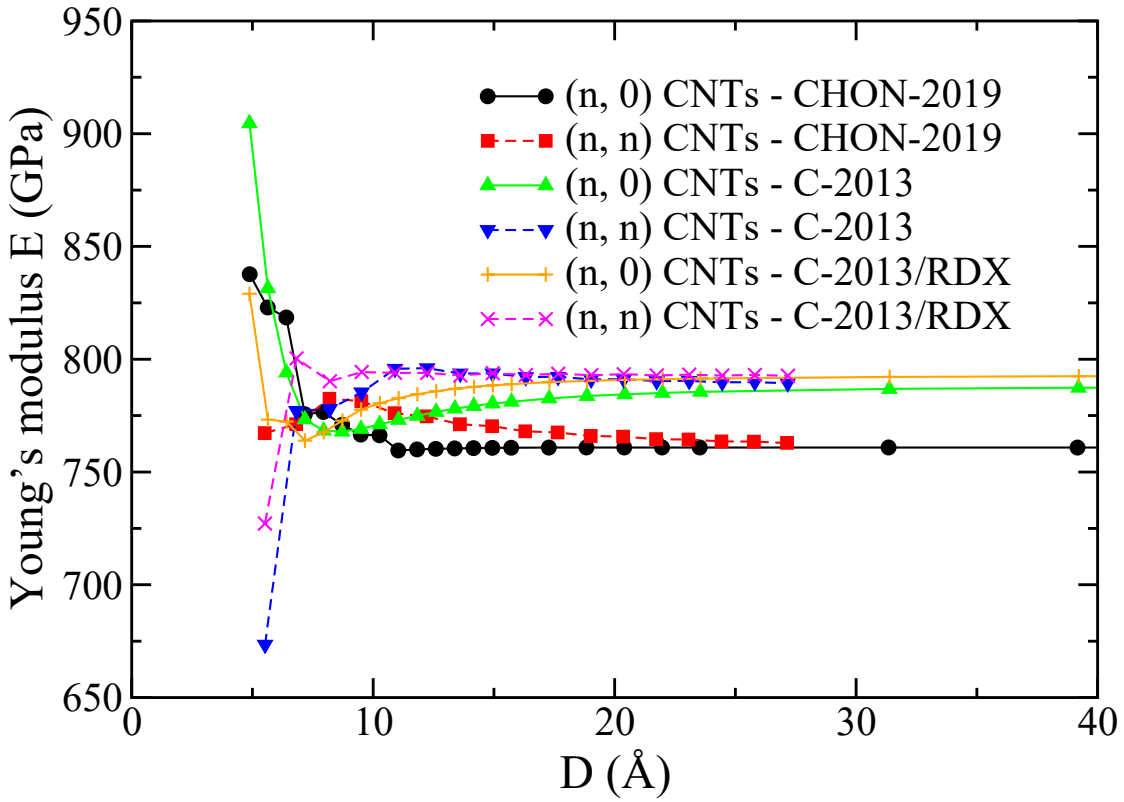

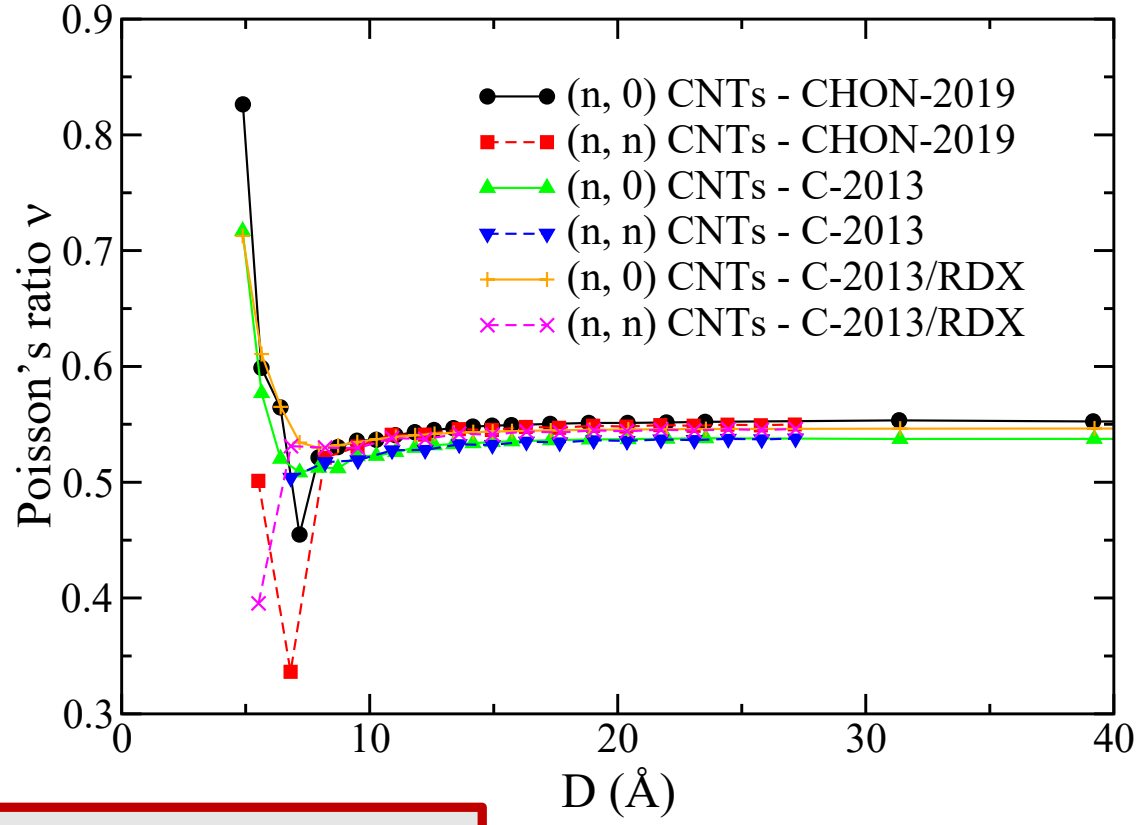

Conclusion:

Excluding the nanotubes for D < 10 A, results very similar to graphene with small variation.

Fullerene energetics

PCCP

Pentagon adjacency as a determinant of fullerene stability

E. Albertazzi,[a] C. Domene,[b] P. W. Fowler,[b] T. Heine,[b] G. Seifert,[c] C. Van Alsenoy[d] and F. Zerbetto[e]

[a] *LAMEL, Consiglio Nazionale delle Richerche, via Gobetti 108, 40129 Bologna, Italy*
[b] *School of Chemistry, University of Exeter, Stocker Road, Exeter, UK EX4 4QD*
[c] *Universität-GH Paderborn, FB6 Theoretische Physik, D-33095 Paderborn, Germany*
[d] *Department of Chemistry, University of Antwerp (UIA), Universiteitsplein 1, B-2610 Antwerp, Belgium*
[e] *Dipartimento di Chimica, 'G. Ciamician', Università di Bologna, via F. Selmi 2, 40126 Bologna, Italy*

Received 1st March 1999, Accepted 26th April 1999

Optimisation of geometries of all 40 fullerene isomers of C_{40}, using methods from molecular mechanics and tight-binding to full *ab initio* SCF and DFT approaches, confirms minimisation of pentagon adjacency as a major factor in relative stability. The consensus predictions of 11 out of 12 methods are that the isomer of lowest total energy is the D_2 cage with the smallest possible adjacency count, and that energies rise linearly with the number of adjacencies. Quantum mechanical methods predict a slope of 80–100 kJ mol^{-1} per adjacency. Molecular mechanics methods are outliers, with the Tersoff potential giving a different minimum and its Brenner modification a poor correlation and much smaller penalty.

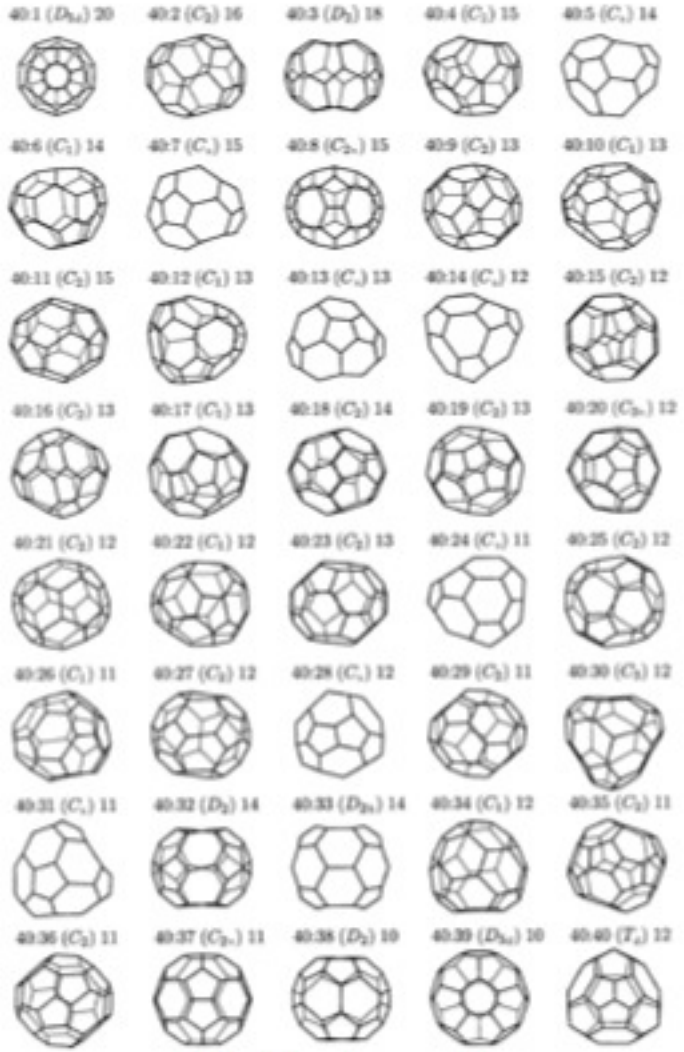

Fig. 1 Fullerene isomers of C_{40}.

Phys. Chem. Chem. Phys. **1**, 2913 (1999)

Fullerene energetics

PCCP

Pentagon adjacency as a determinant of fullerene stability

E. Albertazzi,[a] C. Domene,[b] P. W. Fowler,[b] T. Heine,[b] G. Seifert,[c] C. Van Alsenoy[d] and F. Zerbetto[e]

[a] *LAMEL, Consiglio Nazionale delle Richerche, via Gobetti 108, 40129 Bologna, Italy*
[b] *School of Chemistry, University of Exeter, Stocker Road, Exeter, UK EX4 4QD*
[c] *Universität-GH Paderborn, FB6 Theoretische Physik, D-33095 Paderborn, Germany*
[d] *Department of Chemistry, University of Antwerp (UIA), Universiteitsplein 1, B-2610 Antwerp, Belgium*
[e] *Dipartimento di Chimica, 'G. Ciamician', Università di Bologna, via F. Selmi 2, 40126 Bologna, Italy*

Received 1st March 1999, Accepted 26th April 1999

Optimisation of geometries of all 40 fullerene isomers of C_{40}, using methods from molecular mechanics and tight-binding to full *ab initio* SCF and DFT approaches, confirms minimisation of pentagon adjacency as a major factor in relative stability. The consensus predictions of 11 out of 12 methods are that the isomer of lowest total energy is the D_2 cage with the smallest possible adjacency count, and that energies rise linearly with the number of adjacencies. Quantum mechanical methods predict a slope of 80–100 kJ mol^{-1} per adjacency. Molecular mechanics methods are outliers, with the Tersoff potential giving a different minimum and its Brenner modification a poor correlation and much smaller penalty.

Phys. Chem. Chem. Phys. **1**, 2913 (1999)

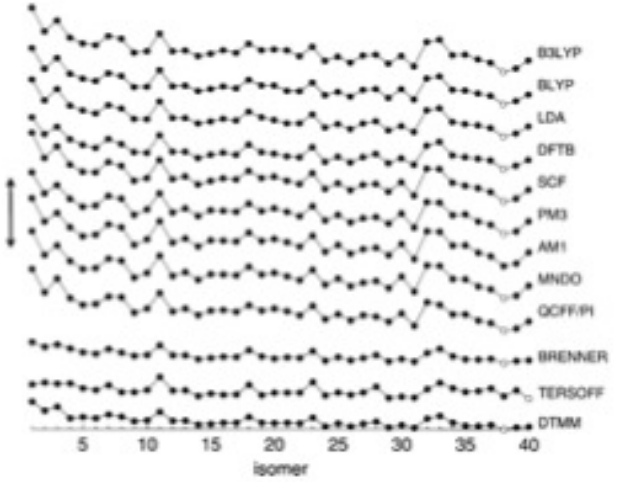

Fig. 3 Parallel trends in calculated energies of C_{40} fullerenes. Points representing energies relative to 40:38 are plotted against position in the isomer sequence, and joined by straight line segments to guide the eye. Curves for the 12 methods of Table 1 are offset by 500 kJ mol^{-1} in the energy of 40:38, with the scale indicated by the double-headed arrow representing 1000 kJ mol^{-1}.

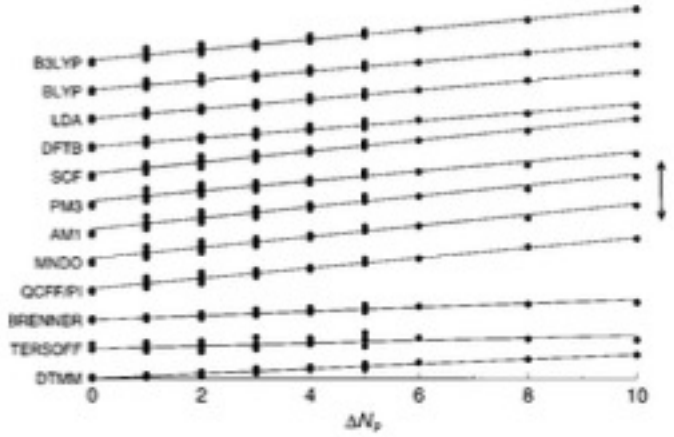

Fig. 4 Correlation of energy and pentagon adjacencies for the C_{40} fullerene isomers. Energies (ΔE/kJ mol^{-1}) are quoted relative to that of 40:38 and pentagon adjacencies ΔN_p are relative to the minimal achievable value ($N_p = 10$ for 40:38). Data sets are offset by 500 kJ mol^{-1} as in Fig. 3, and again the arrow indicates a scale of 1000 kJ mol^{-1}. Slopes for the 12 fitted lines (kJ mol^{-1}) from the top of the figure are 92.1, 82.5, 85.4, 78.0, 99.5, 87.5, 97.3, 97.1, 90.7, 36.1, 24.4 and 42.2. Intercepts (with offsets removed) are 60.9, 43.3, 35.8, 35.4, 67.2, 94.8, 103.7, 86.3, 56.1, 15.2, 13.3 and 0.2. All correlations have $r^2 \geq 0.92$ apart from BRENNER ($r^2 = 0.87$) and TERSOFF ($r^2 = 0.41$).

Fullerene energetics

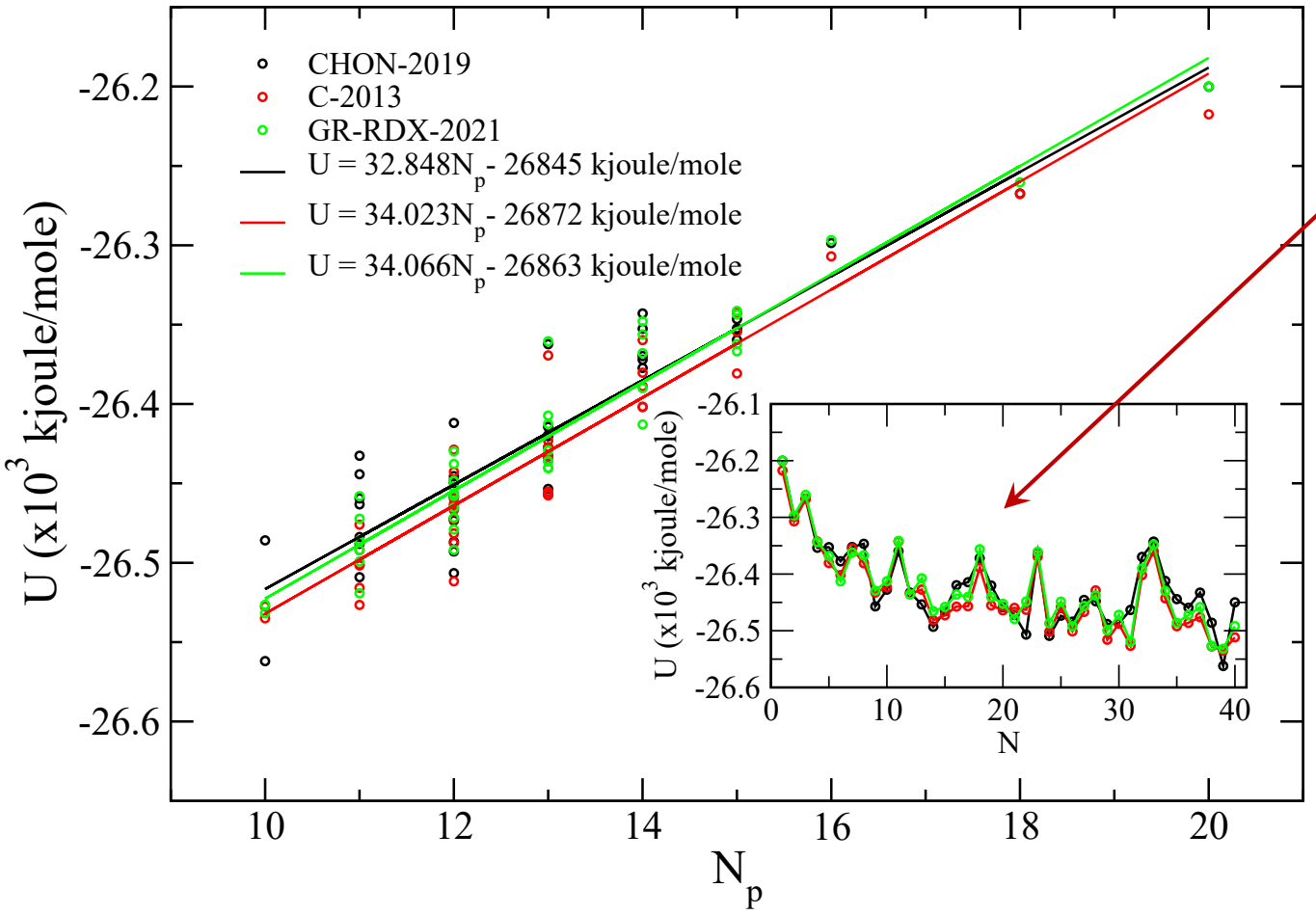

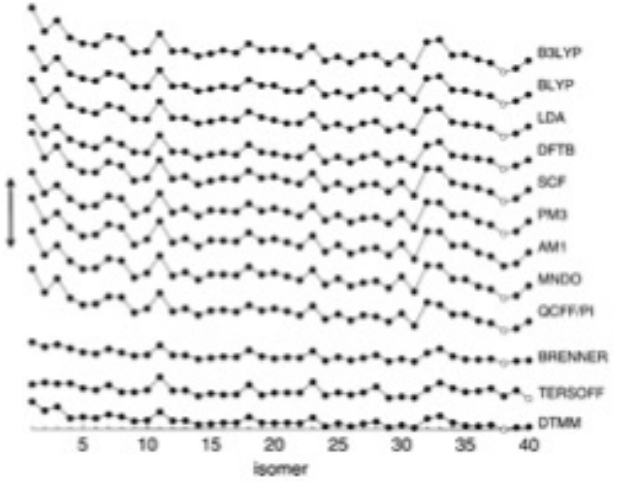

Fig. 3 Parallel trends in calculated energies of C_{40} fullerenes. Points representing energies relative to 40:38 are plotted against position in the isomer sequence, and joined by straight line segments to guide the eye. Curves for the 12 methods of Table 1 are offset by 500 kJ mol^{-1} in the energy of 40:38, with the scale indicated by the double-headed arrow representing 1000 kJ mol^{-1}.

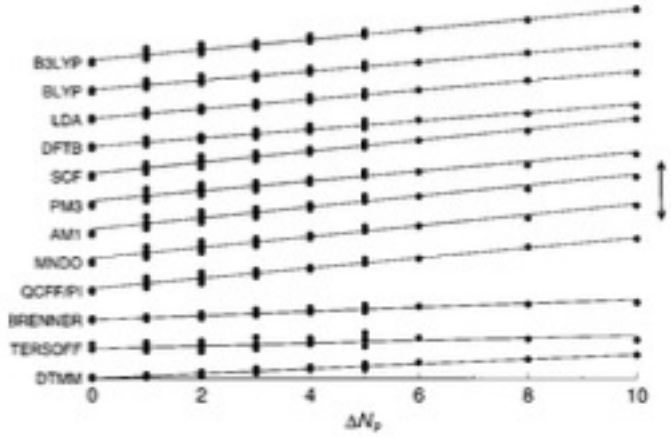

Fig. 4 Correlation of energy and pentagon adjacencies for the C_{40} fullerene isomers. Energies (ΔE/kJ mol^{-1}) are quoted relative to that of 40:38 and pentagon adjacencies ΔN_p are relative to the minimal achievable value ($N_p = 10$ for 40:38). Data sets are offset by 500 kJ mol^{-1} as in Fig. 3, and again the arrow indicates a scale of 1000 kJ mol^{-1}. Slopes for the 12 fitted lines (kJ mol^{-1}) from the top of the figure are 92.1, 82.5, 85.4, 78.0, 99.5, 87.5, 97.3, 97.1, 90.7, 36.1, 24.4 and 42.2. Intercepts (with offsets removed) are 60.9, 43.3, 35.8, 35.4, 67.2, 94.8, 103.7, 86.3, 56.1, 15.2, 13.3 and 0.2. All correlations have $r^2 \geq 0.92$ apart from BRENNER ($r^2 = 0.87$) and TERSOFF ($r^2 = 0.41$).

Fullerene energetics

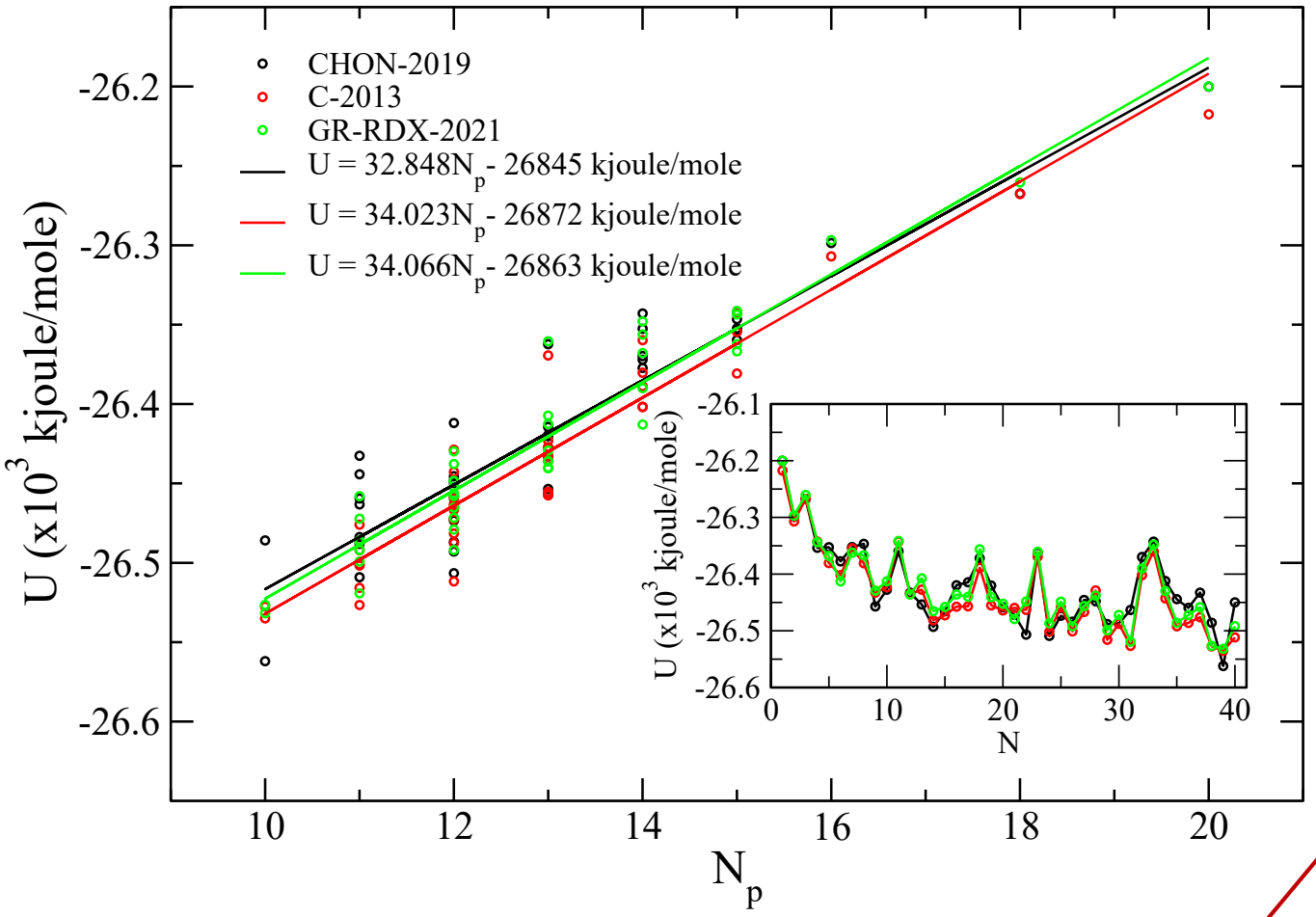

Method	Slope (kjoule/mole)
SCF	99.5
AM1	97.3
MNDO	97.1
B3LYP	92.1
QCFF/PI	90.7
LDA	85.4
BLYP	82.5
DFTB	78.0
SCF	99.5
DTMM	42.2
Fthenakis et al	40.5
Brenner	36.1
GR-RDX-2021	**34.1**
C-2013	**34.0**
CHON-2019	**32.8**
Tersoff	24.4

Fthenakis et al, Phys. Chem. Chem. Phys. **19**, 30925 (2017))

Fullerene energetics

Conclusion:

Very small slope values, although comparable to the slopes obtained using other classical potentials.

However…

Method	Slope (kjoule/mole)
SCF	99.5
AM1	97.3
MNDO	97.1
B3LYP	92.1
QCFF/PI	90.7
LDA	85.4
BLYP	82.5
DFTB	78.0
SCF	99.5
DTMM	42.2
Fthenakis et al	40.5
Brenner	36.1
GR-RDX-2021	**34.1**
C-2013	**34.0**
CHON-2019	**32.8**
Tersoff	24.4

Fullerene energetics

For the 1812 C_{60} fullerene isomers

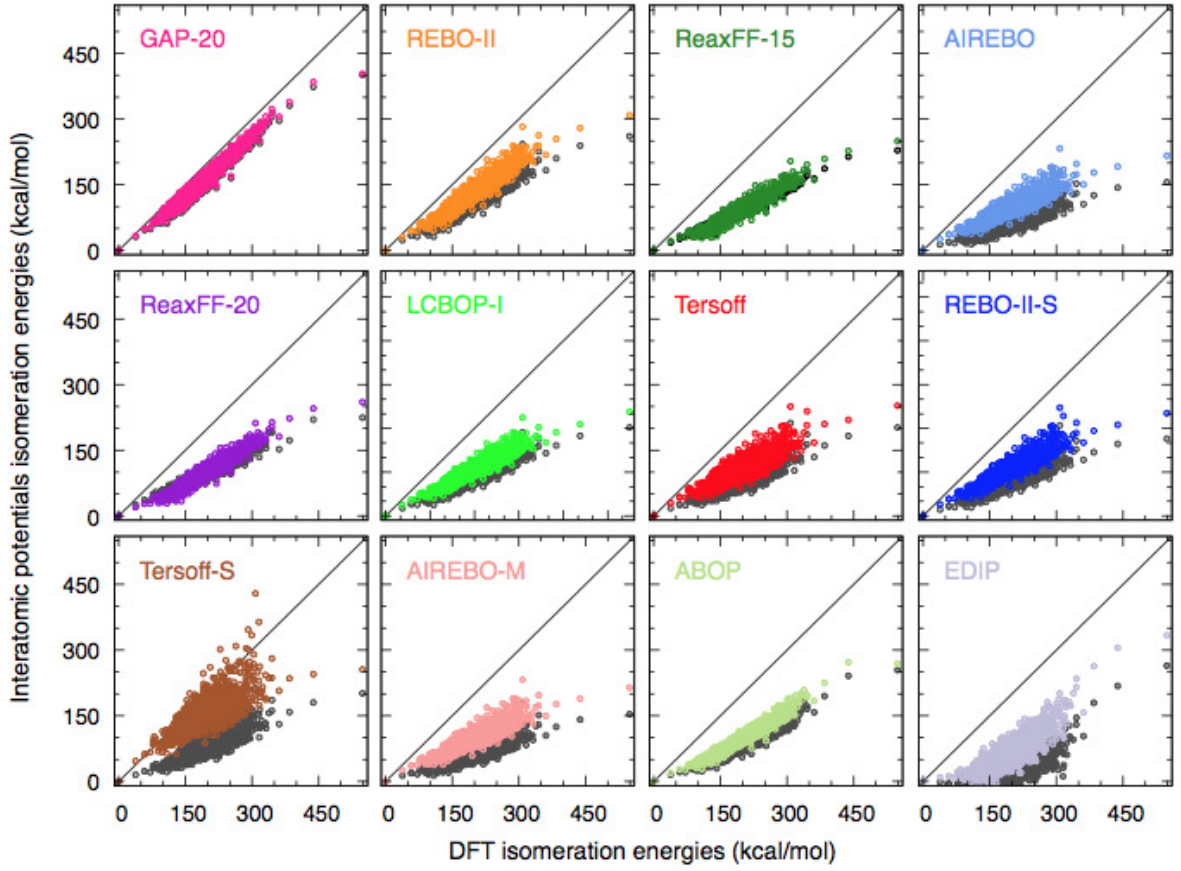

Figure 2. Correlation between the PW6B95-D3/Def2-QZVP isomerization energies and the force-field isomerization energies calculated using the PBE-D3/Def2-TZVP geometries (colored points) and the structures optimized with each of the force fields (gray points).

Aghajamali and Karton, Chem. Phys. Lett. **779**, 138853 (2021)

Method	Slope (kjoule/mole)
SCF	99.5
AM1	97.3
MNDO	97.1
B3LYP	92.1
QCFF/PI	90.7
LDA	85.4
BLYP	82.5
DFTB	78.0
SCF	99.5
DTMM	42.2
Fthenakis et al	40.5
Brenner	36.1
GR-RDX-2021	**34.1**
C-2013	**34.0**
CHON-2019	**32.8**
Tersoff	24.4

Fullerene energetics

For the 1812 C_{60} fullerene isomers

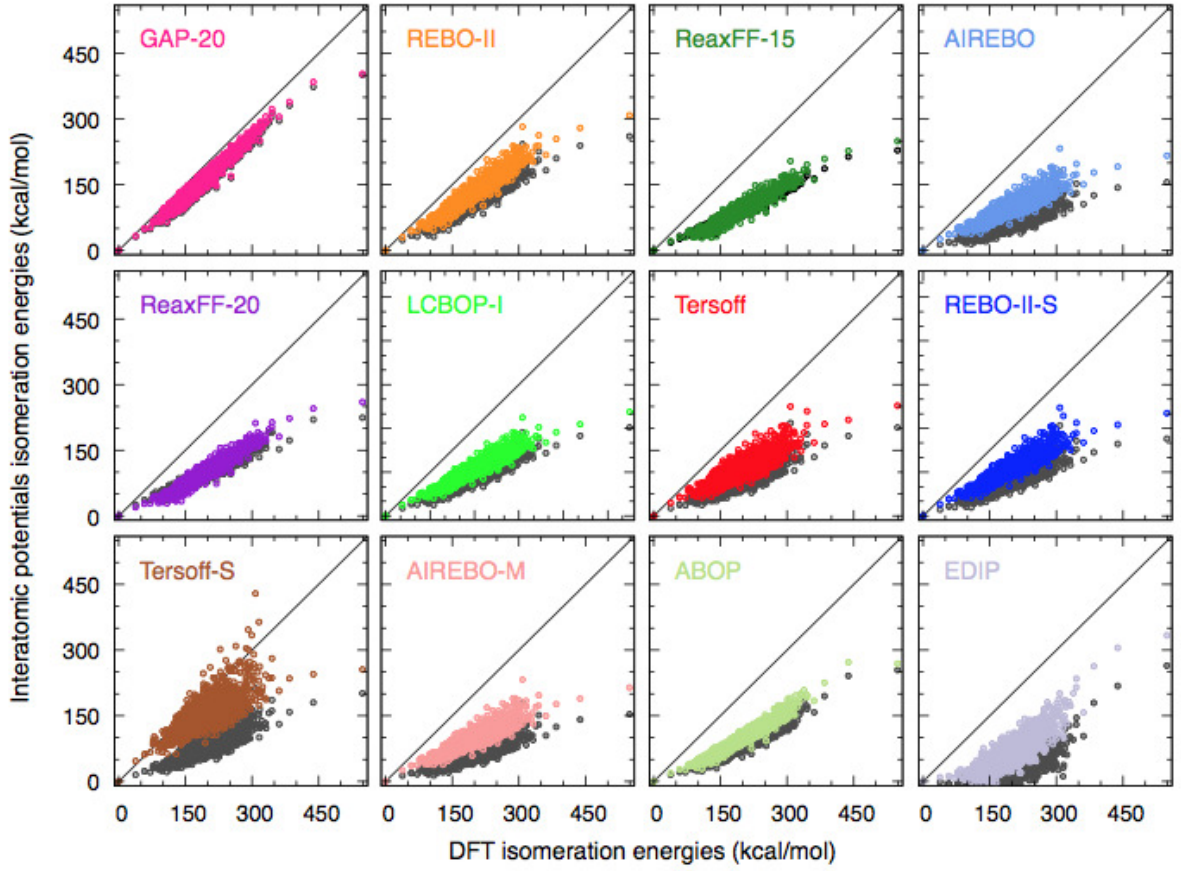

Figure 2. Correlation between the PW6B95-D3/Def2-QZVP isomerization energies and the force-field isomerization energies calculated using the PBE-D3/Def2-TZVP geometries (colored points) and the structures optimized with each of the force fields (gray points).

Aghajamali and Karton, Chem. Phys. Lett. **779**, 138853 (2021)

- All classical potentials predict smaller energy values compared to the corresponding DFT/GGA values.
- Considering that all potentials predict that the energy rise linearly with the number of pentagon adjacencies N_p, the slope of the classical potentials will be smaller than that of DFT/GGA.
- Therefore, **the small slope seems to be an internal problem of ALL classical potentials… which needs improvement.**

Fullerene energetics – Icosahedral C_{60}

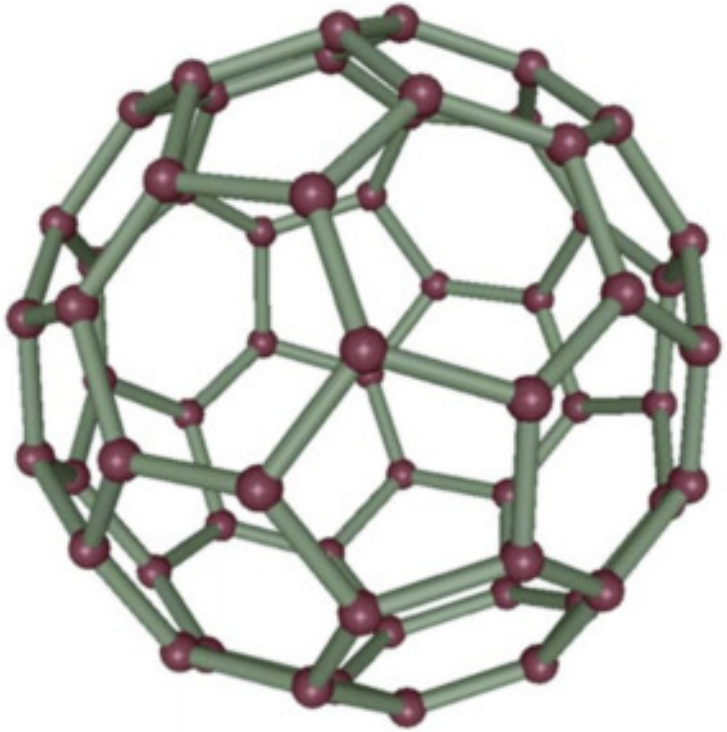

$\Delta U/N = U_{C60}/60 - U_{graphene}/1008$

ReaxFF	ΔU/N (eV/atom)
CHON-2019	**0.3625**
C-2013	**0.3759**
GR-RDX-2021	**0.3767**
Experimental*	0.41±0.02
DFT-GGA/PBE**	0.38
DFT***	0.384
DFT****	0.380

*Chen at al, *Appl. Phys. Lett.* **59**, 2956 (1991)
Wirz et al, *J. Comp. Chem.* **37, 10 (2016)
***Lusk and Carr, *Phys. Rev. Lett.* **100**, 175503 (2008)
****Rocquefelte et al, *Nano Lett.* **4**, 805 (2004)

Response to strain - Graphene

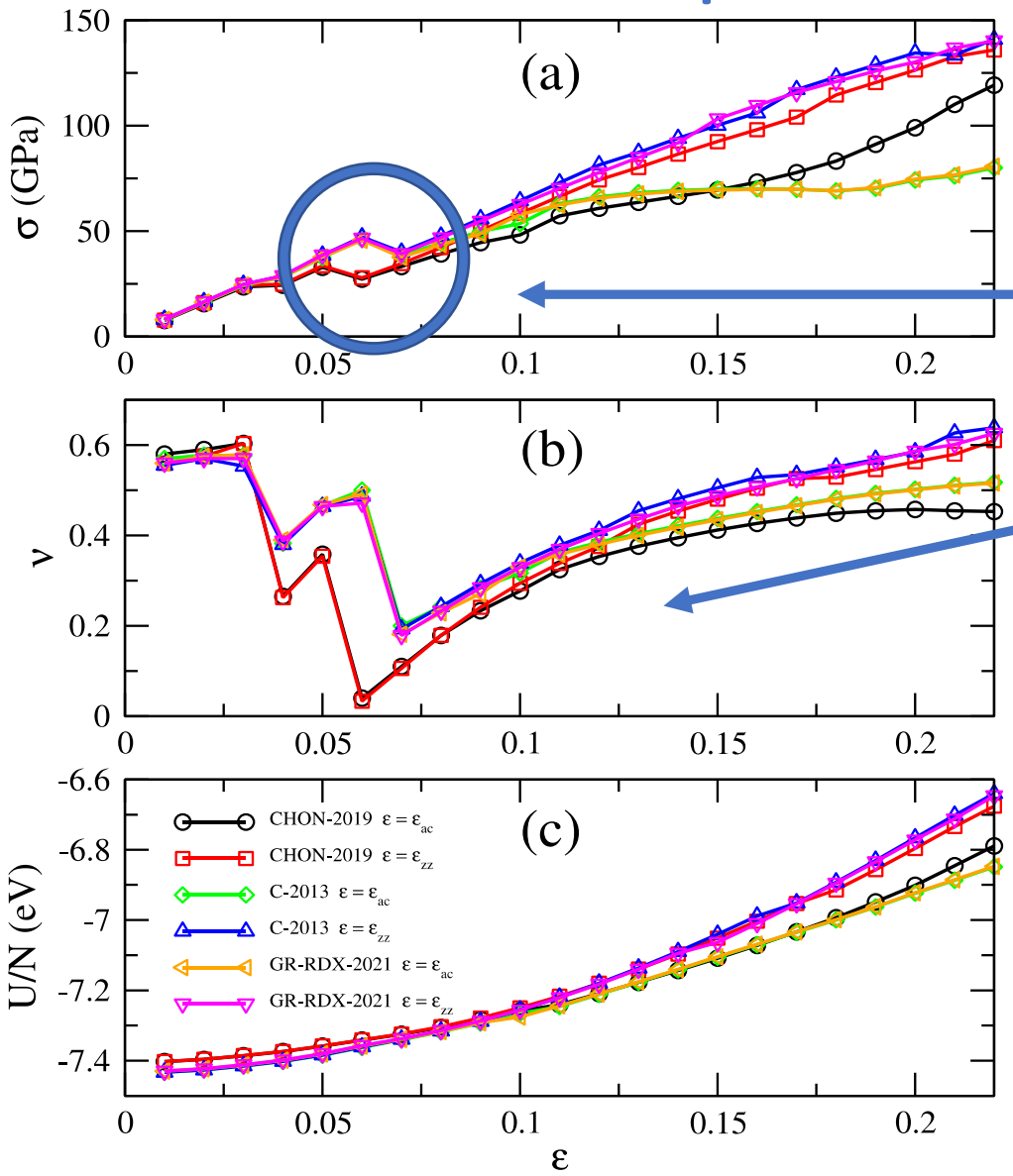

Comment 1: More or less, similar behavior from the three potentials.

Comment 2: Unexpected jump of stress for strain near 0.05.

Comment 3: Unexpected (incorrect) behavior of Poisson's ration versus strain.

Comment 4: Different behavior for strain along arm chair and zig-zag directions for $\varepsilon \gtrsim 0.1$.

Response to strain (up to fracture) – Carbon nanotubes

Energy – Looks normal

(n,0)

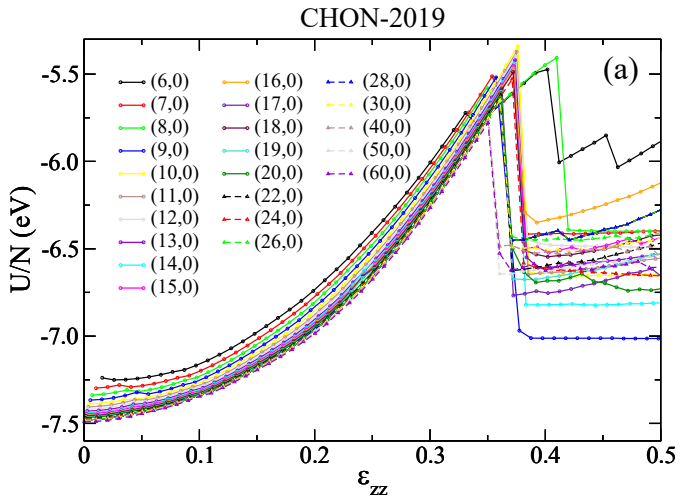

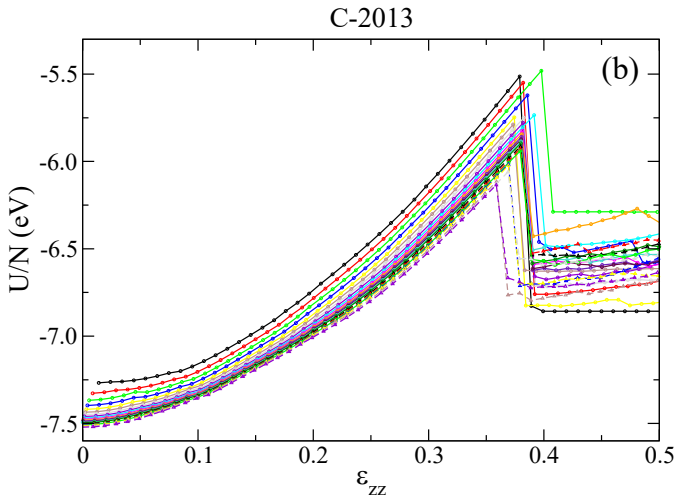

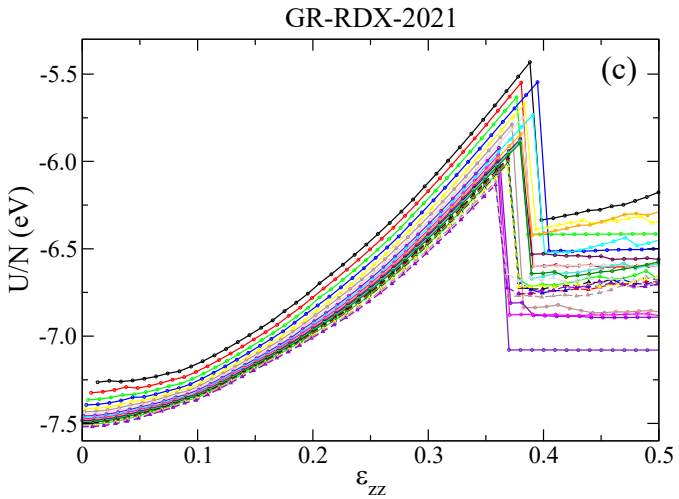

(n,n)

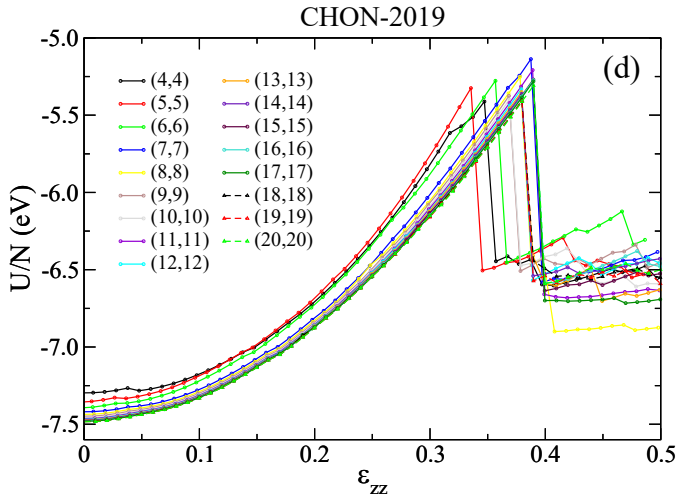

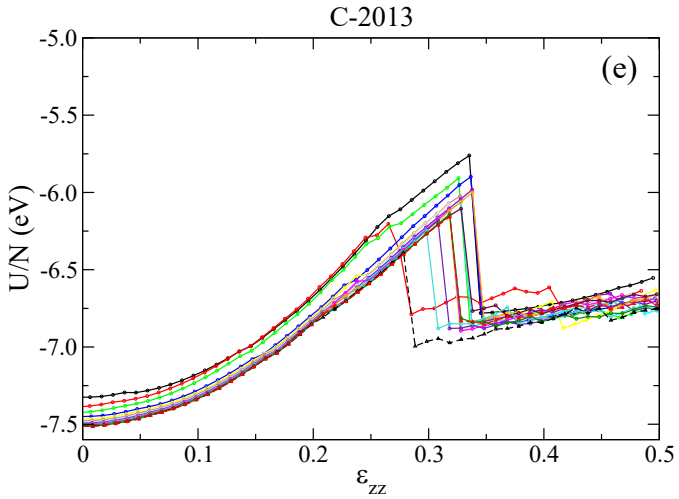

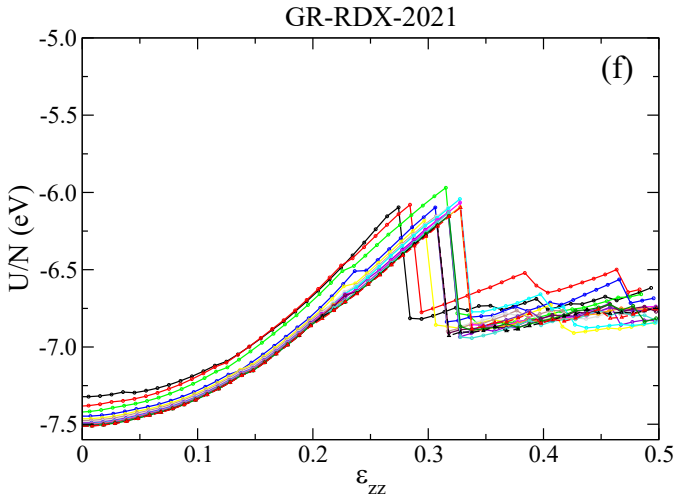

Response to strain (up to fracture) – Carbon nanotubes

Stress – Same unexpected jumps as in graphene

(n,0)

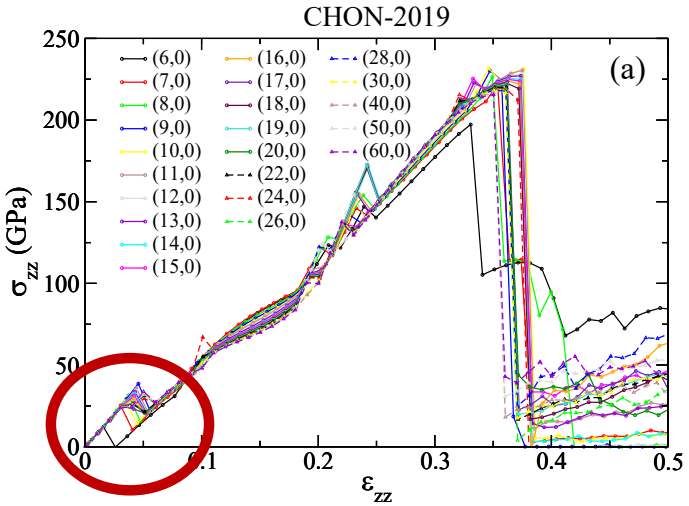

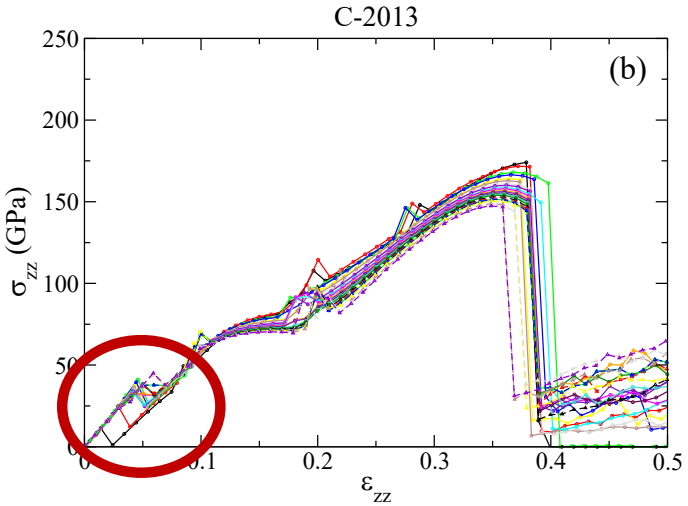

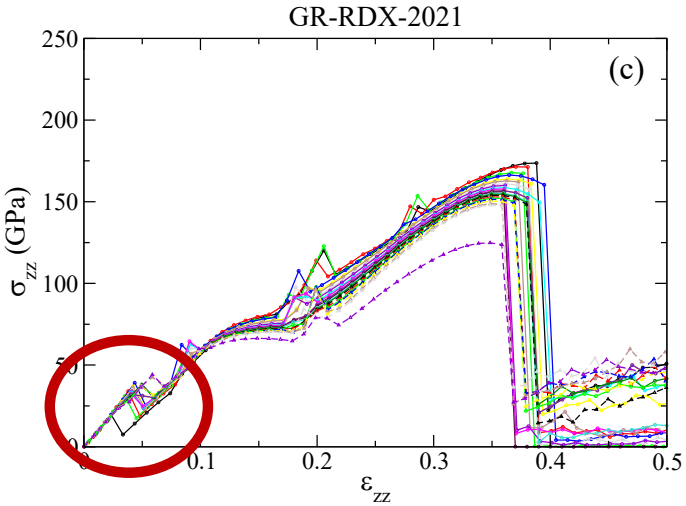

(n,n)

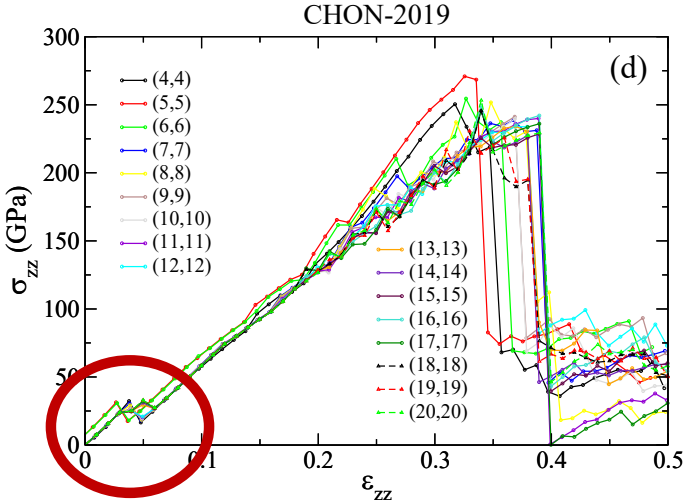

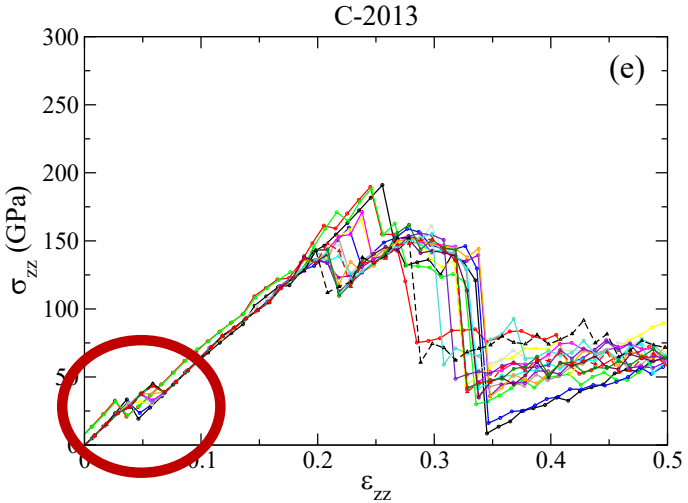

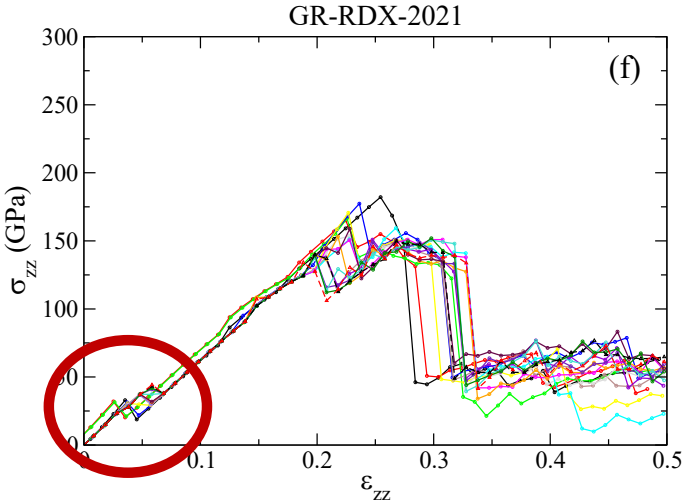

Response to strain (up to fracture) – Carbon nanotubes

Poisson's ratio – Unexpected (incorrect) behavior, as in graphene

(n,0)

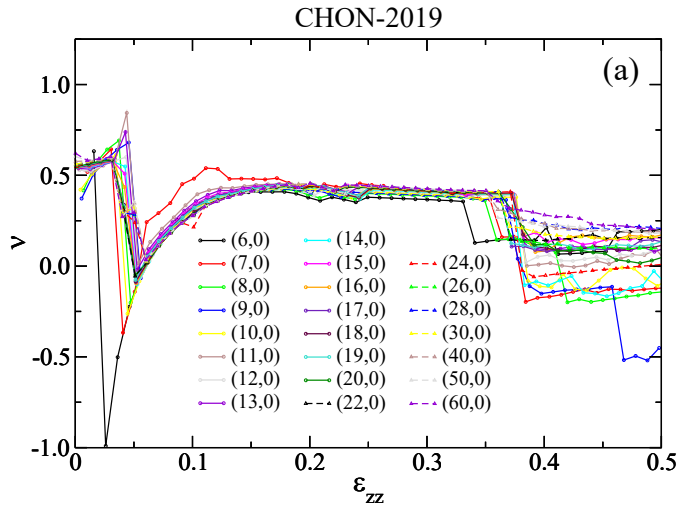

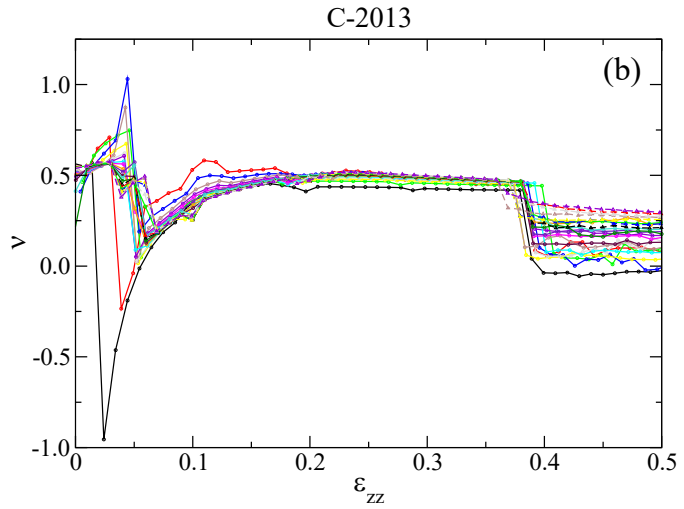

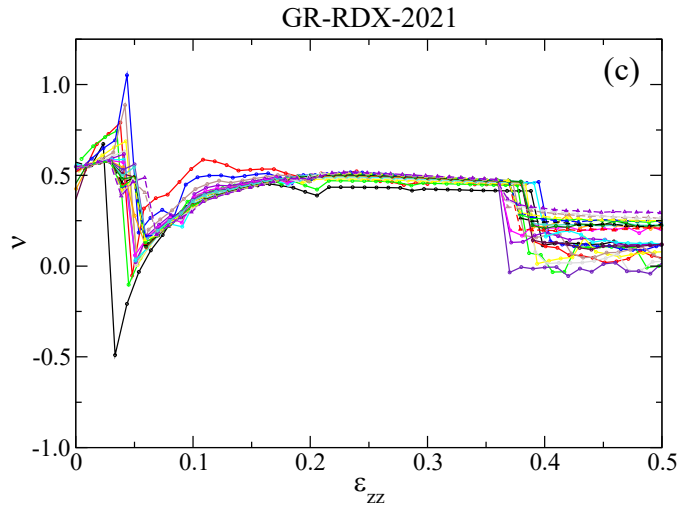

(n,n)

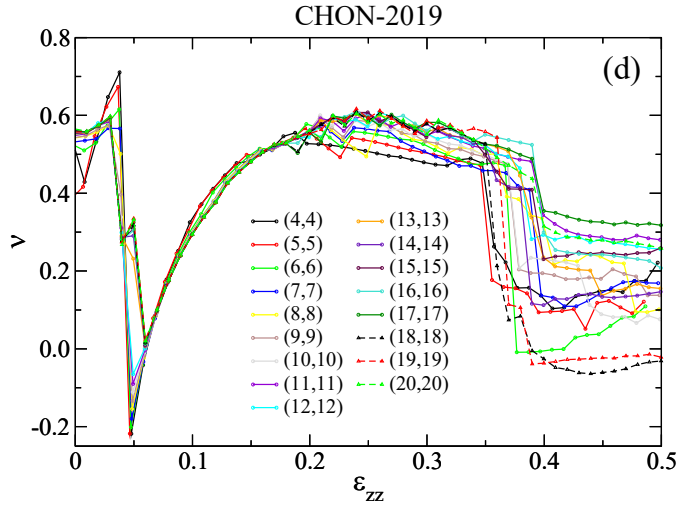

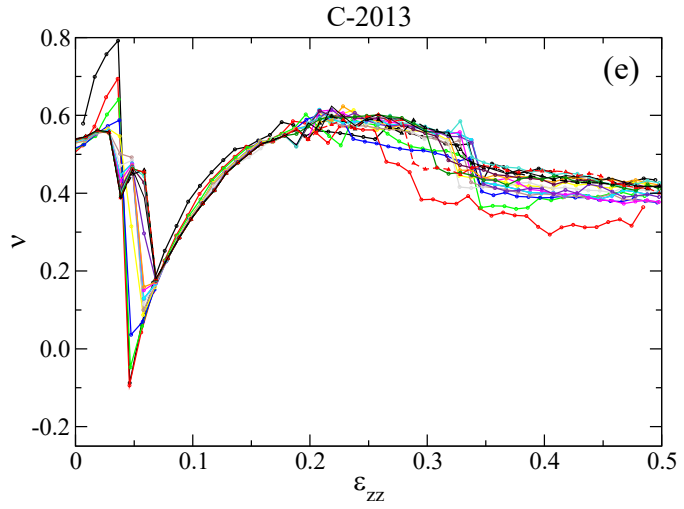

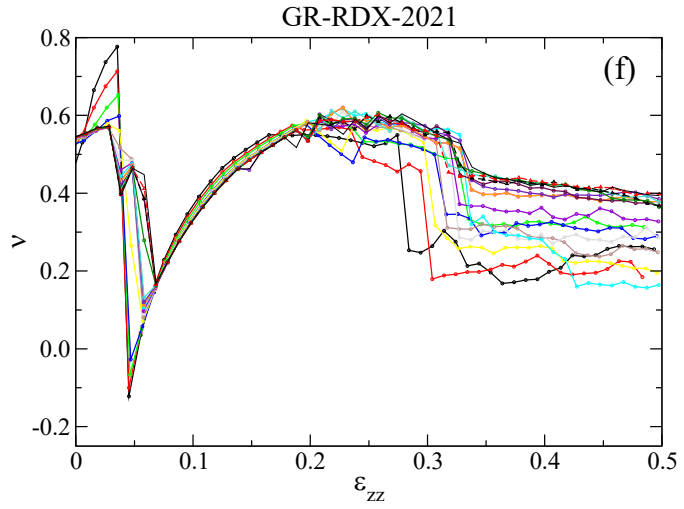

Why that behavior under strain?

- CHON-2019
- Energy and stress scan for constant strain values along x (arm chair) direction.
- $0 \le \varepsilon_{xx} \le 0.20$
  - strain step $\delta\varepsilon_{xx} = 0.01$
- $-0.10 \le \varepsilon_{yy} \le 0$
  - Strain step $\delta\varepsilon_{xx} = 0.001$ for $-0.10 \le \varepsilon_{yy} \le -0.025$
  - Strain step $\delta\varepsilon_{xx} = 0.0001$ for $-0.10 \le \varepsilon_{yy} \le -0.025$

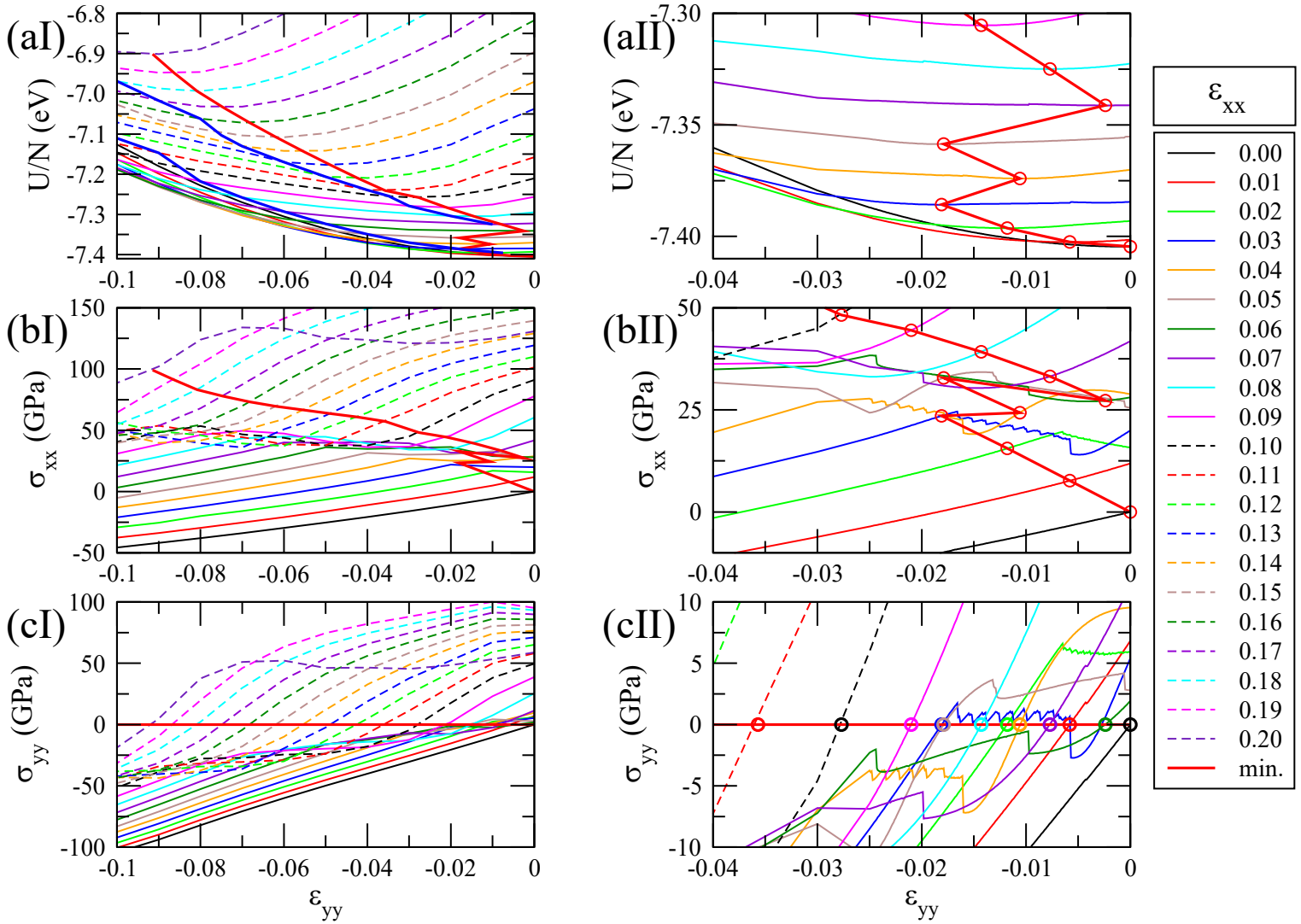

Why that behavior under strain?

- CHON-2019
- Energy and stress scan for constant strain values along x (arm chair) direction.
- $0 \le \varepsilon_{xx} \le 0.20$
  - strain step $\delta\varepsilon_{xx} = 0.01$
- $-0.10 \le \varepsilon_{yy} \le 0$
  - Strain step $\delta\varepsilon_{xx} = 0.001$ for $-0.10 \le \varepsilon_{yy} \le -0.025$
  - Strain step $\delta\varepsilon_{xx} = 0.0001$ for $-0.10 \le \varepsilon_{yy} \le -0.025$

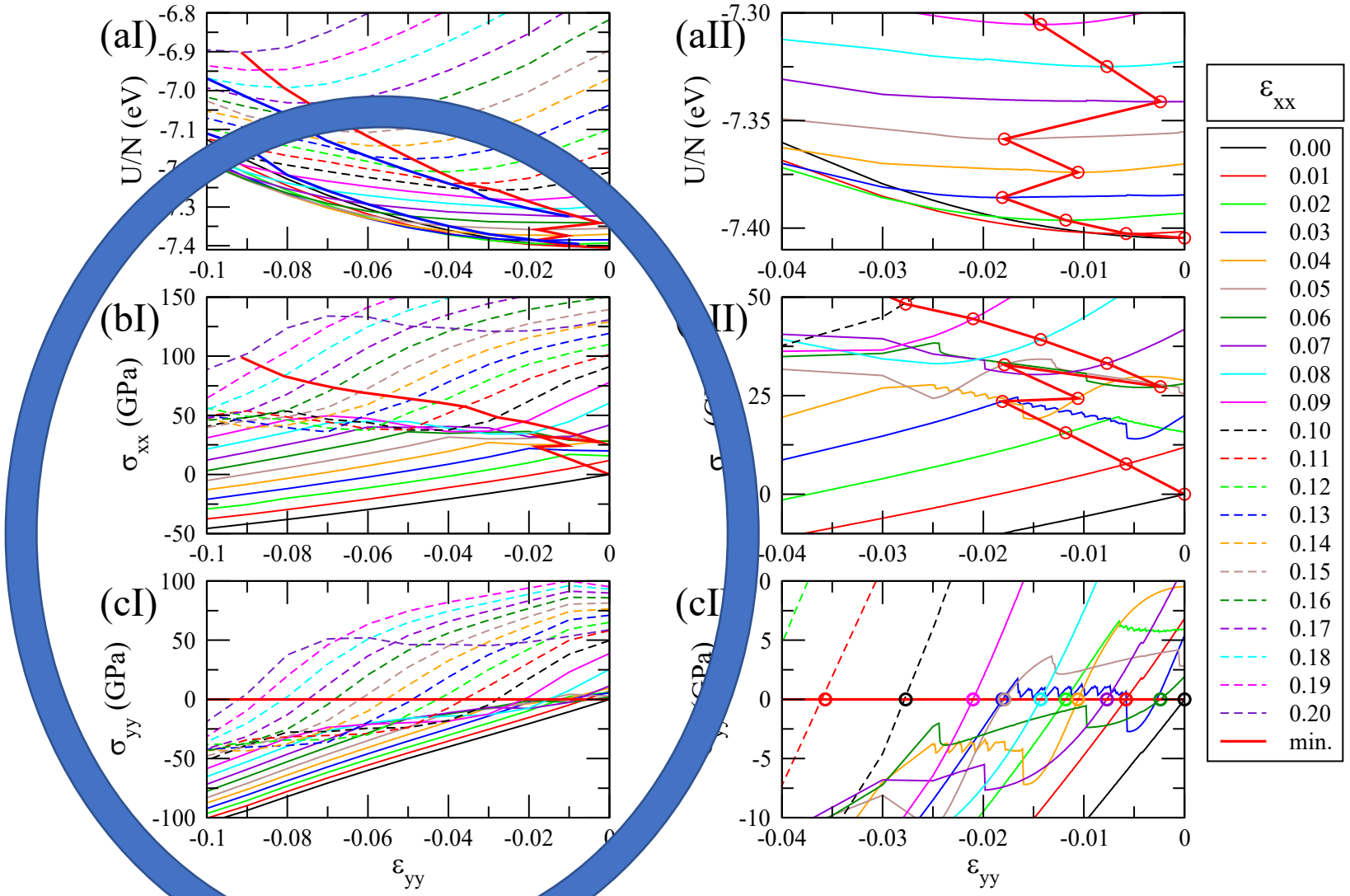

Why that behavior under strain?

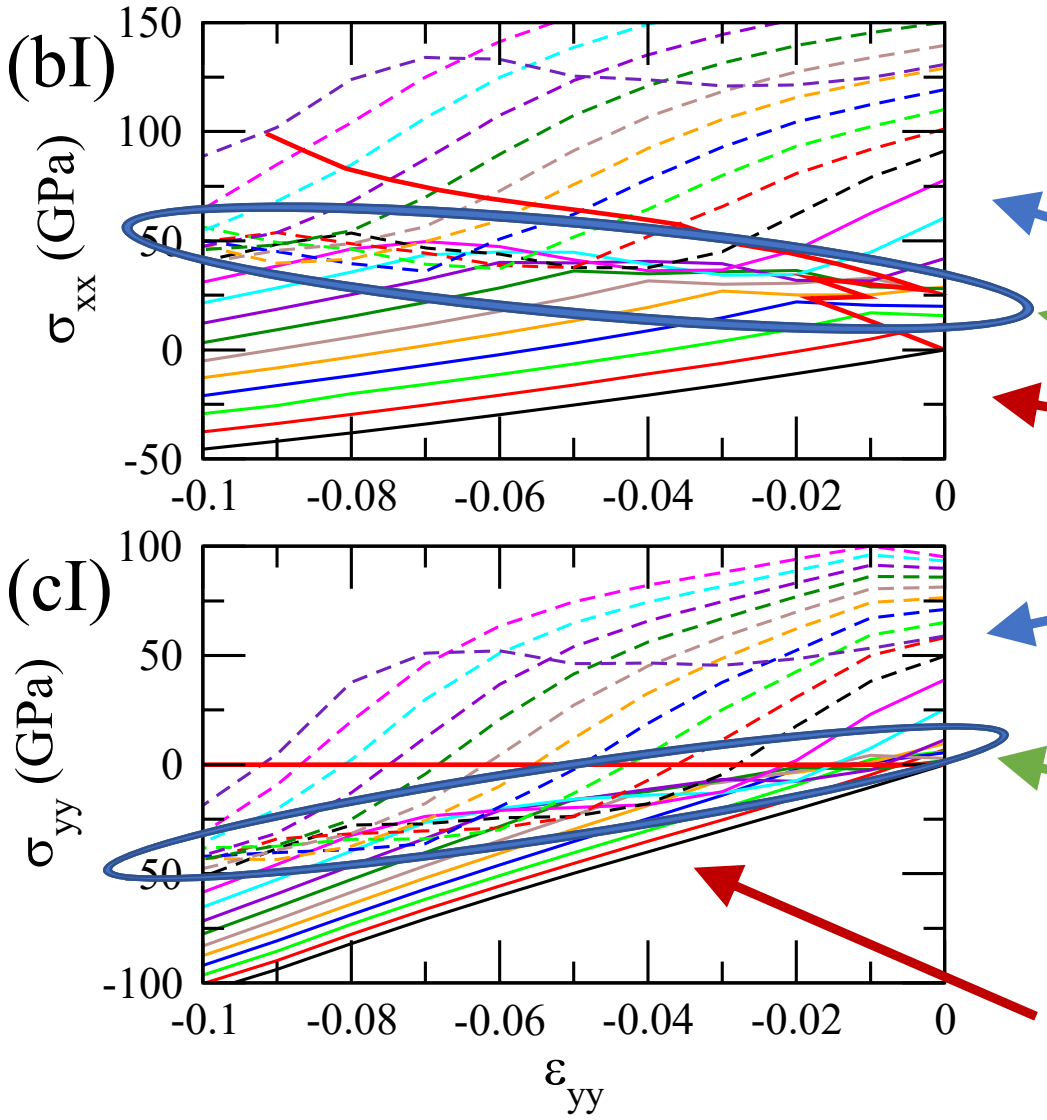

- Stress changes slope
- Three different slope “values”
  - Above that area
  - Inside that area
  - Below that area

Why that behavior under strain?

- CHON-2019
- Energy and stress scan for constant strain values along x (arm chair) direction.
- $0 \le \varepsilon_{xx} \le 0.20$
  - strain step $\delta\varepsilon_{xx} = 0.01$
- $-0.10 \le \varepsilon_{yy} \le 0$
  - Strain step $\delta\varepsilon_{xx} = 0.001$ for $-0.10 \le \varepsilon_{yy} \le -0.025$
  - Strain step $\delta\varepsilon_{xx} = 0.0001$ for $-0.10 \le \varepsilon_{yy} \le -0.025$

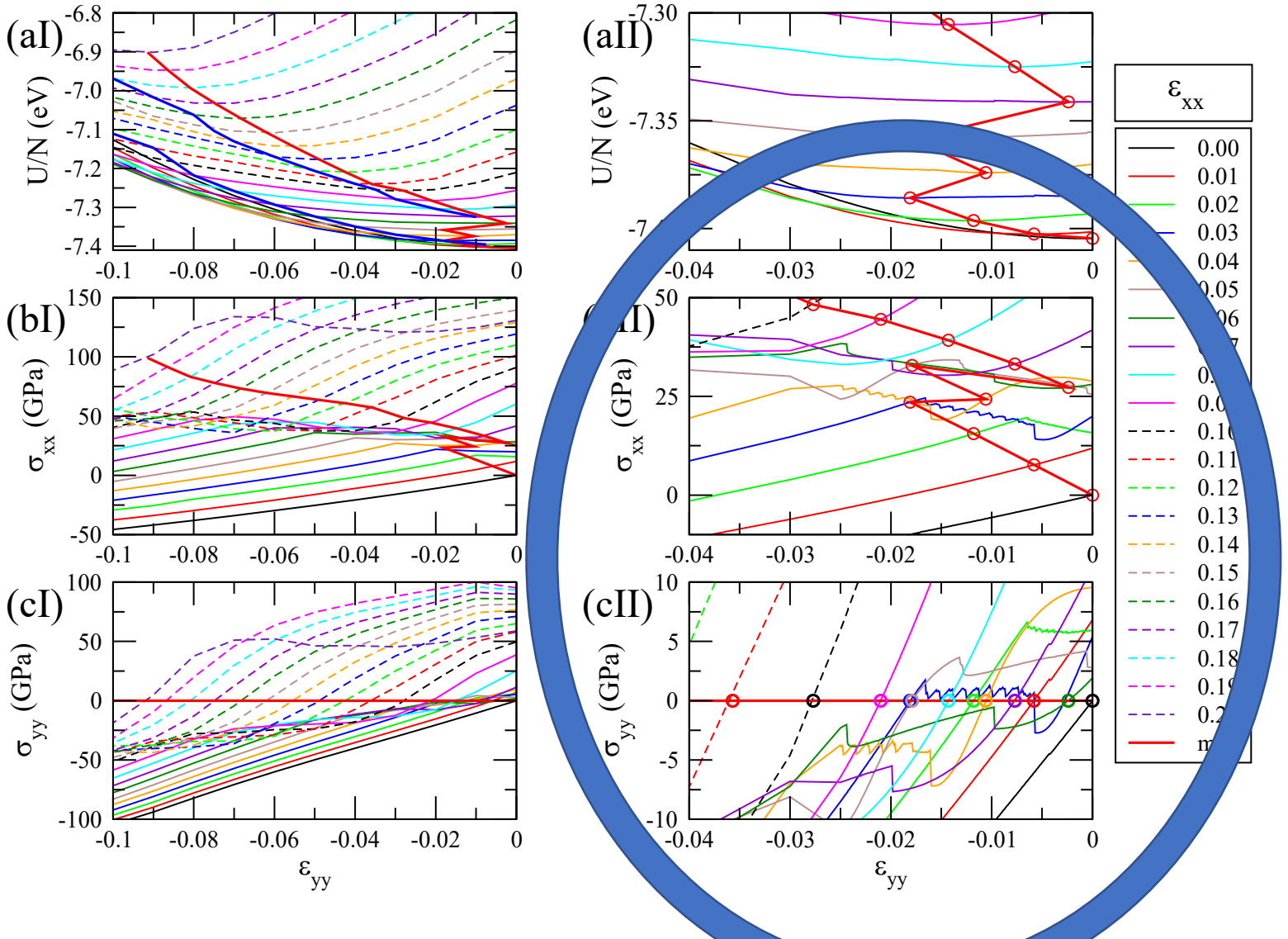

Why that behavior under strain?

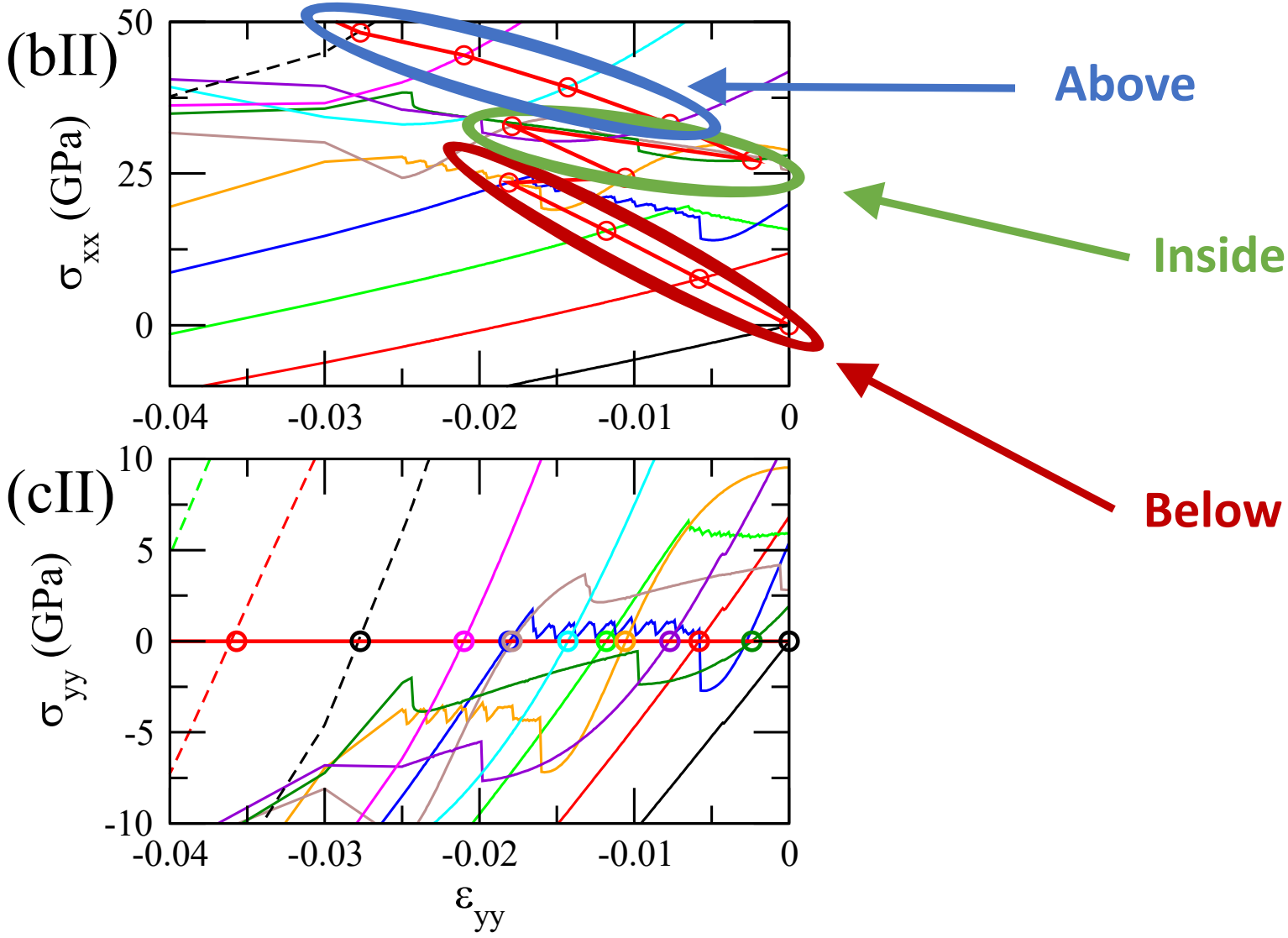

The equilibrium structure under strain near ε_{yy} = 0.05 falls in one of the three areas having different slope.

Why that behavior under strain?

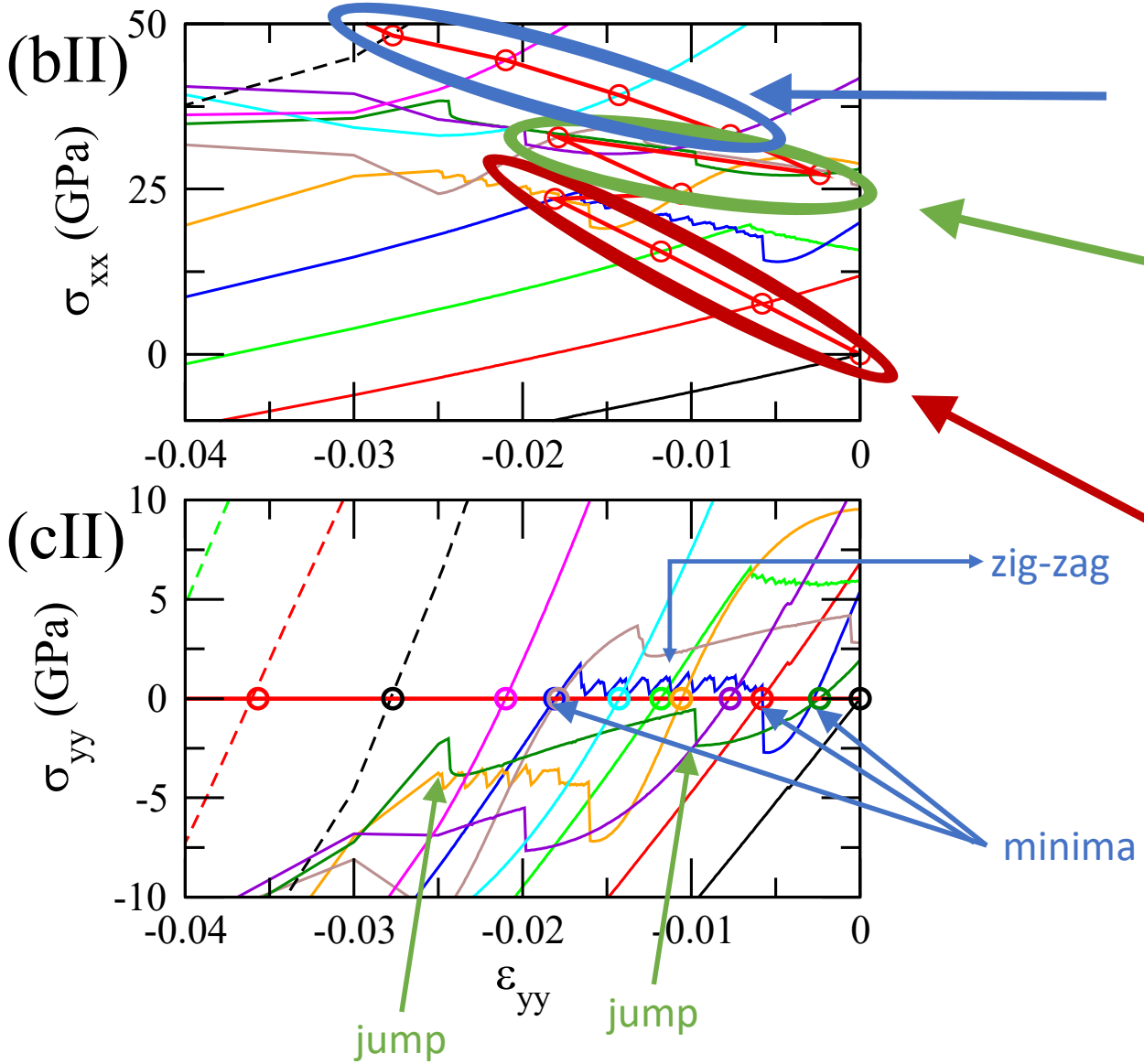

Above

Inside

Below

The equilibrium structure under strain near ε_{yy} = 0.05 falls in one of the three areas having different slope.

Jumps or zig-zag behavior of σ_{yy}
Three minima for ε_{xx} = 0.03

Moreover …

CHON-2019 again

- Energy and stress scan for constant strain values along y (zig-zag) direction.
- $0.08 \leq \varepsilon_{yy} \leq 0.23$
  - Strain step $\delta\varepsilon_{yy} = 0.01$
- $-0.15 \leq \varepsilon_{xx} \leq 0$
  - Strain step $\delta\varepsilon_{xx} = 0.001$

- **Discontinuities in stress**
- **Discontinuities in energy**

Two minima

Jump of stress at equilibrium

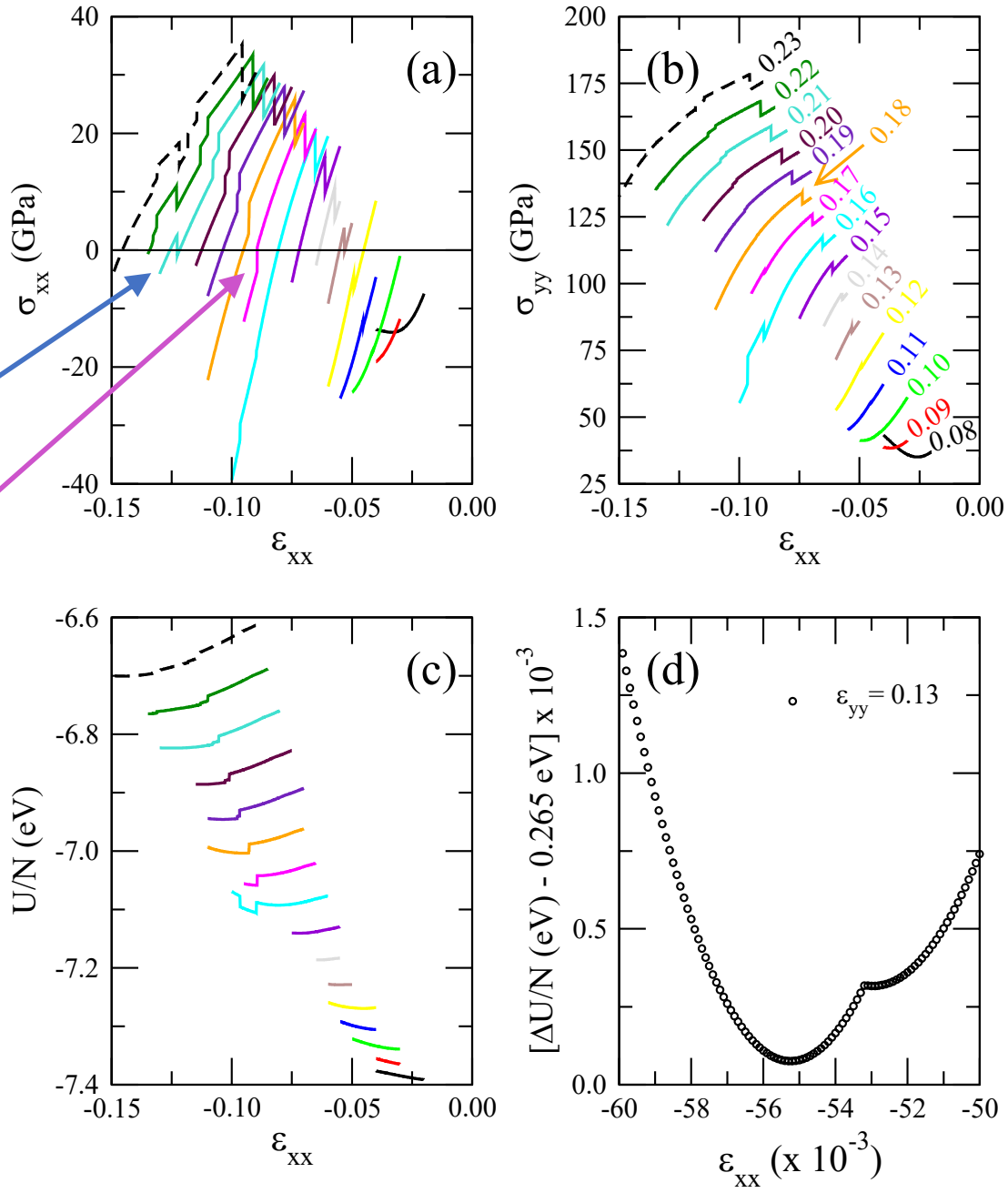

Fracture of carbon nanotubes

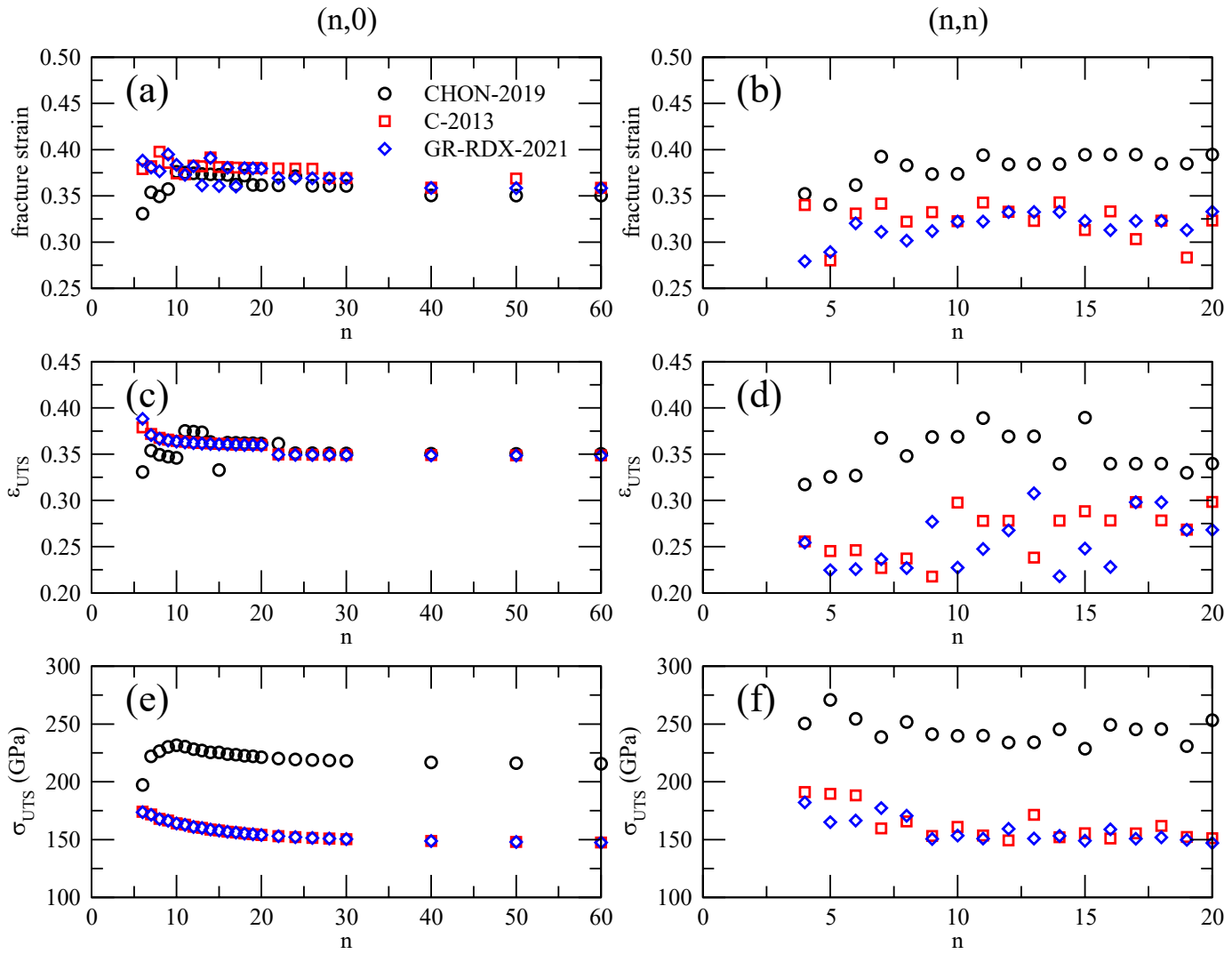

Conclusions

- The three ReaxFF provide similar results for graphene
- Good predictions for energetic and structural properties of graphene and carbon nanotubes
- Overestimated vacancy formation energies
- Underestimation of SW and inverse SW formation energies
- Reasonable energy barriers for the permeation of CO2 through pyridinic graphene pores
- Reasonable results for fullerene isomer energies with small slope for the adjacent pentagon penalty rule
- Reasonable phonon dispersion relation for graphene. More or less agreement with DFT.
- Underestimation of Young's modulus and overestimation of Poisson's ratio for graphene and carbon nanotubes
- Unusual behavior of stress-strain plots and the Poisson's ratio vs strain for graphene and carbon nanotubes
- Graphene potential energy surface contains artifacts that have to be improved (energy and stress discontinuities, slope change)

Thank you for your attention